

NORTHWESTERN UNIVERSITY

A NUMERICAL METHOD FOR COMPUTING OCEAN ACOUSTIC MODES

A DISSERTATION

SUBMITTED TO THE GRADUATE SCHOOL

IN PARTIAL FULFILLMENT OF THE REQUIREMENTS

for the degree

DOCTOR OF PHILOSOPHY

Field of Engineering Sciences and Applied Mathematics

By

MICHAEL BLAIR PORTER

Evanston, Illinois

June 1984

ABSTRACT

A Numerical Method For Computing Ocean Acoustic Modes

by Michael Blair Porter

We present a fast finite difference method for computing the propagation numbers and corresponding normal modes for various oceanic scenarios. Specifically, we consider the problem of computing the acoustic field due to a time harmonic source in a stratified ocean of constant depth. We consider three related models. In the first, the ocean is stationary and the ocean subbottom is modelled as a completely rigid medium. In the second, we allow for a laminar shear flow parallel to the ocean bottom. In the third, we allow for coupling into an elastic subbottom with depth dependent P- and S-wave speeds.

The numerical method is a combination of well-known numerical procedures such as, Sturm sequences, the bisection method, Newton's and Brent's methods, the compound matrix method, Richardson extrapolation and inverse iteration. We also introduce a modified extrapolation procedure which substantially increases the speed and accuracy of the computation.

Advisor: Professor Edward L. Reiss

ACKNOWLEDGEMENTS

The advice and support of my advisor, Professor Edward L. Reiss, was instrumental in the completion of this work and is deeply appreciated. In addition, I have also benefitted from numerous discussions with Professors G. Kriegsmann, S. Stein, T. Mahar and E. Bareiss, and I gratefully acknowledge their contribution. Finally, I specifically thank the members of the examination committee for performing the non-trivial task of editing and reviewing the dissertation.

TABLE OF CONTENTS

Abstract	ii
Aknowledgements	iii
List of Tables	v
List of Figures	vi
CHAPTER 1 INTRODUCTION	1
CHAPTER 2 THE CLASSICAL OCEAN ACOUSTICS PROBLEM	12
2.1 Introduction	12
2.2 The Method	14
2.3 Applications of the Method	20
2.4 Relation to the Shooting Method	24
CHAPTER 3 ACOUSTIC PROPAGATION IN DUCTS WITH SHEAR FLOWS	27
3.1 Introduction	27
3.2 Formulation	28
3.3 Properties of the Equation	30
3.4 The Method	34
3.5 Applications of the Method	39
CHAPTER 4 BOTTOM INTERACTING ACOUSTIC PROPAGATION	44
4.1 Introduction	44
4.2 Formulation	46
4.3 The Method	47
4.4 Applications of the Method	54
CHAPTER 5 CONCLUSIONS	58
TABLES	62
FIGURES	93
REFERENCES	111
VITA	125

LIST OF TABLES

2.1	Numerical eigenvalues for the Mathieu problem	62
2.2	Standard extrapolations for the Mathieu problem	63
2.3	Modified extrapolations for the Mathieu problem	64
2.4	Numerical eigenvalues for the Munk profile	65
2.5	Standard extrapolations for the Munk profile	67
2.6	Modified extrapolations for the Munk profile	69
2.7	Numerical eigenvalues for the double-duct problem	71
2.8	Modified extrapolations for the double-duct problem	72
2.9	Comparison of execution times using different techniques to generate the initial guesses	73
3.1	Numerical eigenvalues for the Munk profile with a shear flow	74
3.2	Standard extrapolations for the Munk profile with a shear flow	76
3.3	Modified extrapolations for the Munk profile with a shear flow	78
3.4	Comparison of eigenvalues for the Munk profile with and without a shear flow	80
3.5	Numerical eigenvalues for the aeroacoustic problem	81
3.6	Standard extrapolations for the aeroacoustic problem	82
3.7	Modified extrapolations for the aeroacoustic problem	83
4.1	Numerical eigenvalues for the shallow water problem	84
4.2	Standard extrapolations for the shallow water problem	86
4.3	Numerical eigenvalues for the Munk profile with an elastic bottom	88
4.4	Standard extrapolations for the Munk profile with an elastic bottom	90
4.5	Comparison of eigenvalues for the Munk profile with an elastic bottom and with a rigid bottom	92

LIST OF FIGURES

2.1	Munk sound speed profile	93
2.2	Selected modes for the Munk sound speed profile	94
2.3	Sound speed profile for the double-duct problem	96
2.4	First nine modes for the double-duct problem	97
3.1	First nine modes for the aeroacoustic problem with $M=.5$	100
3.2	First six modes for the aeroacoustic problem with $M=.1$	103
4.1	Mode 3 for the shallow water problem	105
4.2	Mode 9 for the shallow water problem	106
4.3	Mode 15 for the shallow water problem	107
4.4	Mode 1 for the Munk profile with an elastic bottom	108
4.5	Mode 10 for the Munk profile with an elastic bottom	109
4.6	Mode 21 for the Munk profile with an elastic bottom	110

CHAPTER 1

INTRODUCTION

The problem of computing the acoustic field in the ocean arises from both military and civilian concerns including, the detection and tracking of submarines, sub-surface communication, and navigation. The ocean surface and the ocean bottom form an acoustic duct which facilitates the long-range propagation of sound. In addition, there may exist internal ducts due to gradients in the sound speed. This type of problem is very similar to a variety of other guided-wave problems which arise in the study of, for instance, optical fibers, microwave guide, surface acoustic wave devices, seismic wave propagation, ionospheric radio wave propagation, and the Shrodinger equation. Thus, although the ocean acoustic problem will be the focus of this work, the techniques developed have broad applicability.

There are a variety of methods that have been used to compute the acoustic field in an oceanic environment, e.g., ray tracing, the parabolic equation method, the fast field program, and the method of normal modes. Each of these approaches has advantages for different occasions. In particular, ray tracing is most effective for the near-field due to the expense of numerically integrating the ray equations into the far-field, and for high-frequencies due to the asymptotics used to derive the model. The parabolic equation method

is useful for including the effect of weak range variations in the sound speed but is only accurate in narrow spatial domains. The fast field program is appropriate for computing the acoustic field in the entire ocean due to a fixed source. Normal mode programs are desirable when the problem must be solved repeatedly for several source and receiver locations and for far-field, low-frequency problems. They are also important as a means of verifying more sophisticated models applied to simpler test problems. In addition, the normal mode model, like the ray-tracing model, provides special physical insights into the problem. In this work we shall consider the normal-mode model.

The normal mode model assumes that the sound speed is a function of depth but not range and that the ocean bottom lies at a constant depth. This is often a realistic assumption for oceanic problems; the sound speed is influenced primarily by the increase in temperature towards the ocean surface, the increase in pressure towards the ocean bottom, and the vertical dependence of the salinity. Normal mode methods may also be applied to range-dependent problems by dividing the range into segments and computing a modal solution in each segment. Thus, despite the apparent simplicity of the model, the normal mode methods have proven extremely useful for computing acoustic propagation.

The normal mode representation is obtained by considering a time

harmonic source for the time dependence and then using separation of variables on the resulting two-dimensional partial differential equation for the acoustic pressure. In cylindrical coordinates the solutions for the radial equation are Hankel functions while in rectangular coordinates one obtains sines and cosines. In either case the modes corresponding to the depth variable, z , satisfy the same second-order differential equation. Often, the ocean surface is assumed to be a perfect pressure release and the ocean subbottom is assumed to be perfectly rigid. In this case, one obtains a Sturm-Liouville eigenvalue problem with a Dirichlet boundary condition at the surface and a Neumann boundary condition at the ocean bottom. The spectrum of the problem consists of a finite number of positive eigenvalues corresponding to propagating modes and an infinite number of negative eigenvalues corresponding to growing or decaying solutions. These latter modes are normally omitted from the field synthesis.

The sound speed profiles encountered in the ocean are usually sufficiently complex that numerical methods are required. In addition, the eigenvalues of this problem are the squares of the horizontal wavenumbers and must be determined very accurately since errors in these eigenvalues appear as phase shifts in the range dependence of the pressure. If the range is large then these phase shifts will seriously degrade the accuracy of the solution. In

addition, the number of propagating modes is roughly proportional to the frequency of the source multiplied by the ocean depth, therefore for high frequencies and/or deep oceans the modal problem can be extremely expensive to solve.

Existing methods have been based on two overlapping classes of methods: the method of coefficient approximation (Stickler, 1975; Gordon, 1979) and shooting methods (Ferris, et al., 1970; Beisner, 1974; Dozier, 1975). In the method of coefficient approximation the depth variable is divided into a series of layers and in each layer the coefficients in the differential equation are approximated by a function for which the differential equation may be analytically solved. The most obvious choice is to use a piecewise constant approximation in which case the analytic solution in each layer is a combination of sines and cosines. The most popular choice, however, seems to be to use a piecewise-linear approximation. This yields Airy functions or equivalently Hankel functions of order $1/3$. The piecewise-linear model naturally yields better approximations to the eigenvalues for the same number of layers and, according to its proponents, is also more efficient. The chief drawback is that a complicated subprogram for computing the Airy functions is required.

Loss of precision in implementations of the method of coefficient approximation has been reported under various circumstances (Gordon, 1979). This problem is probably resolvable by choosing Airy functions

rather than Hankel functions but in any case it indicates that a coefficient approximation method must be very carefully implemented.

Regardless of the approximation chosen, one obtains a matrix eigenvalue problem with transcendental functions for the elements. The eigenvalues may then be found by solving for the zeros of the determinant using some root finder. Existing programs for the acoustic problem require that an initial guess be provided by the user, estimated by extrapolation using lower order eigenvalues, or estimated by the WKB method. This approach is ineffective for the lowest order modes which tend to be somewhat erratically spaced. The discussion in Chapter 2 provides a solution to this problem based on a bisection technique and indeed this approach has recently been applied to other Sturm-Liouville problems (Mikhailov and Vulchanov, 1983).

In the shooting method one integrates from one boundary to the other and adjusts a trial eigenvalue, using some root finder, until the boundary condition at the terminal point is satisfied. One initial condition is obtained from the boundary condition and a second is selected arbitrarily and normalizes the eigenfunction. One advantage of the shooting method is simplicity, since packages for solving initial value problems are generally readily available. On the other hand, the integration will quite often be unstable as physical problems often have one or more ducts. Outside the ducts the lower order modes grow or decay exponentially. It is then important that

the differential equation be integrated in the direction of exponential growth for if the integration is performed in the opposite direction round-off errors invariably lead to the growth of the unwanted complement. This problem is readily resolved by multiple shooting however only parallel shooting appears to have been used to date.

In Chapter 2 we introduce a new method based on finite differences combined with Richardson extrapolation. Richardson extrapolation has found widespread use in a variety of areas, especially numerical quadrature (the Romberg method) and the integration of systems of ordinary differential equations (the Gragg-Burlisch-Stoer method). An excellent discussion of extrapolation methods may be found in the paper by Joyce (1971). Fundamentally, Richardson extrapolation is based on obtaining a sequence of approximations to the exact solution and using a knowledge of the behavior of the error in the approximations to extrapolate to the exact solution. For the problems we consider, this method is applied by obtaining approximations to the exact eigenvalues via a finite difference scheme. It can be shown that for the difference schemes we employ, the error in the approximate eigenvalues can be written as a power series in h^2 , where h is the mesh width. The extrapolation is then obtained by fitting a polynomial in h^2 to the sequence of approximations and then computing the value of the polynomial at $h=0$, i.e., for a zero mesh width. We

also introduce a modified form of Richardson extrapolation in which the error is represented as a sum of two functions. The first is a transcendental function which gives the error as a function of the mesh width, h , that would be obtained for a constant sound speed problem. The second function is a polynomial in h^2 which represents a perturbation in the error due to the deviation of the sound speed from a constant value. The modified extrapolation procedure provides substantially better results than the standard Richardson extrapolation for the higher order modes.

Naturally the efficiency of the overall method is strongly influenced by the manner in which the approximate solutions are obtained. The finite difference scheme we have employed yields an algebraic eigenvalue problem for which many efficient algorithms have been developed. In particular we have selected an algorithm based on Sturm sequences combined with inverse iteration. In Section 2.3 this method is interpreted as a shooting approach which provides valuable insights into this latter class of methods. Specifically, this discussion relates the Sturm sequence procedure to a zero counting in the eigenfunctions and thus suggests a bisection procedure which may be applied to obviate the need for initial guesses in other programs. This discussion also indicates that one-sided shooting is effective if only eigenvalues are required as, for instance, in dispersion curve calculations. In comparison to existing methods for solving the modal

equation, this approach is extremely simple due to the simple difference approach used, and efficient over a wide range of accuracy requirements due to the use of extrapolation. The Sturm sequence provides an efficient procedure for systematically computing all of the propagating modes (or specified subsets) without the requirement of an initial guess. In addition, the use of inverse iteration to compute the eigenfunctions provides a stable method for computing the eigenfunction regardless of the number of ducts present.

In Chapter 3 we extend this technique to the case when a laminar shear flow is present. This problem arises from the desire to reduce noise in jet engine ducts and air conditioning systems or for assessing the effect of ocean currents on long-range acoustic propagation. The results presented in Section 3.5 suggest that these effects may indeed be significant in realistic oceanic scenarios. Existing numerical procedures include the shooting method (Mungur, 1969; Shankar, 1972) and the Rayleigh-Ritz method (Savkar, 1971). The governing equation is a second-order eigenvalue problem in which the eigenvalue appears nonlinearly. The nonlinear occurrence of the eigenvalue is, according to expectation, also manifested in the discretized algebraic eigenvalue problem and introduces a number of new features. In particular, the Sturm sequence procedure is not immediately applicable and in Section 3.3 we generalize this procedure in a framework which allows it to be incorporated in other numerical methods as well.

The models considered in Chapters 2 and 3 assume that the ocean bottom is perfectly rigid, which, depending on the specific local geology, may or may not be a reasonable assumption. For instance, a bottom structure in the Western North Atlantic which is described by Beebe and McDaniel (1980) features the following morphologies over a range of 130 km: gravel and sand; sand and gravel; silt; sand; till; and clay. For deep-water problems the sound speed profile is generally dominated by the increase in pressure with depth. This positive sound speed gradient traps the lower order modes and prevents them from interacting significantly with the ocean bottom. Thus, for deep-water problems a rigid bottom model is likely to yield accurate results even when the ocean bottom is quite soft. Conversely, the rigid bottom model is often questionable for shallow water problems. Ultimately, the significance of the ocean bottom model must be assessed by comparing experimental results to numerical results both with and without an enhanced bottom model. Some recent efforts in this area are summarized in Proceedings of a Conference on Bottom Interacting Ocean Acoustics (Kuperman and Jensen, 1980).

The ocean subbottom may be incorporated in a variety of ways. If a portion of the subbottom is extremely soft then it may be treated as a fluid layer overlying a fluid half-space, neglecting the effect of shear waves (Beisner, 1974; Stickler, 1975; Gordon, 1979), or alternatively as a fluid layer overlying an elastic half-space

(Tolstoy, 1960; Essen, 1980; Ferla, et al., 1980). Still further improvements may be obtained by using an arbitrary sequence of elastic layers with constant P- and S-wave velocities in each layer. This model has only recently been applied to ocean acoustics problems but has been considered extensively in the seismological literature, where it is known as the Thomson-Haskell method or the propagator matrix method (Thomson, 1950; Haskell, 1953; Knopoff, 1964; Dunkin, 1965; Thrower, 1965; Gilbert and Backus, 1966). One also finds implementations of shooting methods (Takeuchi and Saito, 1972) and more recently the finite element method with cubic splines (Wiggins, 1976). The latter has primarily been applied to problems with spherical geometry but the problems are essentially the same and have followed a parallel development.

In Chapter 4, we have incorporated the effect of the ocean subbottom into the model of Chapter 2 by performing an integration through the elastic subbottom to compute an impedance condition at the ocean/subbottom interface. The techniques applied in Chapter 2 to the rigid bottom model then apply directly to this new model with the exception that the Sturm sequence procedure is invalid due to the complicated functional dependence of the impedance condition on the eigenvalue parameter. We have therefore replaced the Sturm sequence procedure with a deflation technique in order to compute the eigenvalues at each mesh. In addition, the standard Richardson

extrapolation was employed rather than the modified form due to the greater computational expense required to compute the eigenvalues for a constant property problem, which are required for the modified extrapolation procedure.

Finally, we conclude this work in Chapter 5 with comments about possible extensions or improvements which may be useful for other problems.

CHAPTER 2

THE CLASSICAL OCEAN ACOUSTICS PROBLEM

2.1 Introduction

In a stratified cylindrically-symmetric ocean being excited by continuous wave radiation of angular frequency ω , the acoustic pressure can be written in the form

$$P(r,z,t) = \sum_j c_j H_0^{(1)}(k_j r) p_j(z) e^{-i\omega t}, \quad (2.1)$$

where the depth variable, z , ranges from 0 at the ocean surface to D at the ocean bottom. The propagation numbers k_j and the normal modes $p_j(z)$ are then the eigenvalues and eigenfunctions, respectively, of the following Sturm-Liouville problem:

$$\begin{aligned} p'' + (\omega^2/c^2(z) - k^2)p &= 0 \\ p(0) &= 0 \\ p'(D) &= 0. \end{aligned} \quad (2.2)$$

Here, ω is the circular frequency of the source and $c(z)$ is the ocean sound speed. The boundary conditions in (2.2) imply that the ocean surface ($z=0$) is free, i.e., it is the pressure release condition, and that the ocean bottom ($z=D$) is rigid.

There are only a finite number of eigenvalues of (2.2) that are real. Then by the properties of the Hankel function they correspond to propagating modes in the sum (2.1). The remaining eigenvalues correspond to evanescent or non-propagating modes.

As discussed in Chapter 1, explicit solutions of (2.2) can be obtained only for relatively simple sound speed profiles $c(z)$. The profiles encountered in the ocean are usually sufficiently complex that numerical methods are employed to solve (2.2). For example, coefficient approximation methods (Stickler, 1975; Gordon, 1979) and shooting methods (Beisner, 1974; Dozier, 1975) are widely used. Typically, the errors in the eigenvalues k_j that are determined from numerical solutions of (2.2) increase with j . Furthermore, as we observe from (2.1) these errors appear as phase shifts in the range dependence of p . Specifically, the phase shifts are proportional to the products of these errors and r . Thus, if r is large as occurs in long-range propagation, the phase shifts caused by the numerical errors in k_j will seriously degrade the accuracy of the series representation (2.1). This suggests the need for extremely accurate determination of the eigenvalues of (2.2).

In addition, we observe that if $c(z)$ is replaced by its average value, \bar{c} , in (2.2) one obtains $m = (\omega/\bar{c})(D/\pi)$ as an estimate of the number of propagating modes. Thus for "high" frequency sources and/or deep oceans, the number of propagating modes is large. These and other factors in the repeated use of (2.1) to represent acoustic fields suggest that the numerical methods must be fast in addition to accurate. In this chapter we present a numerical procedure which satisfies these requirements. It is a combination of well-known

numerical techniques such as finite difference approximations and Richardson extrapolation. The method is described in Section 2.2 and then applied in Section 2.3 to three examples to demonstrate its speed and accuracy. They are a Mathieu equation for which the eigenvalues are tabulated (Abramowitz and Stegun, 1964), the well-known Munk profile (Munk, 1974) for the sound speed, and finally a double-duct profile. In Section 2.4 we present a brief discussion of the relationship between the present method and shooting methods for solving (2.2).

2.2 The Method

To solve (2.2) numerically we first define a mesh by dividing the interval $0 < z < D$ into N equal subintervals by the points $z_i = ih$, $i = 0, 1, \dots, N$ where the mesh width h is defined by $h = D/N$. Then using the standard three-point difference approximation to the second derivative in (2.2) and the centered difference approximation to the first derivative in (2.2), we obtain the algebraic eigenvalue problem

$$A\mathbf{p} = h^2 k^2 \mathbf{p} \quad (2.3)$$

as an approximation to the eigenvalue problem (2.2). Here, \mathbf{p} is the N -dimensional vector with components p_1, p_2, \dots, p_N . These components approximate the eigenfunctions of (2.2) at the mesh points. In addition, the tridiagonal $N \times N$ matrix A is defined by

is equal to the number of eigenvalues greater than k^2 , where zeros in the sequence are deleted.

In the first step of the method we find an isolating interval for each eigenvalue k_j^2 , i.e., an interval in k^2 which contains only the eigenvalue k_j^2 . For the first, or largest, eigenvalue an upper bound is obtained from Gerschgorin's Theorem (Wilkinson, 1965). Zero is taken as the lower bound since only propagating modes (positive eigenvalues) are to be obtained. This interval is successively bisected until it contains only the first eigenvalue, a condition that is determined by counting the sign changes in the Sturm sequence. This process is repeated for each subsequent eigenvalue. Now, however, the previous eigenvalue's lower bound is an upper bound for the next eigenvalue. In addition, lower bounds for the current eigenvalue may have already been computed during the bisection process for the previous eigenvalues. The isolating intervals provide initial estimates for each eigenvalue. More accurate approximations of each eigenvalue are then obtained by Brent's Method (Brent, 1971) which combines bisection, linear interpolation and inverse quadratic interpolation and guarantees convergence to the isolated eigenvalue.

In Richardson's extrapolation method (Joyce, 1971; Dahlquist and Bjorck, 1974) improved estimates for the eigenvalues of the continuous problem (2.2) are obtained by extrapolating to zero mesh width using the numerical approximations to the eigenvalues, $k_j^2(h)$, of the

algebraic problem (2.3). In the standard extrapolation method the converged numerical value with mesh width h for the j th eigenvalue $k_j^2(h)$ is expressed as

$$k_j^2(h) = b_0 + b_2 h^2 + b_4 h^4 + \dots + b_{2(m-1)} h^{2(m-1)}. \quad (2.7)$$

Here, b_0 is the Richardson approximation to the j th eigenvalue of (2.2). The constant b_0 is then determined from the linear system that results from applying (2.7) to a sequence of successively finer meshes $\{h_j\} = h_1, h_2, \dots, h_m$. Since this approximation depends on the sequence of mesh widths that is employed we denote the Richardson approximation corresponding to the meshes h_p, h_{p+1}, \dots, h_q by $k_j^2(p, \dots, q)$. Successive extrapolations are generated recursively by the relation

$$k_j^2(p, \dots, q) = \frac{h^2(p)k^2(p+1, \dots, q) - h^2(q)k^2(p, \dots, q-1)}{h^2(p) - h^2(q)} \quad (2.8)$$

as we can obtain from (2.7).

In addition, we employ a modified Richardson extrapolation procedure which was motivated by the analysis by Paine, et al. (1981). Thus, the Richardson expansion (2.7) is now replaced by

$$\hat{k}_j^2(h) = (k_j^I)^2(h) - (k_j^I)^2(0) + b_0 + b_2 h^2 + b_4 h^4 + \dots \quad (2.9)$$

Here the eigenvalues $(k_j^I)^2(h)$, which are defined by

$$\begin{aligned} (k_j^I)^2(h) &= \omega^2/\bar{c}^2 - [\sin\{(j-.5)(\pi/D)(h/2)\}/(h/2)]^2 \\ (k_j^I)^2(0) &= \omega^2/\bar{c}^2 - [(j-.5)(\pi/D)]^2 \end{aligned} \quad (2.10)$$

are the exact eigenvalues of (2.2) and (2.3), respectively with $c(z)$

replaced by its average value \bar{c} . That is, they are the exact eigenvalues of the continuous and algebraic eigenvalue problems for similar isovelocity profile. Then the modified Richardson approximations which we denote by $\hat{k}_j^2(p, \dots, q)$ are computed as before but now using (2.9). The recursion formula (2.8) may also be applied to compute the modified extrapolation. The analysis in (Paine, et al., 1981) suggests that the modified extrapolation method moderates the error growth with increasing mode number.

The Sturm sequence procedure for isolating each eigenvalue of the algebraic system is used only for the first mesh, i.e., for $h=h_1$, and not for the subsequent meshes. Initial guesses for the eigenvalues corresponding to the second and subsequent meshes are obtained by using the modified extrapolation procedure but extrapolating to the desired mesh size. Thus, for the second and subsequent meshes, isolating intervals for the eigenvalues are not obtained and Brent's method is not applicable. Therefore, Newton's method is employed, starting from the initial guesses to solve for the numerical eigenvalues.

The mesh selection is motivated by two considerations. First, if the mesh is refined too rapidly, then the initial guess obtained from the previous mesh may be sufficiently inaccurate that the Newton iteration converges to the wrong mode. On the other hand, if the meshes are refined too slowly then the extrapolation is not as effective. We

have found it convenient to use the following meshes:

$$N = [\Im_m \{1.0, 1.2, 1.5, 1.9, 2.5, 3.2, 4.0, 5.0\}] \quad (2.11)$$

$$m = (\omega / \bar{c}) D / \pi.$$

Here, m is an estimate of the number of propagating modes provided from the isovelocity profile with the same depth and frequency and with a sound speed, \bar{c} , equal to the average sound speed. The square brackets in (2.11) denote the integer part.

After the eigenvalues are obtained to the desired accuracy, the eigenvectors are found by inverse iteration (Wilkinson, 1965) using the difference equations and eigenvalues of the final mesh.

A related extrapolation method was previously developed for the one-dimensional Schrodinger equation (Truhlar, 1972). The present method has the following new features which provide improved speed and accuracy.

1. A quadratically convergent root finder is employed rather than the linearly convergent method of bisection apparently used in (Truhlar, 1972).
2. The eigenvalues of the previous mesh are used to provide the initial guesses for the eigenvalues of the next refined mesh.
3. We use a modified Richardson extrapolation procedure.

Finally, we remark that we have experimented with generalizations of

our finite difference method by using Numerov's method (Dahlquist and Bjorck, 1974; Dozier, 1975) and a five-point difference scheme to obtain more accurate approximations to (2.2). We find that the standard three-point difference scheme is both simpler to implement and more efficient than these higher order schemes. When a fourth-order difference scheme, such as Numerov's method, is used in the extrapolation procedure, the error in the eigenvalues has the following form:

$$k_j^2(h) = b_0 + b_4 h^4 + b_6 h^6 + \dots \quad (2.12)$$

Consequently, each extrapolation increases the order of the method by two, and after L extrapolations it is a $4+2(L-1)$ order method. This same order can be obtained with $L+1$ extrapolations using the standard three-point difference scheme, however, the standard scheme requires about half as much computation time for the same number of mesh points.

We have also applied extrapolation techniques to a coefficient approximation scheme using constant sound speed layers and find the present method to be more efficient.

2.3 Applications of the Method

We now present three applications of our method to demonstrate its convergence properties, speed and accuracy, and finally, its versatility. In the first problem we consider an eigenvalue problem

for Mathieu's equation for which

$$p'' + \left[\frac{249 - \cos(2z/1000)}{1000^2} - k^2 \right] p = 0 \quad (2.13)$$

$$p(0) = 0$$

$$p'(500\pi) = 0.$$

In Table 2.1a we present the first eight numerically determined eigenvalues of the corresponding algebraic problems (2.3) for the mesh widths indicated in the table (recall that $h=D/N$). In Table 2.1b the errors in these numerical eigenvalues are shown. The error is the difference between the numerically determined eigenvalues given in Table 2.1a and the "exact" eigenvalues. The exact eigenvalues are computed by our method using extrapolations with several more refined meshes. They agree to 13 digits with tabulated values (Abramowitz and Stegun, 1964). We observe that for each mesh the errors increase monotonically with the mode number, which is indicated by j in Table 2.1. The symbol ET in the tables denotes the execution time in seconds on the Northwestern Cyber 170/730 to compute all the eigenvalues corresponding to each mesh width.

The results of successive standard Richardson extrapolations are shown in Table 2.2. Of course, the first columns in Tables 2.1 and 2.2 are equal, however, a comparison of the subsequent columns in Tables 2.1 and 2.2 shows the dramatic decreases in the errors that are achieved by the extrapolation. Each successive extrapolation reduces the error by a factor of 100 to 1000. The 100-fold error reduction which is

obtained with one additional extrapolation would require a ten times finer mesh and a similar increase in execution time if it were obtained simply by mesh reduction.

The eigenvalues obtained using the modified extrapolation process are given in Table 2.3. In comparison to the standard extrapolations of Table 2.2, the growth in the error with increasing mode number is dramatically reduced. This occurs particularly for the coarser meshes. Thus, the numerical results suggest that if the speed of computation is a controlling factor in the computation, so that the least refined mesh consistent with accuracy is desired, the modified extrapolation procedure then becomes more effective.

The second example that we consider is an ocean whose sound speed varies in accordance with the Munk profile (Munk, 1974). Thus, we have

$$\omega=87/s$$

$$D=5000m$$

$$c(x)=1500[1+.00737(x-1+e^{-x})] \text{ m/s} \quad (2.14)$$

$$x=2(z-1300)/1300.$$

where we have used parameter values suggested by Dozier (1975). Numerically determined eigenvalues for certain selected modes are shown in Table 2.4a for the indicated mesh widths. Finer meshes are required because of the relatively large number of propagating modes. The corresponding errors in these eigenvalues are given in Table 2.4b.

The standard and modified Richardson extrapolated eigenvalues and their respective errors are presented in Tables 2.5 and 2.6. Again we observe, the substantial increase in accuracy due to the Richardson extrapolation.

The sound speed profile given in (2.14) is graphed in Figure 2.1, and some selected numerically determined modes are shown in Figure 2.2. With these parameter values only modes 17 and 18 are RSR (refracted-surface reflected) modes.

In the final example we consider the double-duct profile sketched in Figure 2.3. Specifically, we have

$$\omega = 8 \times 1550 / \sqrt{4000} \quad (2.15)$$

$$D = 2000 \text{m}$$

$$c(z) = 1550 / \sqrt{1 + (.6 + .8z/D)(1 - \cos(4\pi z/D))} / 64 \text{ m/s}$$

Thus, we are considering the problem,

$$p'' - [\{64 + (.6 + .8z/D)(1 - \cos(4\pi z/D))\} / 4000 - k^2] p = 0$$

$$p(0) = 0 \quad (2.16)$$

$$p'(2000) = 0.$$

The first nine eigenvalues at several meshes are displayed in Table 2.7 and the corresponding eigenfunctions are graphed in Figure 2.4. For the parameters (2.15) there are approximately 80 propagating modes. The execution times reflect only the time required to compute the first nine eigenvalues. Successive extrapolations using the

modified scheme are given in Table 2.8.

These examples suggest that the modified extrapolation procedure is superior to the standard Richardson extrapolation with the most dramatic improvements obtained when the error is largest, i.e., for high-order modes, coarse meshes and low-order extrapolation. Thus, the modified extrapolation procedure is particularly effective for the RSRBR (refracted surface-reflected bottom-reflected) modes. On the other hand, in the double-duct problem, in which we computed only the RR (refracted-refracted) modes the standard and modified extrapolation procedures would yield virtually identical results.

The merit of using the modified extrapolation scheme to generate an initial guess is demonstrated in Table 2.9. The first row contains the execution time required at each mesh when the bisection process is repeated for each new mesh. In the second row we used one point Richardson extrapolation, i.e., the eigenvalue from the previous mesh was used as an initial guess and in the third row we used one-point modified Richardson extrapolation. In the fourth row we used N-point standard Richardson extrapolation and finally, in the fifth row we used the N-point modified extrapolation and obtained the best results.

2.4 Relation to the Shooting Method

Some aspects of the finite difference method that we use are closely

related to the shooting method employed by previous investigators, see, e.g., Beisner (1974) and Dozier (1975). The shooting method using the three-point difference approximation generates the value p_i from two preceding values p_{i-1} and p_{i-2} by the formula

$$p_i = [h^2 k^2 - \{2 - h^2 \omega^2 / c^2(z_i)\}] p_{i-1} - p_{i-2}. \quad (2.17)$$

The surface boundary condition determines the value $p_1 = p(0) = 0$. We define the value of $p_1 = p(h)$ by $p_1 = 1$, since the eigenfunction is known only within an arbitrary multiplicative constant. The shooting parameter k^2 is then determined so that $p_{N-1} = p_{N+1}$, i.e., until $p'(D) = 0$. Initial guesses for the value of k^2 must be given to apply the shooting method, e.g., the WKB method has been employed. Initial guesses for the higher-order modes may be obtained by extrapolation from the lower-order modes. In addition, it follows from Sturm-Liouville theory that the j th mode has j zeros and so by counting the sign changes in the $\{p_j\}$ sequence it can be verified that convergence is to the desired mode.

The shooting (2.17) and characteristic polynomial (2.6) recursions are identical. Furthermore, the process of counting zeros is identified with the Sturm sequence property that the number of sign changes in the sequence is equal to the number of eigenvalues greater than k^2 .

An important difference between the finite difference and shooting methods is in the computation of the eigenvectors. Since one-sided

shooting is unstable when integrating into intervals in which the solution decays (Froberg, 1965), the elements of the Sturm sequence cannot be used directly to construct the eigenvectors. Other methods, such as an analog of parallel shooting, have been employed for the algebraic eigenvalue problem to partially obviate this difficulty (Wilkinson, 1965). However, inverse iteration, which we employ in the final step of our method has the computational advantage of not being degraded as one-sided shooting or parallel shooting would be, for profiles with multiple ducts.

CHAPTER 3

ACOUSTIC PROPAGATION IN DUCTS WITH SHEAR FLOWS

3.1 Introduction

In this chapter we extend the methods of the previous chapter to problems involving acoustic propagation in ducts and in layers with fluid flows. Typical examples of such problems are: the propagation from a sound source in the ocean in the presence of a current; the propagation of sound through a duct of a jet engine; and the propagation in boundary layer or other shear flows over flat plates. In the last example, the flow may extend to "infinity" normal to the plate, in which case the normal modes contribute to the more general spectral representation of the acoustic field. However, such flows over flat plates are frequently modeled by a finite layer of fluid flowing over the plate with the pressure on the upper surface of the layer taken as the far field pressure distribution.

As in the stationary medium problem treated above, the normal modes for the duct can be determined analytically only for relatively simple flows and sound speed distributions. More generally, it is necessary to determine them numerically. In this chapter, we consider problems of two-dimensional stratified flows, such as boundary layer or other shear flows, through ducts of finite depth D , where the sound speed of the fluid is also stratified. The appropriate normal mode problem for

such flows is then reduced to an eigenvalue problem for a second-order, linear ordinary differential equation. Since the acoustic medium is stratified, the coefficients in this equation depend only on the depth variable, z . The eigenvalue parameter, k , is the propagation number of the acoustic waves and the eigenfunctions are the normal modes. Since k occurs nonlinearly in this equation, it is a non-standard Sturm-Liouville eigenvalue problem unless the flow velocity is identically constant.

The normal mode problem is formulated in Section 3.2. In Section 3.3 we discuss those mathematical properties of the modal equation which are required for the numerical method and in Section 3.4 we describe the method. Finally, to demonstrate the performance of the method it is applied to two problems in Section 3.5. In the first problem we consider a parabolic profile for the stratified flow velocity to simulate an ocean current. The well known Munk profile (Munk, 1974) is employed for the stratified ocean sound speed. In the second problem the flow velocity is linearly stratified and the sound speed is constant thus simulating the flow in a shear layer over a flat plate.

3.2 Formulation

The two-dimensional basic flow velocity $\underline{U}(z)$, which is parallel to the rigid wall ($z=D$), is given by

$$\underline{U}(z) = (u^0(z), 0, 0) \quad (3.1)$$

where the horizontal flow velocity, $u^0(z)$, is a specified function. The upper layer of the duct is at $z=0$, so that the z coordinate is directed downward. The two-dimensional Euler's equations for the isentropic flow of a compressible fluid are then linearized about the steady stratified flow (3.1) to obtain the acoustic equations. Then by eliminating the density and the entropy from the resulting equations we determine that the acoustic velocity vector \underline{u}^* , which has components $[u^*(x,z,t), 0, w^*(x,z,t)]$, and the reduced acoustic pressure $p^* = \rho P$, where P is the physical pressure, and ρ is the constant fluid density of this flow, satisfy a system of three partial differential equations. We seek solutions of these equations in the form

$$\begin{aligned} u^*(x,z,t) &= u(z)e^{i(kx-\omega t)} & , w^*(x,z,t) &= w(z)e^{i(kx-\omega t)} \\ p^*(x,z,t) &= p(z)e^{i(kx-\omega t)} & , \end{aligned} \quad (3.2)$$

where ω is a specified circular frequency and the propagation numbers k are to be determined. The depth dependent amplitudes then satisfy a system of three ordinary differential equations. By eliminating $u(z)$ and $w(z)$ from these resulting equations, we can show that $p(z)$ satisfies the following self-adjoint, second-order ordinary differential equation,

$$[p'/a(z;\omega,k)]' + b(z;\omega,k)p = 0 \quad (3.3)$$

where primes denote differentiation with respect to z and the functions $a(z;\omega,k)$ and $b(z;\omega,k)$ are defined by

$$a(z;\omega,k) = (\omega - ku^0(z))^2, \quad (3.4)$$

$$b(z;\omega,k)=1/c^2(z)-k^2/a(z;\omega,k),$$

and $c(z)$ is the specified stratified sound speed of the fluid.

To complete the formulation of the boundary value problem we specify the boundary conditions that on the upper surface of the duct ($z=0$) the pressure is a constant which we set equal to zero. On the lower surface ($z=D$) the acoustic normal velocity vanishes. Thus we have

$$p(0)=0, \quad p'(D)/a(D)=0. \quad (3.5)$$

In summary, the eigenvalue problem is: for specified shear flows $u^0(z)$, circular frequencies ω of the source and sound velocities $c(z)$, determine the propagation numbers $k=k_j$ of the acoustic field (3.2) for which (3.3)-(3.5) have non-trivial solutions (normal modes) $p_j(z)$. It is not a standard Sturm-Liouville eigenvalue problem since (3.3) depends nonlinearly on the parameter k .

If the medium is stationary, so that $u^0(z)=0$, then (3.3)-(3.5) is reduced to

$$p''+(\omega^2/c^2(z)-k^2)p=0, \quad p(0)=p'(D)=0. \quad (3.6)$$

which is a standard Sturm-Liouville eigenvalue since it depends linearly on the parameter k^2 .

3.3 Properties of the Equation

We now establish certain mathematical results that are required for the numerical solution of (3.3)-(3.5). We shall be interested in subsonic flows so we assume that $\max(u^0(z)) < \min(c(z))$.

Theorem 1: The real eigenvalues k of (3.3), satisfy either

$$\omega/k > \min(u^0(z) + c(z)) \text{ or } \omega/k < \max(u^0(z) - c(z)). \quad (3.7)$$

Proof: Multiply both sides of the differential equation (3.3) by p and integrate the result from $z=0$ to $z=D$. Then integrating by parts and using the boundary conditions we get

$$-\int_0^D [p'(z)]^2/a(z) dz + \int_0^D b(z)[p(z)]^2 dz = 0. \quad (3.8)$$

We note that this integration by parts must also be valid if $a(z)$ vanishes within the interval as physical constraints dictate that p and p'/a be bounded. Since $a(z) \geq 0$ it follows from (3.8) that there exists an interval in $(0, D)$ in which $b(z) > 0$. Therefore, in this interval we have from the definition of $b(z)$ in (3.4) that $c^2 < (\omega/k - u^0)^2$ from which the desired result follows. The theorem states that the bound on the phase velocity is increased or decreased by the flow velocity, depending on whether the wave is travelling upstream or downstream.

Theorem 2: For $\omega > 0$ and $k > 0$, the number of eigenvalues greater than k is obtained by integrating (3.3) with the initial conditions $p(0)=0$, $p'(0)=1$, and then calculating the index function $I(k)$, which is defined by

$$I(k) = \text{the number of zeros of } p(z) \text{ in } (0, D] + \begin{cases} 1 & \text{if } p(D)p'(D) < 0, \\ 0 & \text{if } p(D)p'(D) \geq 0. \end{cases} \quad (3.9)$$

To prove this theorem we first require the following extension of an existing oscillation result (Hille, 1969) for the solutions of (3.3).

Lemma 1: Let $p(z)$ and $P(z)$ satisfy the initial value problems

$$(p'/a)' + bp = 0; \quad p(0)=0; \quad p'(0)=1 \quad (3.10)$$

$$(P'/A)' + BP = 0; \quad P(0)=0; \quad P'(0)=1$$

where the continuous coefficients satisfy the conditions $A > a > 0$ and $B > b$ for all z . The Prufer variables, $r(z)$, $R(z)$, $t(z)$ and $T(z)$ are defined by

$$\begin{aligned} p(z) &= r(z) \sin t(z), & p'(z) &= r(z) \cos t(z); \\ P(z) &= R(z) \sin T(z), & P'(z) &= R(z) \cos T(z). \end{aligned} \quad (3.11)$$

Then the phases satisfy the inequality,

$$T(z) > t(z), \quad \text{for } z > 0. \quad (3.12)$$

Proof: It is easy to show that the Prufer variables satisfy the following differential equations:

$$\begin{aligned} r' &= \{([a(z)-b(z)]/2) \sin 2t\} r & ; r(0) &= 1 \\ t' &= a(z) \cos^2 t + b(z) \sin^2 t & ; t(0) &= 0 \end{aligned} \quad (3.13)$$

Now suppose $t(z_0) = T(z_0) = t_0$ for some positive z_0 .

At such a point,

$$\begin{aligned} t'(z_0) &= a(z_0) \cos^2 t_0 + b(z_0) \sin^2 t_0 \\ T'(z_0) &= A(z_0) \cos^2 t_0 + B(z_0) \sin^2 t_0 \end{aligned} \quad (3.14)$$

From which it is clear that $T'(z_0) > t'(z_0)$. Thus if the T - and

t-curves ever cross, then the T-curve must approach from below the t-curve. This implies that there can be at most one crossing and this occurs at $z=0$. This proves the claim.

We note that the differential equation for r , has the solution

$$r(z) = e^{\int_0^z ([a(s)-b(s)]/2) \sin 2t(s) ds} \quad (3.15)$$

and so $r(z)$ is bounded away from zero and infinity. It follows that the zeros of $p(z)$ occur when the phase function, t , is an odd multiple of $\pi/2$ and the zeros of $p'(z)$ occur when t is an even multiple of $\pi/2$.

Proof of Theorem 2: We first establish that $I(k_{\max})=0$, where k_{\max} is the upper bound on the eigenvalues implied by Theorem 1. After multiplying (3.3) by p and integrating from 0 to z we obtain,

$$p(z)p'(z)/a(z) - \int_0^z (p')^2/a(z) dz + \int_0^z p^2/b(z) dz = 0. \quad (3.16)$$

When $k=k_{\max}$, $b(z)$ is negative and so we must have $p(z)p'(z) > 0$. Hence, p has no zeros and $I(k_{\max})=0$.

As k is decreased, $a(z;k)$ and $b(z;k)$ both increase. It follows from the lemma that the phase function $t(z;k)$ increases as k is decreased. Since the eigenvalues occur at points where $t(D;k)$ is an odd multiple of $\pi/2$ and $0 < t(D;k_{\max}) < \pi/2$, the number of eigenvalues greater than k is obtained as the largest n for which $t(D;k) > (2n-1)\pi/2$. Thus, the problem of determining the number of eigenvalues less than k is reduced to that of determining the number of rotations in the phase function.

We do not compute the phase function explicitly, so we need to be able to count rotations in $p(z)$. If for some z_0 , $t=m\pi$ then

$$t'(z_0) = a(z_0)\cos^2(m\pi) + b(z_0)\sin^2(m\pi) = a(z_0) > 0. \quad (3.17)$$

This implies that $t(z)$ can cross through a line $t=m\pi$ at most once during the integration from $z=0$. Thus m , the number of whole multiples of π contained in $t(D)$ can be obtained by counting the zeros of $p(z)$. Now, if $(2m)\pi/2 \leq t(D;k) < (2m+1)\pi/2$ then n , the number of eigenvalues greater than k , will be equal to m , but if $(2m+1)\pi/2 < t(D;k) < (2m+2)\pi/2$ then n is equal to $m+1$. Clearly, the former case occurs when $p(D)p'(D) \geq 0$ and the latter when $p(D)p'(D) < 0$, thus establishing the theorem.

Theorem 2 may be extended to the other quadrants of the ω - k plane with minor changes.

3.4 The Method

We first define a mesh by dividing the interval $0 < z < D$ into N equal subintervals by the points $z_i = ih$, $i=0,1,\dots,N$, where the mesh width h is defined by $h=D/N$. We then approximate the differential equation (3.3) on this mesh by replacing the first derivative in this self-adjoint operator by a standard two-point centered difference approximation, centered at the midpoint of a subinterval. This leads to the difference approximation

$$\left[(a_{i-1/2}^{-1})p_{i-1} - (a_{i-1/2}^{-1} + a_{i+1/2}^{-1})p_i + (a_{i+1/2}^{-1})p_{i+1} \right] + h^2 b_i p_i = 0,$$

$$i=1,2,\dots,N, \quad (3.18)$$

where we have used the notation

$$a_{i+1/2} = a(z_{i+1/2}), \quad b_i = b(z_i) \quad (3.19)$$

and p_i , $i=0,1,\dots,N$ are approximations to the eigenfunctions evaluated at the mesh points. The quantity p_{N+1} is the value of p corresponding to the fictitious point $z_{N+1}=D+h$. The boundary conditions in (3.5) are approximated by

$$p_0=0, \quad (3.20a)$$

$$a_{N-1/2}^{-1}(p_N - p_{N-1}) + a_{N+1/2}^{-1}(p_{N+1} - p_N) = 0. \quad (3.20b)$$

By solving (3.20b) for p_{N+1} and substituting the result into (3.18) with $i=N$, we finally obtain the algebraic eigenvalue problem

$$A(k)\underline{p}=0 \quad (3.21)$$

as an approximation to the continuous eigenvalue problem (3.3)-(3.5). Here \underline{p} is the N -dimensional vector with components p_1, \dots, p_N and the tridiagonal $N \times N$ matrix A is defined by

$$A = \begin{bmatrix} -(a_{1/2}^{-1} + a_{3/2}^{-1}) + h^2 b_1 & a_{3/2}^{-1} & & \\ a_{1-1/2}^{-1} & -(a_{i-1/2}^{-1} + a_{i+1/2}^{-1}) + h^2 b_i & a_{i+1/2}^{-1} & \\ & & & \\ & & 2a_{N-1/2}^{-1} & -2a_{N-1/2}^{-1} + h^2 b_N \end{bmatrix} \quad (3.22)$$

The midpoint "averaged" difference approximation in (3.20b) for the derivative yields a matrix with elements involving only values of $a(z)$ and $b(z)$ inside the domain.

The modified Richardson extrapolation procedure which we introduced in Chapter 2, is used to obtain more accurate estimates of the eigenvalues of the continuous problem (3.3)-(3.5) from the eigenvalues $k_j(h)$ of the algebraic problem (3.21). Thus, we express the j th eigenvalue $k_j(h)$ of (3.21) with mesh width h as

$$\hat{k}_j(h) = k_j^I(0) - k_j^I(h) + c_0 + c_1 h^2 + \dots \quad (3.23)$$

Here $k_j^I(h)$ is the j th eigenvalue of the algebraic eigenvalue problem (3.21) where the sound speed and convection velocities are replaced by "averaged" values \bar{c} and \bar{u}^0 respectively. These eigenvalues satisfy the dispersion relation,

$$[(\omega - k_j^I \bar{u}^0) / \bar{c}]^2 - (k_j^I)^2 = e_j^2(h), \quad (3.24)$$

where $e_j(h)$ is defined by

$$e_j(h) = \sin\{(j-.5)(\pi/D)(h/2)\} / (h/2). \quad (3.25)$$

and c_0, c_2, \dots , are constants. The constant c_0 is then the modified Richardson approximation to the j th eigenvalue of (3.3)-(3.5) and may be determined recursively as described in Chapter 2. As before, we denote the standard and modified Richardson approximations corresponding to the meshes h_p, h_{p+1}, \dots, h_q by $k_j(p, \dots, q)$ and $\hat{k}_j(p, \dots, q)$, respectively.

We now describe how we obtain the values $k_j(h_p)$ for the sequence of mesh widths. For the coarsest mesh width, we first find an isolating interval for each eigenvalue k_j . This is defined as an interval in k

which contains only the eigenvalue k_j . For the first, or largest, eigenvalue an upper bound for this interval is given by Theorem 1. Zero is taken as the lower bound since we are considering only modes which propagate to the right, i.e., in the downstream direction. This interval is successively bisected until it contains only the first eigenvalue. In Chapter 2 this condition was determined for the algebraic problem corresponding to (3.21) by counting sign changes in the Sturm sequence. Since the algebraic system (3.21) is nonlinear in the eigenvalue parameter, the Sturm sequence method is not directly applicable to the present problem. In Theorem 2 we derived an index function which gives a zero-counting procedure for the present problem and may be viewed as a generalization of the Sturm counting method.

This process is repeated for each subsequent eigenvalue. Now, however, the previous eigenvalue's lower bound is an upper bound for the next eigenvalue. In addition, lower bounds for the current eigenvalue may have already been computed during the bisection process for the previous eigenvalues. The isolating intervals provide initial estimates for each eigenvalue. More accurate approximations of each eigenvalue are then obtained by solving for the roots of the characteristic equation by Brent's method (Brent, 1971) which combines bisection, linear interpolation and inverse quadratic interpolation. Convergence is then guaranteed to the isolated eigenvalue.

A characteristic function for the eigenvalue problem, that is, a

function with zeros at the eigenvalues, may be obtained by setting $p_1=1$ and using the first $N-1$ difference equations of (3.21) to recursively generate p_i , $i=1,\dots,N$. By substituting the P_{N-1} and P_N into the final difference equation, we obtain the residual, $r(k)$, which is given by $r(k)=2a_{N-1/2}^{-1}P_{N-1}+(-2a_{N-1/2}^{-1}+h^2b_N)P_N$. This residual is then a characteristic function for the eigenvalue problem as it much vanish if k is to be an eigenvalue. Clearly this process may be interpreted as an integration of (3.3)-(3.5) and thus the computation of the characteristic function simultaneously generates the information required to compute the index function of Theorem 2. In addition, it is easy to verify that the p_i so generated, differ from the principal minors of $-A$ by products of the squares of the off-diagonal elements. It follows that the index function gives the number of sign changes in the principal minors of $-A$ and that the present method is indeed a generalization of the Sturm sequence method previously employed. We also note that the upper bound on the eigenvalues implied by Theorem 1, may be obtained from the discrete problem (3.21) by using the same technique which is normally used to prove Gerschgorin's Theorem.

Initial guesses for the eigenvalues corresponding to the second and subsequent meshes are obtained by using the modified Richardson extrapolation procedure, but now extrapolating to the desired mesh size. Since isolating intervals are not obtained for these meshes,

Brent's method is not applicable. We then use the secant method to refine the root, although other procedures such as Newton's method motivated by convergence and speed of computation, as discussed in Chapter 2.

After the eigenvalues are obtained to the desired accuracy by the modified Richardson extrapolation procedure, the eigenfunctions are found by an inverse iteration (Wilkinson, 1965) defined by

$$\begin{aligned} \underline{p}^0 &= 1, \\ \underline{A} \underline{p}^{l+1} &= \underline{p}^l \quad l=1,2,\dots, \end{aligned} \quad (3.26)$$

where the eigenvalues and difference equations of the final mesh are employed.

3.5 Applications of the Method

We now present two applications to demonstrate the method. The first application is motivated by acoustic propagation in the deep ocean in the presence of a current. We consider a parabolic profile for the current $u^0(z)$ and a Munk profile for the stratified sound velocity $c(z)$ using the parameters suggested by Dozier (1975) and employed previously in Chapter 2. Specifically, we employ the following parameters:

$$\begin{aligned}
 \omega &= 8\pi/s, \\
 D &= 5000\text{m}, \\
 u^0(z) &= 1.5[(z-D)/D]^2 \text{ m/s}, \\
 c(x) &= 1500[1. + .00737(x-1+e^{-x})] \text{ m/s},
 \end{aligned}
 \tag{3.27}$$

where the parameter x is defined by $x=2(z-1300)/1300$. The Mach number for this flow is approximately $1/1000$. In Table 3.1a we present the numerically determined eigenvalues corresponding to the downstream travelling modes for the indicated mesh widths ($h=D/N$). The column labeled "exact" contains the eigenvalues numerically determined by our method using extrapolations with several more refined meshes. The symbol ET in these tables denotes the execution time in seconds on the Northwestern Cyber 170/730 to compute all the given eigenvalues corresponding to each mesh width. The errors in these eigenvalues, which are defined as the difference between them and the "exact" eigenvalues are shown in Table 3.1b. In Table 3.2 we present the eigenvalues obtained by the standard Richardson extrapolation procedure, and their errors, and in Table 3.3 we present the same information for the modified Richardson extrapolation procedure.

We observe from Table 3.1 the anticipated $O(h^2)$ convergence in that doubling the number of mesh points reduces the error by a factor of about 4. In contrast, the errors in the eigenvalues obtained from both the standard and modified extrapolation procedures are reduced by as much as a factor of 1000 with each additional extrapolation, for

the first few eigenvalues. In addition, the modified extrapolation procedure provides the same dramatic reduction in error for the higher-order modes previously observed in the stationary medium problem.

These results show that the efficiencies of the methods for the present problem and the stationary medium problem treated in Chapter 2, are comparable, with one significant difference: the extrapolation process for the present problem is less effective for the modes close to cut-off. This occurs even with $u^0=0$ in the present problem. This discrepancy is a result of extrapolating with k rather than with k^2 , as we did in Chapter 2. Intuitively, this occurs because the values $k^2(h)$ move smoothly along the real line as h is refined but the values of $k(h)$ lie along either the real or the imaginary axes, and a pair of eigenvalues on the real line can coalesce at the origin and then split along the imaginary axis as h decreases. The extrapolation process cannot determine this abrupt transition because real values of k will always yield real extrapolates. Although none of the eigenvalues we have computed in Table 3.2 actually split, it can be shown that proximity to the splitting point is sufficient to adversely effect the convergence.

In Table 3.4 the eigenvalues from this convected problem are compared to the eigenvalues obtained when $u^0=0$. The change varies from $2.3 \times 10^{-6}/m$ to $3.6 \times 10^{-6}/m$, an effect that would be significant at

ranges of approximately 300 km and beyond. A reasonable estimate of this effect of slow convective flows can be obtained by comparison to a related problem with the sound speed and convection velocities replaced by their average values. Taking the first term of the Taylor series in \bar{u}^0 for the dispersion relation, $k(\omega; \bar{u}^0)$, one obtains,

$$\begin{aligned} k(u^0) &= \omega^2/\bar{c}^2 - e^2 - \omega \bar{u}^0/\bar{c}^2 + o((\bar{u}^0)^2) \\ &\approx k(0) - (\omega/\bar{c})(\bar{u}^0/\bar{c}). \end{aligned} \quad (3.28)$$

For the Munk profile, this yields

$$\begin{aligned} k(1/3) &= k(0) - [8\pi/1520][(1/3)/1520] \\ &= k(0) - 3.6 \times 10^{-6}. \end{aligned} \quad (3.29)$$

In the second application of our method, which we call the aeroacoustic problem, we employ the following parameters:

$$\begin{aligned} \omega &= 3300\pi/\text{s}, \\ D &= 1\text{m}, \\ u^0(z) &= 165(z-D)/D \text{ m/s}, \\ c &= 330 \text{ m/s} \end{aligned} \quad (3.30)$$

Then the corresponding dimensionless acoustic wave number $\omega D/c = 10\pi$ and the Mach number of the subsonic flow equals $1/2$. These parameters correspond to acoustic propagation at moderate subsonic flow velocities in a strongly sheared layer over the rigid surface ($z=D$), where the "upper surface" of the layer is approximated by a constant pressure surface. Since the depth of the layer is usually considered

to be infinite the imposed boundary condition implies that we are only considering trapped modes.

In Table 3.5, we present the numerically determined eigenvalues and results are substantially the same as in the previous problem, that is, the standard Richardson extrapolation method yields substantially more accurate eigenvalues and the modified Richardson extrapolation provides further improvements for the higher-order modes.

Graphs of the eigenfunctions corresponding to the first 9 eigenvalues are presented in Figure 3.1. The lower-order modes, modes 1 to 5, are trapped near the wall ($z=1.0$) while the higher order modes, modes 6 to 9, are oscillatory throughout the interval and hence convey energy to the surface ($z=0$).

In addition, we have applied our method to the aeroacoustic problem with a Mach number of $1/10$. The first six modes are graphed in Figure 3.2. The shear flow is less effective in forming an acoustic duct at this lower Mach number as can be observed by comparing Figures 1 and 2. Thus, for a given mode, more energy is carried to the free surface ($z=0$) at the lower values of the Mach number.

CHAPTER 4

BOTTOM INTERACTING ACOUSTIC PROPAGATION

4.1 Introduction

In the preceding models the ocean subbottom has been treated as a rigid body and therefore replaced by a boundary condition that the normal derivative of the pressure vanish at the ocean bottom. An alternative is to model the ocean subbottom as an elastic half-space, in which case one obtains an impedance condition requiring that some combination of the pressure and its normal derivative vanish. In either of these approaches, one may elect to declare the model's ocean bottom to lie beneath that of the true ocean bottom and therefore model a portion as a fluid layer. None of these approaches is entirely satisfactory for bottom-interacting modes, for they fail to take into account variations in both the P- and S-wave velocities in the ocean subbottom.

As noted in Chapter 1, a number of existing programs use coefficient approximation in the ocean, that is, the ocean is treated as a sequence of layers with, for instance, constant or linearly varying properties in each layer. Within each layer the problem is solved analytically. In this case, it is natural to extend these models by replacing the elastic subbottom by a sequence of layers with constant P- and S-wave velocities in each layer. This yields the so-called

Thomson-Haskell method and its variants (Schwab, 1981). A popular complaint about this method is that it is unphysical to use constant property layers for a medium in which the properties vary with depth. A similar complaint might be levelled against any numerical method, however in terms of other criteria such as simplicity, the Thomson-Haskell methods fall short; the propagator matrices are 4x4 or 5x5 when compounded and the individual elements are complicated combinations of transcendental functions.

In Chapter 2, we presented an alternate model for the ocean based on finite differences combined with Richardson extrapolation, which we concluded possessed the two desirable properties of efficiency and simplicity. In this chapter, we describe a simple extension of this technique to allow for coupling into an elastic subbottom with continuously varying P- and S-wave velocities. The governing equations are presented in Section 4.2, followed by a description of the modifications in Section 4.3. In Section 4.4, we present the results of two test problems to demonstrate its performance. The first problem is a shallow water scenario with a soft bottom. The second is a deep water scenario with a Munk sound speed profile in the ocean (Munk, 1974) and a linear profile for the P- and S-wave velocities in the subbottom. The significance of the elastic bottom is illustrated by comparing to the results to those obtained when the subbottom is modeled as a completely rigid body.

4.2 Formulation

After separating out an x and t dependence of the form $e^{i(kx-\omega t)}$ one obtains the following second-order differential equation for the pressure as a function of the depth variable z :

$$p'' + (\omega^2/c^2(z) - k^2)p = 0 \quad (4.1)$$

where ω is the angular frequency of the source and $c(z)$ is the sound speed. At the ocean surface the pressure vanishes:

$$p(0) = 0. \quad (4.2)$$

In the elastic subbottom the modal equation is fourth-order (Aki and Richards, 1980):

$$\begin{bmatrix} r_1 \\ r_2 \\ r_3 \\ r_4 \end{bmatrix}' = \begin{bmatrix} 0 & -1 & 1/(\rho c_s^2) & 0 \\ k^2(c_p^2 - 2c_s^2)/c_p^2 & 0 & 0 & 1/(\rho c_p^2) \\ k^2 t(z) - \omega^2 \rho & 0 & 0 & -(c_p^2 - 2c_s^2)/c_p^2 \\ 0 & -\omega^2 \rho & k^2 & 0 \end{bmatrix} \begin{bmatrix} r_1 \\ r_2 \\ r_3 \\ r_4 \end{bmatrix} \quad (4.3)$$

where,

$$t(z) = \rho [c_p^4 - (c_p^2 - 2c_s^2)^2] / c_p^2 \quad (4.4)$$

and,

$$\begin{aligned} r_1 &= u/ik, \\ r_2 &= w, \\ r_3 &= \tau_{zx}/ik, \end{aligned} \quad (4.5)$$

$$r_4 = \tau_{zz}.$$

The quantities u , w , τ_{zz} and τ_{zx} denote the x displacement, z displacement, normal stress and tangential stress respectively. In addition c_p , c_s and ρ are the P-wave speed, S-wave speed and density respectively. At the interface, we require that w , τ_{zz} and τ_{zx} be continuous:

$$\begin{aligned} r_2(D_1) &= p'(D_1)/\omega^2, \\ r_3(D_1) &= 0, \\ r_4(D_1) &= -p(D_1), \end{aligned} \tag{4.6}$$

where D_1 is the depth of the ocean. The subbottom of thickness D_2 is terminated with a completely rigid basement at which the normal and tangential displacements must vanish:

$$\begin{aligned} r_1(D_1 + D_2) &= 0, \\ r_2(D_1 + D_2) &= 0. \end{aligned} \tag{4.7}$$

4.3 The Method

The modal equation in the ocean is treated in the same fashion as in Chapter 2 with the exception that the rigid bottom boundary condition is replaced by an impedance condition of the form $f(k^2)p + g(k^2)p' = 0$, where $f(k^2)$ and $g(k^2)$ are for the moment undefined functions which depend on the properties of the elastic subbottom. We divide the interval $[0, D_1]$ into N_1 equal subintervals by the points $z_i = ih_1$, $i = 0, 1, \dots, N_1$ where the mesh width $h_1 = D_1/N_1$. Then using the standard

three-point difference approximation to the second derivative in (4.1) and the centered difference approximation to the first derivative in the impedance condition we obtain the algebraic eigenvalue problem

$$A(k^2)\underline{p}=0 \tag{4.8}$$

as an approximation to the eigenvalue problem (4.1)-(4.7). Here \underline{p} is the N_1 -dimensional vector with components p_1, p_2, \dots, p_{N_1} . The tridiagonal matrix A is given by

$$A = \begin{bmatrix} a_1 - h_1^2 k^2 & 1 & & & \\ 1 & a_2 - h_1^2 k^2 & 1 & & \\ & \diagdown & \diagdown & \diagdown & \\ \bigcirc & & & & \\ & & & & \bigcirc \\ & & & 1 & a_{N_1-1} - h_1^2 k^2 & 1 \\ & & & 2g(k^2) & g(k^2)(a_{N_1} - h_1^2 k^2) - 2h_f(k^2) & \end{bmatrix} \tag{4.9}$$

where the coefficients a_i are defined by

$$a_i = 2 - h_1^2 \omega^2 / c^2(z_i), \quad i=1,2,\dots,N_1. \tag{4.10}$$

Now, suppose \underline{r} and \underline{s} are two linearly independent solutions obtained by integrating the modal equations in the elastic subbottom from the rigid basement up to the interface with initial conditions given by

$$\begin{aligned} \underline{r}(D_1 + D_2) &= (0, 0, 1, 0), \\ \underline{s}(D_1 + D_2) &= (0, 0, 0, 1). \end{aligned} \tag{4.11}$$

If k^2 is to be an eigenvalue then it must be possible to form a linear combination, $\underline{A}r + \underline{B}s$, of these solutions satisfying the interface conditions at $z=D_1$, that is,

$$\begin{bmatrix} r_2 & s_2 \\ r_3 & s_3 \\ r_4 & s_4 \end{bmatrix} \begin{bmatrix} A \\ B \end{bmatrix} = \begin{bmatrix} p'/\omega^2 \\ 0 \\ -p \end{bmatrix} \quad (4.12)$$

In order for a solution to exist we must have

$$\omega^2 [r_2 s_3 - r_3 s_2] p - [r_3 s_4 - r_4 s_3] p' = 0. \quad (4.13)$$

Thus, in principle the functions $f(k^2)$ and $g(k^2)$ might be computed by integrating (4.3) twice from the rigid layer up to the interface with different initial condition. In practice the \underline{r} and \underline{s} functions so computed have a tendency to become linearly dependent. This difficulty is readily resolved by the compound matrix method (Ng and Reid, 1979; Gilbert and Backus, 1966). We introduce the following variables:

$$\begin{aligned} Y_1 &= r_1 s_2 - r_2 s_1 \\ Y_2 &= r_3 s_4 - r_4 s_3 \\ Y_3 &= r_1 s_3 - r_3 s_1 \\ Y_4 &= -(r_2 s_3 - r_3 s_2) \\ Y_5 &= -(r_1 s_4 - r_4 s_1) \\ Y_6 &= -(r_2 s_4 - r_4 s_2) \end{aligned} \quad (4.14)$$

Evidently $f(k^2)$ is identified with $\omega^2 Y_4$ and $g(k^2)$ with Y_2 . By differentiating these equations and using (4.3) to eliminate the

derivatives of \underline{r} and \underline{s} that appear, one obtains the following differential equation satisfied by \underline{Y} :

$$\begin{bmatrix} Y_1 \\ Y_2 \\ Y_3 \\ Y_4 \\ Y_5 \end{bmatrix}' = \begin{bmatrix} 0 & 0 & 0 & 1/(\rho c_s^2) & -1/(\rho c_p^2) \\ 0 & 0 & 0 & -\omega^2 \rho & -[k^2 t(z) - \omega^2 \rho] \\ 0 & 0 & 0 & 1 & (c_p^2 - 2c_s^2)/c_p^2 \\ k^2 t(z) - \omega^2 \rho & 1/(\rho c_p^2) & -k^2(c_p^2 - 2c_s^2)/c_p^2 & 0 & 0 \\ \omega^2 \rho & -1/(\rho c_s^2) & -2k^2 & 0 & 0 \end{bmatrix} \begin{bmatrix} Y_1 \\ Y_2 \\ Y_3 \\ Y_4 \\ Y_5 \end{bmatrix} \quad (4.15)$$

The differential equation for Y_6 reduces to $Y_6 = -k^2 Y_4$ and has been eliminated from this system. The initial conditions for these equations are obtained by substituting those for \underline{r} and \underline{s} into the definition of \underline{Y} :

$$\begin{aligned} Y_1(D_1 + D_2) &= 0, \\ Y_2(D_1 + D_2) &= 1, \\ Y_3(D_1 + D_2) &= 0, \\ Y_4(D_1 + D_2) &= 0, \\ Y_5(D_1 + D_2) &= 0. \end{aligned} \quad (4.16)$$

The differential equations are then integrated using the modified midpoint method (Burlisch, 1966; Dahlquist, 1974) which is an explicit second-order integrator for first order systems of the form $Y' = f(z, Y)$ and is given by

$$\begin{aligned} y_0 &= y(z_0), \\ y_1 &= y_0 + h_2 f(z_0, y_0), \\ y_{i+1} &= y_{i-1} + 2h_2 f(z_i, y_i), \quad i=1, 2, \dots, N_2 \end{aligned}$$

$$Y_i = (y_{i-1} + 2y_i + y_{i+1})/4, \quad \text{for } i \text{ even.} \quad (4.17)$$

This final step is a filter required to stabilize the integration. Since we are only interested in the values of the functions at the terminal point at $z=D_1$ we need only filter at that point. The number of subintervals in the subbottom, N_2 , must be even.

Now that $f(k^2)$ and $g(k^2)$ are defined we may proceed with the solution of the eigenvalue problem. For a given k^2 we compute the coefficients of the impedance condition and then the determinant $d(k^2)$ of (4.9) via the following recursion,

$$\begin{aligned} p_0 &= 0, \\ p_1 &= 1, \\ p_i &= (a_i - h_1^2 k^2) p_{i-1} - p_{i-2}, \quad i=2, \dots, N_1-1 \\ d(k^2) &= [g(k^2)(a_{N_1} - h^2 k^2) + 2hf(k^2)] p_{N_1-1} - 2g(k^2) p_{N_1-2}. \end{aligned} \quad (4.18)$$

This is equivalent to shooting down from the ocean surface to the interface and computing $f(k^2)p(D_1) - g(k^2)p'(D_1)$. Subsequently k^2 is adjusted such that $d(k^2)$ vanishes using some root finder. We have elected to use the secant method.

If an initial guess is not available then it is desirable to have a procedure for systematically producing all of the eigenvalues corresponding to right-travelling propagating modes, i.e., positive real k^2 . When the impedance condition is simple, as it was for the completely rigid bottom model treated in Chapter 2, a bisection

procedure can be devised based on the number of zeros in the eigenfunctions. For more complicated interface conditions, it is not clear how to generalize this procedure. We note that a more conventional generalized eigenvalue problem of the form $A_p = k^2 B_p$ is readily obtained by merely incorporating difference equations for (4.3) into the matrix. The Sturm sequence method has been extended to this case, provided A and B are symmetric and B is positive definite (Wilkinson, 1962). A and B are readily symmetrized but the existence of complex eigenvalues k^2 for many simple problems, e.g., elastic waves in plates, suggests that it will not in general be possible to produce a positive definite B at the same time.

An alternate procedure, which we have used in our test problems, is to apply the secant method beginning at a $k = k_{\max}$ equal to the upper bound on the eigenvalues. A good estimate for k_{\max} may be obtained from $\omega / \min(c, c_p, c_s)$. It can be shown that when the roots are real the secant method will converge to the largest root. It has also been shown that if the shift suggested by the secant method at each step is doubled then the secant method can at most cross over one root. Thus when the sign changes one can switch back to the standard secant method and still be assured of convergence to the desired root (Wilkinson, 1965). The next largest root is in turn found by deflating all previous known roots. The deflation is accomplished by returning the determinant with known roots divided out as follows

$$d(k^2) = d(k^2) \left[\prod_j k_j^2 / (k^2 - k_j^2) \right]. \quad (4.19)$$

As in the previous problems, we have applied Richardson extrapolation to increase the accuracy in the eigenvalues. Thus we solve the eigenvalue problem (4.8) at several meshes and extrapolate to zero mesh width using a polynomial fit of the form

$$k_j^2(h) = b_0 + b_2 h^2 + b_4 h^4 + \dots \quad (4.20)$$

In general, $k_j^2(h)$ would be a bivariate polynomial involving the mesh width in the ocean and the mesh width in the subbottom. However, we refine both meshes simultaneously, maintaining the proportions of the two mesh widths, and thus the polynomial is reduced to a univariate form. In (4.20), b_0 is the Richardson approximation to the j th eigenvalue of (4.8) and is computed recursively as described in Chapter 2. We shall denote this Richardson approximation corresponding to the meshes h_p, h_{p+1}, \dots, h_q by $k_j^2(p, \dots, q)$ as usual. As before, we also use the extrapolation procedure to produce an initial guess at a refined mesh, thereby bypassing the deflation procedure.

Once the eigenvalues have been computed to the desired accuracy, the eigenfunctions may be found by an inverse iteration (Wilkinson, 1965) of the form $A(k^2) \underline{p}^{l+1} = \underline{p}^l$ starting with $\underline{p}^0 = 1$. For the purpose of computing propagation loss this spares the expense of computing unnecessary eigenfunctions in the elastic subbottom. If, on the other hand eigenfunctions are desired in the elastic subbottom, it is

probably best to incorporate difference equations for the elastic subbottom into the matrix and apply inverse iteration to the entire matrix. For our computations of the eigenfunctions we have used the Trapezoidal method to obtain difference equations in the subbottom. All of the previously described techniques may be applied to this alternative formulation, yielding a more complicated but approximately as efficient method. We note that it is possible to derive a set of differential equations for the compound matrix method, which can be integrated backwards once from the interface to produce the eigenfunctions (Ng and Reid, 1979). However, these equations are exact for an exact forward integration and it is not clear what the effect of using discretized solutions is on the accuracy of the reverse integration.

4.4 Applications of the Method

We now present two applications of our method to demonstrate its performance. In the first problem we consider a shallow water environment with a constant sound speed of 1500m/s in the ocean and S- and P-wave speeds of 700m/s and 1700m/s respectively in the subbottom. The ocean depth is 300m and has a density of 1gm/cm^3 while the subbottom has a depth of 200m and a density of 2gm/cm^3 . The circular frequency is $\omega=30\pi/\text{s}$.

The numerically determined eigenvalues and corresponding errors are

presented in Table 4.1. The exact eigenvalues for this problem were determined by a compound matrix formulation of the Thomson-Haskell method. The error table reflects the second order convergence of the scheme in that a doubling of the number of mesh points reduces the error by a factor of about 4. The extrapolations and their errors are presented in Table 4.2. In contrast to the unextrapolated eigenvalues, the errors are reduced by as much as a factor of 1000 with each extrapolation. The quantity ET in these tables is the execution time required on the Northwestern Cyber 170/730 to compute all the given eigenvalues for the indicated mesh width. The row labelled " N_1/N_2 " contains the number of subintervals in the ocean over the number of subintervals in the subbottom.

In Figures 4.1-4.3 we have graphed the eigenfunctions for modes 3,9 and 15. Note the scaling information in the figure captions. The eigensolution (p, r_1, r_2, r_3, r_4) has been scaled such that $\max |p(z)|=1$. These modes are representative of three classes of modes which exist for this problem. The first class, modes 1-7, are seismic modes, i.e., modes which have phase velocities less than the sound speed in the ocean and are consequently evanescent in the ocean. The second class of modes, modes 8-10, have a phase velocity greater than both the S-wave speed in the subbottom and the sound speed in the ocean but less than the P-wave speed in the subbottom. These modes are oscillatory in the ocean but only the S-wave component is oscillatory

in the subbottom. The third class of modes, modes 11-18, have a phase speed greater than the S- or P-wave speeds in both the ocean and the subbottom and are therefore oscillatory throughout the region.

The second example that we consider is an ocean with a Munk sound speed profile overlying a relatively rigid subbottom with linearly increasing S- and P-wave speeds. The parameter values for the Munk profile are those previously employed in Chapters 2 and 3. Thus we have,

$$\begin{aligned}
 \omega &= 8\pi/s \\
 D_1 &= 5000\text{m}, \\
 D_2 &= 1000\text{m}, \\
 c(x) &= 1500[1 + 0.00737(x-1+e^{-x})] \text{ m/s}, \quad x = 2(z-1300)/1300, \\
 c_p(z) &= 4700 + 100(z-D_1)/D_2 \text{ m/s}, \\
 c_s(z) &= 2000 + 100(z-D_1)/D_2 \text{ m/s}.
 \end{aligned}
 \tag{4.21}$$

In Table 4.3 we have displayed the eigenvalues and their errors at several meshes. Successive extrapolations and their errors are given in Table 4.4. The column labelled "exact" was obtained by our program using higher-order extrapolation. For this problem there exists 8 classes of modes including an interfacial mode characterized by evanescence away from the interface. Representatives of some of these classes of modes are graphed in Figures 4.4-4.6.

The significance of the elastic bottom is illustrated in Table 4.5 in which we have presented the eigenvalues for this problem and the

eigenvalues for a problem with the same sound speed profile in the ocean but with the subbottom modeled as a perfectly rigid medium. Naturally, there is no equivalent for the interface mode. Modes 2-6, which are trapped in the duct of the Munk profile are largely unaffected by the subbottom model as expected. In contrast, the highest-order modes of the two models appear to be completely unrelated. These results suggest that even with relatively rigid ocean bottoms, significant energy may be coupled into the subbottom by modes which are not trapped in an oceanic duct.

CHAPTER 5

CONCLUSIONS

We now consider possible modifications, improvements and extensions of the method. The time required to solve for the eigenvalues at a given mesh might conceivably be reduced by using a different root finder. Since most program libraries provide a variety of root finders, it is in principle, a simple matter to compare each of them on several test problems. In view of the different classes of modes present in a typical ocean acoustic scenario e.g., modes trapped in internal ducts (RR modes) and boundary interacting modes (RSRBR modes), and the concomitant changes in the local behavior of the determinant, it would not be surprising if one root finder performed better for one class of modes and another for another class. Thus a more sophisticated code might automatically select the optimal root finder. In regard to the choices of the secant and the Newton root finders, we note that the Newton method is better behaved for extremely small tolerances than the secant method (Wilkinson, 1965) in that, the secant method may shoot off unpredictably if too small a tolerance is specified. On the other hand, the derivative required by Newton's method may not always be readily computable in which case the secant method is attractive. In terms of the efficiency of the two methods, asymptotic formulas suggest that the secant method is superior, though in limited testing for the stationary medium problem we found this not to be the case.

It is tempting to employ variable-order extrapolation in yet a third manner in the method by using it to compute a root. (The secant method would then be a special case of this root finder.) We have done some experiments with this root finder and obtained favorable results. It should be borne in mind that the expense of computing the function for which the zeros are required, i.e., the determinant of the matrix of difference equations, justifies a considerable expenditure of effort to reduce the number of function calls.

The use of a polynomial fit to the eigenvalues as a function of the mesh width is historically the most popular as well as the most obvious choice, though there is certainly no necessity to restrict oneself to this form. Indeed, the widely used GBS method (Burlisch and Stoer, 1966) for solving initial value problems employs a rational polynomial or Pade approximant. For the initial value problem it has often been stated that this approach is superior and occasionally evidence has been presented to support this. We have performed limited testing on an isovelocity problem and found insignificant differences, though additional testing is certainly merited.

Borrowing further from the experience of initial value problem solvers raises the question of whether an uneven mesh might be more efficient. For the stationary problem treated in Chapter 2, the properties of the solution are sufficiently well understood that it would be a simple

matter to automatically select an uneven mesh for each mode or for groups of modes, with a finer mesh where the oscillation is greatest. By tabulating the sound speed for the finest mesh, the expense of setting up the matrix may be reduced. The use of artificial internal boundaries for the computation of internally trapped modes (RR modes) may also be employed, as suggested by Ferla, Jensen and Kuperman (1982).

The elastic problem of Chapter 4 presents a number of new features. Like the convected acoustic equation treated in Chapter 3, there may exist backward travelling modes, i.e., modes with phase and group velocities of opposite sign. In addition, there may exist modes with a cut-off frequency corresponding to a non-zero wavenumber. The deflation technique has performed well in the test problems considered though it would be desirable to generalize the Sturm sequence method and with it gain the ability to efficiently select out specified modes. It is interesting to note that although the Sturm sequence procedure has not been extended to the arbitrary generalized algebraic eigenvalue problem, it is possible to obtain this information for an arbitrary polynomial via the Routh-Hurwitz theory. In principle this immediately implies a technique for treating the algebraic eigenvalue problem by constructing the characteristic polynomial. In practice the computation of the characteristic polynomial is both expensive and unstable (Wilkinson, 1965). Nevertheless, the duality of the problems

suggests that an effective Sturm sequence procedure might be obtained for the generalized algebraic eigenvalue problem. Such a procedure is important not just to computing elastic normal modes, but also to problems in hydrodynamic stability, vibrations of structures and a variety of other problems.

Finally, we note that the programs may be readily modified to accommodate multiple interfaces or a depth dependent density. Absorption may also be included in the usual manner either a priori by introducing an imaginary component in the sound speed profile or a posteriori via a perturbation technique. Alternatively, absorption might be included by employing a viscoelastic or porous viscoelastic model. We also note that if an eigenvalue is to be computed with an accuracy very close to the machine precision then the difference schemes should be implemented in "summed-form" (Dahlquist and Bjorck, 1974; Friar, 1978). That is, the three-point recursions corresponding to the second-order modal equations, should be reduced to two two-point recursions corresponding to a pair of first-order equations.

Table 2.1a Numerical eigenvalues $K^2(p)=10^4 x k^2(p)$
for the Mathieu problem.

N=	23	27	34	43	
ET=	.0320	.0150	.0150	.0280	
j	$K^2(1)$	$K^2(2)$	$K^2(3)$	$K^2(4)$	"Exact"
1	2.4852984161	2.4852970550	2.4852957256	2.4852948750	2.4852934565
2	2.4001782107	2.4000917631	2.4000072419	2.3999531269	2.3998628016
3	2.2423687693	2.2417064749	2.2410580514	2.2406424340	2.2399479099
4	2.0092366186	2.0067094600	2.0042301876	2.0026384386	1.9999739573
5	1.7051683913	1.6983223636	1.6915877916	1.6872545372	1.6799843748
6	1.3358389303	1.3207261614	1.3058087319	1.2961839183	1.2799895833
7	0.9081312255	0.8790302449	0.8501873622	0.8315161183	0.7999925595
8	0.4300138418	0.3792089530	0.3286120258	0.2957314732	0.2399944196

Table 2.1b Errors in numerical eigenvalues $e(p)=k^2-k^2(p)$
for the Mathieu problem.

N=	23	27	34	43
ET=	.0320	.0150	.0150	.0280
j	$e(1)$	$e(2)$	$e(3)$	$e(4)$
1	-4.9E-10	-3.5E-10	-2.2E-10	-1.4E-10
2	-3.1E-08	-2.2E-08	-1.4E-08	-9.0E-09
3	-2.4E-07	-1.7E-07	-1.1E-07	-6.9E-08
4	-9.2E-07	-6.7E-07	-4.2E-07	-2.6E-07
5	-2.5E-06	-1.8E-06	-1.1E-06	-7.2E-07
6	-5.5E-06	-4.0E-06	-2.5E-06	-1.6E-06
7	-1.0E-05	-7.9E-06	-5.0E-06	-3.1E-06
8	-1.9E-05	-1.3E-05	-8.8E-06	-5.5E-06

Table 2.2a Standard extrapolations $K^2(p, \dots, q) = 10^4 x k^2(p, \dots, q)$
for the Mathieu problem.

N=	23	27	34	43	
ET=	.0320	.0150	.0150	.0280	
j	$K^2(1)$	$K^2(1,2)$	$K^2(1,2,3)$	$K^2(1,2,3,4)$	"Exact"
1	2.4852984161	2.4852934551	2.4852934565	2.4852934565	2.4852934565
2	2.4001782107	2.3998631090	2.3998628018	2.3998628016	2.3998628016
3	2.2423687693	2.2399547064	2.2399479167	2.2399479099	2.2399479099
4	2.0092366186	2.0000251255	1.9999740544	1.9999739574	1.9999739573
5	1.7051683913	1.6802146202	1.6799850911	1.6799843756	1.6799843748
6	1.3358389303	1.2807528877	1.2799931252	1.2799895894	1.2799895833
7	0.9081312255	0.8020581510	0.8000059517	0.7999925926	0.7999925595
8	0.4300138418	0.2448300221	0.2400362101	0.2399945583	0.2399944196

Table 2.2b Errors in standard extrapolations $e(p, \dots, q) = k^2 - K^2(p, \dots, q)$
for the Mathieu problem.

N=	23	27	34	43
ET=	.0320	.0150	.0150	.0280
j	$e(1)$	$e(1,2)$	$e(1,2,3)$	$e(1,2,3,4)$
1	-4.9E-10	1.3E-13	-3.1E-16	6.2E-17
2	-3.1E-08	-3.0E-11	-1.5E-14	-4.9E-17
3	-2.4E-07	-6.7E-10	-6.8E-13	-7.8E-17
4	-9.2E-07	-5.1E-09	-9.7E-12	-5.7E-15
5	-2.5E-06	-2.3E-08	-7.1E-11	-8.0E-14
6	-5.5E-06	-7.6E-08	-3.5E-10	-6.1E-13
7	-1.0E-05	-2.0E-07	-1.3E-09	-3.3E-12
8	-1.9E-05	-4.8E-07	-4.1E-09	-1.3E-11

Table 2.3a Modified extrapolations $\hat{k}^2(p, \dots, q) = 10^4 x \hat{k}^2(p, \dots, q)$
for the Mathieu problem.

N=	23	27	34	43	
ET=	.0320	.0150	.0150	.0280	
j	$\hat{k}^2(1)$	$\hat{k}^2(1,2)$	$\hat{k}^2(1,2,3)$	$\hat{k}^2(1,2,3,4)$	"Exact"
1	2.4852945298	2.4852934547	2.4852934565	2.4852934564	2.4852934565
2	2.3998638124	2.3998627897	2.3998628017	2.3998628016	2.3998628016
3	2.2399488826	2.2399478790	2.2399479102	2.2399479099	2.2399479099
4	1.9999749911	1.9999738957	1.9999739585	1.9999739573	1.9999739573
5	1.6799854735	1.6799842687	1.6799843781	1.6799843747	1.6799843748
6	1.2799907614	1.2799894157	1.2799895911	1.2799895831	1.2799895833
7	0.7999938374	0.7999923086	0.7999925757	0.7999925589	0.7999925595
8	0.2399958237	0.2399940563	0.2399944510	0.2399944182	0.2399944196

Table 2.3b Errors in modified extrapolations $\hat{e}(p, \dots, q) = k^2 - \hat{k}^2(p, \dots, q)$
for the Mathieu problem.

N=	23	27	34	43
ET=	.0320	.0150	.0150	.0280
j	$\hat{e}(1)$	$\hat{e}(1,2)$	$\hat{e}(1,2,3)$	$\hat{e}(1,2,3,4)$
1	-1.0E-10	1.7E-13	-3.1E-16	7.9E-17
2	-1.0E-10	1.1E-12	-4.7E-15	-5.5E-17
3	-9.7E-11	3.0E-12	-3.1E-14	1.6E-16
4	-1.0E-10	6.1E-12	-1.1E-13	1.1E-15
5	-1.0E-10	1.0E-11	-3.3E-13	5.4E-15
6	-1.1E-10	1.6E-11	-7.7E-13	1.8E-14
7	-1.2E-10	2.5E-11	-1.6E-12	5.4E-14
8	-1.4E-10	3.6E-11	-3.1E-12	1.3E-13

Table 2.4a Numerical eigenvalues $K^2(p)=10^3 x k^2(p)$
for the Munk profile.

N=	268	321	402	509	
ET=	2.8570	1.5820	1.6980	1.5970	
j	$K^2(1)$	$K^2(2)$	$K^2(3)$	$K^2(4)$	"Exact"
1	3.3563831469	3.3563827650	3.3563824465	3.3563822357	3.3563818863
5	3.2991005678	3.2990875105	3.2990766285	3.2990694272	3.2990574928
9	3.2470718156	3.2470319752	3.2469987862	3.2469768297	3.2469404541
13	3.1987746315	3.1986976127	3.1986334761	3.1985910580	3.1985208041
17	3.1541731417	3.1540630239	3.1539713960	3.1539108309	3.1538105814
21	3.1043750682	3.1041172179	3.1039021779	3.1037597972	3.1035237024
25	3.0368104016	3.0362991701	3.0358725646	3.0355899767	3.0351211679
29	2.9559009269	2.9549819056	2.9542144804	2.9537058630	2.9528616052
33	2.8625216362	2.8609843054	2.8596996200	2.8588477113	2.8574327908
37	2.7571242285	2.7546959557	2.7526651520	2.7513176737	2.7490782651
41	2.6400582045	2.6363970543	2.6333325835	2.6312979477	2.6279142481
45	2.5116449357	2.5063325887	2.5018819615	2.4989249576	2.4940037256
49	2.3722043890	2.3647393182	2.3584789923	2.3543165264	2.3473836367
53	2.2220665844	2.2118575377	2.2032869781	2.1975838839	2.1880769223
57	2.0615768883	2.0479367091	2.0364726412	2.0288375714	2.0160984812
61	1.8910984691	1.8732382827	1.8582091552	1.8481905627	1.8314583468
65	1.7110133199	1.6880371097	1.6686777826	1.6557599982	1.6341634845
69	1.5217225003	1.4926220974	1.4680687700	1.4516681825	1.4242188553
73	1.3236459219	1.2872964304	1.2565818235	1.2360431692	1.2016280725
77	1.1172218518	1.0723775297	1.0344263343	1.0090191031	0.9663938189
81	0.9029062294	0.8481968444	0.8018214513	0.7707364133	0.7185181212
85	0.6811718530	0.6150995309	0.5589960529	0.5213419139	0.4580025336
89	0.4525074705	0.3734440531	0.3061886513	0.2609888410	0.1848482642

Table 2.4b Errors in numerical eigenvalues $e(p)=k^2-k^2(p)$
for the Munk profile.

N=	268	321	402	509
ET=	2.8570	1.5820	1.6980	1.5970
j	e(1)	e(2)	e(3)	e(4)
1	-1.2E-09	-8.7E-10	-5.6E-10	-3.4E-10
5	-4.3E-08	-3.0E-08	-1.9E-08	-1.1E-08
9	-1.3E-07	-9.1E-08	-5.8E-08	-3.6E-08
13	-2.5E-07	-1.7E-07	-1.1E-07	-7.0E-08
17	-3.6E-07	-2.5E-07	-1.6E-07	-1.0E-07
21	-8.5E-07	-5.9E-07	-3.7E-07	-2.3E-07
25	-1.6E-06	-1.1E-06	-7.5E-07	-4.6E-07
29	-3.0E-06	-2.1E-06	-1.3E-06	-8.4E-07
33	-5.0E-06	-3.5E-06	-2.2E-06	-1.4E-06
37	-8.0E-06	-5.6E-06	-3.5E-06	-2.2E-06
41	-1.2E-05	-8.4E-06	-5.4E-06	-3.3E-06
45	-1.7E-05	-1.2E-05	-7.8E-06	-4.9E-06
49	-2.4E-05	-1.7E-05	-1.1E-05	-6.9E-06
53	-3.3E-05	-2.3E-05	-1.5E-05	-9.5E-06
57	-4.5E-05	-3.1E-05	-2.0E-05	-1.2E-05
61	-5.9E-05	-4.1E-05	-2.6E-05	-1.6E-05
65	-7.6E-05	-5.3E-05	-3.4E-05	-2.1E-05
69	-9.7E-05	-6.8E-05	-4.3E-05	-2.7E-05
73	-1.2E-04	-8.5E-05	-5.4E-05	-3.4E-05
77	-1.5E-04	-1.0E-04	-6.8E-05	-4.2E-05
81	-1.8E-04	-1.2E-04	-8.3E-05	-5.2E-05
85	-2.2E-04	-1.5E-04	-1.0E-04	-6.3E-05
89	-2.6E-04	-1.8E-04	-1.2E-04	-7.6E-05

Table 2.5a Standard extrapolations $K^2(p, \dots, q) = 10^3 x k^2(p, \dots, q)$
for the Munk profile.

N=	268	321	402	509	
ET=	2.8570	1.5820	1.6980	1.5970	
j	$K^2(1)$	$K^2(1,2)$	$K^2(1,2,3)$	$K^2(1,2,3,4)$	"Exact"
1	3.3563831469	3.3563818862	3.3563818863	3.3563818863	3.3563818863
5	3.2991005678	3.2990574681	3.2990574929	3.2990574928	3.2990574928
9	3.2470718156	3.2469403105	3.2469404543	3.2469404541	3.2469404541
13	3.1987746315	3.1985204080	3.1985208050	3.1985208041	3.1985208041
17	3.1541731417	3.1538096651	3.1538105878	3.1538105814	3.1538105814
21	3.1043750682	3.1035239564	3.1035237062	3.1035237024	3.1035237024
25	3.0368104016	3.0351229296	3.0351211782	3.0351211679	3.0351211679
29	2.9559009269	2.9528674236	2.9528616278	2.9528616051	2.9528616052
33	2.8625216362	2.8574472183	2.8574328376	2.8574327907	2.8574327908
37	2.7571242285	2.7491089916	2.7490783589	2.7490782648	2.7490782651
41	2.6400582045	2.6279734887	2.6279144302	2.6279142476	2.6279142481
45	2.5116449357	2.4941099533	2.4940040683	2.4940037247	2.4940037256
49	2.3722043890	2.3475637009	2.3473842622	2.3473836354	2.3473836367
53	2.2220665844	2.1883685870	2.1880780292	2.1880769204	2.1880769223
57	2.0615768883	2.0165534170	2.0161003820	2.0160984785	2.0160984812
61	1.8910984691	1.8321456080	1.8314615196	1.8314583437	1.8314583468
65	1.7110133199	1.6351734994	1.6341686402	1.6341634815	1.6341634845
69	1.5217225003	1.4256679591	1.4242270274	1.4242188537	1.4242188553
73	1.3236459219	1.2036636063	1.2016407305	1.2016280748	1.2016280725
77	1.1172218518	0.9691998193	0.9664130130	0.9663938298	0.9663938189
81	0.9029062294	0.7223216203	0.7185466617	0.7185181483	0.7185181212
85	0.6811718530	0.4630804878	0.4580442121	0.4580025889	0.4580025336
89	0.4525074705	0.1915351288	0.1849081234	0.1848483664	0.1848482642

Table 2.5b Errors in standard extrapolations $e(p, \dots, q) = k^2 - k^2(p, \dots, q)$
for the Munk profile.

N=	268	321	402	509
ET=	2.8570	1.5820	1.6980	1.5970
j	e(1)	e(1,2)	e(1,2,3)	e(1,2,3,4)
1	-1.2E-09	1.4E-13	-1.2E-15	-1.1E-15
5	-4.3E-08	2.4E-11	-2.0E-14	3.6E-16
9	-1.3E-07	1.4E-10	-2.0E-13	2.7E-16
13	-2.5E-07	3.9E-10	-8.3E-13	7.3E-16
17	-3.6E-07	9.1E-10	-6.3E-12	-2.8E-15
21	-8.5E-07	-2.5E-10	-3.7E-12	9.5E-15
25	-1.6E-06	-1.7E-09	-1.0E-11	2.6E-14
29	-3.0E-06	-5.8E-09	-2.2E-11	6.5E-14
33	-5.0E-06	-1.4E-08	-4.6E-11	1.4E-13
37	-8.0E-06	-3.0E-08	-9.3E-11	2.8E-13
41	-1.2E-05	-5.9E-08	-1.8E-10	5.1E-13
45	-1.7E-05	-1.0E-07	-3.4E-10	8.6E-13
49	-2.4E-05	-1.8E-07	-6.2E-10	1.3E-12
53	-3.3E-05	-2.9E-07	-1.1E-09	1.9E-12
57	-4.5E-05	-4.5E-07	-1.9E-09	2.6E-12
61	-5.9E-05	-6.8E-07	-3.1E-09	3.1E-12
65	-7.6E-05	-1.0E-06	-5.1E-09	3.0E-12
69	-9.7E-05	-1.4E-06	-8.1E-09	1.6E-12
73	-1.2E-04	-2.0E-06	-1.2E-08	-2.3E-12
77	-1.5E-04	-2.8E-06	-1.9E-08	-1.0E-11
81	-1.8E-04	-3.8E-06	-2.8E-08	-2.7E-11
85	-2.2E-04	-5.0E-06	-4.1E-08	-5.5E-11
89	-2.6E-04	-6.6E-06	-5.9E-08	-1.0E-10

Table 2.6a Modified extrapolations $\hat{K}^2(p, \dots, q) = 10^3 x k^2(p, \dots, q)$
for the Munk profile.

N=	268	321	402	509	
ET=	2.8570	1.5820	1.6980	1.5970	
j	$\hat{K}^2(1)$	$\hat{K}^2(1,2)$	$\hat{K}^2(1,2,3)$	$\hat{K}^2(1,2,3,4)$	"Exact"
1	3.3563831466	3.3563818862	3.3563818863	3.3563818863	3.3563818863
5	3.2990987142	3.2990574680	3.2990574929	3.2990574928	3.2990574928
9	3.2470482249	3.2469403051	3.2469404543	3.2469404541	3.2469404541
13	3.1986643410	3.1985203530	3.1985208050	3.1985208041	3.1985208041
17	3.1538384824	3.1538093742	3.1538105877	3.1538105814	3.1538105814
21	3.1035781970	3.1035228870	3.1035237057	3.1035237024	3.1035237024
25	3.0351860538	3.0351198159	3.0351211762	3.0351211679	3.0351211679
29	2.9529294489	2.9528597149	2.9528616209	2.9528616051	2.9528616052
33	2.8575023577	2.8574302840	2.8574328181	2.8574327906	2.8574327908
37	2.7491492323	2.7490750506	2.7490783095	2.7490782648	2.7490782651
41	2.6279865520	2.6279102271	2.6279143168	2.6279142475	2.6279142481
45	2.4940774047	2.4939987916	2.4940038278	2.4940037245	2.4940037256
49	2.3474587792	2.3473776755	2.3473837840	2.3473836349	2.3473836367
53	2.1881536448	2.1880698104	2.1880771289	2.1880769193	2.1880769223
57	2.0161769201	2.0160900849	2.0160987644	2.0160984763	2.0160984812
61	1.8315386543	1.8314485212	1.8314587278	1.8314583394	1.8314583468
65	1.6342458266	1.6341520712	1.6341639886	1.6341634732	1.6341634845
69	1.4243034120	1.4242056814	1.4242195130	1.4242188387	1.4242188553
73	1.2017150380	1.2016129481	1.2016289199	1.2016280485	1.2016280725
77	0.9664834027	0.9663765353	0.9663948991	0.9663937847	0.9663938189
81	0.7186105493	0.7184984482	0.7185194851	0.7185180734	0.7185181212
85	0.4580980504	0.4579802163	0.4580042413	0.4580024674	0.4580025336
89	0.1849471346	0.1848230202	0.1848503867	0.1848481739	0.1848482642

Table 2.6b Errors in modified extrapolations $\hat{e}(p, \dots, q) = k^2 - \hat{k}^2(p, \dots, q)$
for the Munk profile.

N=	268	321	402	509
ET=	2.8570	1.5820	1.6980	1.5970
j	$\hat{e}(1)$	$\hat{e}(1,2)$	$\hat{e}(1,2,3)$	$\hat{e}(1,2,3,4)$
1	-1.2E-09	1.4E-13	-1.2E-15	-1.1E-15
5	-4.1E-08	2.4E-11	-2.0E-14	3.6E-16
9	-1.0E-07	1.4E-10	-2.0E-13	3.6E-16
13	-1.4E-07	4.5E-10	-8.2E-13	8.3E-16
17	-2.7E-08	1.2E-09	-6.2E-12	-2.9E-15
21	-5.4E-08	8.1E-10	-3.2E-12	9.7E-15
25	-6.4E-08	1.3E-09	-8.3E-12	2.7E-14
29	-6.7E-08	1.8E-09	-1.5E-11	6.7E-14
33	-6.9E-08	2.5E-09	-2.7E-11	1.5E-13
37	-7.0E-08	3.2E-09	-4.4E-11	3.1E-13
41	-7.2E-08	4.0E-09	-6.8E-11	5.9E-13
45	-7.3E-08	4.9E-09	-1.0E-10	1.0E-12
49	-7.5E-08	5.9E-09	-1.4E-10	1.8E-12
53	-7.6E-08	7.1E-09	-2.0E-10	3.0E-12
57	-7.8E-08	8.3E-09	-2.8E-10	4.8E-12
61	-8.0E-08	9.8E-09	-3.8E-10	7.4E-12
65	-8.2E-08	1.1E-08	-5.0E-10	1.1E-11
69	-8.4E-08	1.3E-08	-6.5E-10	1.6E-11
73	-8.6E-08	1.5E-08	-8.4E-10	2.4E-11
77	-8.9E-08	1.7E-08	-1.0E-09	3.4E-11
81	-9.2E-08	1.9E-08	-1.3E-09	4.7E-11
85	-9.5E-08	2.2E-08	-1.7E-09	6.6E-11
89	-9.8E-08	2.5E-08	-2.1E-09	9.0E-11

Table 2.7a Numerical eigenvalues $K^2(p)=10^2 x k^2(p)$
for the double-duct problem.

N=	120	144	180	228	
ET=	.1670	.0980	.0910	.1000	
j	$K^2(1)$	$K^2(2)$	$K^2(3)$	$K^2(4)$	"Exact"
1	1.6526983271	1.6526954868	1.6526931649	1.6526916108	1.6526890414
2	1.6383354414	1.6383226852	1.6383122643	1.6383052931	1.6382937740
3	1.6341614265	1.6341595637	1.6341580406	1.6341570211	1.6341553353
4	1.6252176406	1.6251890186	1.6251656593	1.6251500439	1.6251242610
5	1.6225808340	1.6225727635	1.6225661692	1.6225617570	1.6225544651
6	1.6136840516	1.6136407010	1.6136053859	1.6135818105	1.6135429415
7	1.6122902279	1.6122728675	1.6122586894	1.6122492065	1.6122335402
8	1.6046798472	1.6046385327	1.6046050707	1.6045828295	1.6045463297
9	1.6032657934	1.6032334355	1.6032069338	1.6031891707	1.6031597588

Table 2.7b Errors in numerical eigenvalues $e(p)=k^2-k^2(p)$
for the double-duct problem.

N=	120	144	180	228
ET=	.1670	.0980	.0910	.1000
j	$e(1)$	$e(2)$	$e(3)$	$e(4)$
1	-9.2E-08	-6.4E-08	-4.1E-08	-2.5E-08
2	-4.1E-07	-2.8E-07	-1.8E-07	-1.1E-07
3	-6.0E-08	-4.2E-08	-2.7E-08	-1.6E-08
4	-9.3E-07	-6.4E-07	-4.1E-07	-2.5E-07
5	-2.6E-07	-1.8E-07	-1.1E-07	-7.2E-08
6	-1.4E-06	-9.7E-07	-6.2E-07	-3.8E-07
7	-5.6E-07	-3.9E-07	-2.5E-07	-1.5E-07
8	-1.3E-06	-9.2E-07	-5.8E-07	-3.6E-07
9	-1.0E-06	-7.3E-07	-4.7E-07	-2.9E-07

Table 2.8a Modified extrapolations $\hat{K}^2(p, \dots, q) = 10^2 x k^2(p, \dots, q)$
for the double-duct problem.

N=	120	144	180	228	
ET=	.1670	.0980	.0910	.1000	
j	$\hat{K}^2(1)$	$\hat{K}^2(1,2)$	$\hat{K}^2(1,2,3)$	$\hat{K}^2(1,2,3,4)$	"Exact"
1	1.6526983262	1.6526890318	1.6526890414	1.6526890414	1.6526890414
2	1.6383353701	1.6382936937	1.6382937742	1.6382937740	1.6382937740
3	1.6341608761	1.6341553299	1.6341553353	1.6341553353	1.6341553353
4	1.6252155264	1.6251239683	1.6251242621	1.6251242610	1.6251242610
5	1.6225750578	1.6225544197	1.6225544652	1.6225544651	1.6225544651
6	1.6136711647	1.6135421709	1.6135429443	1.6135429414	1.6135429415
7	1.6122650958	1.6122333952	1.6122335413	1.6122335402	1.6122335402
8	1.6046353141	1.6045445964	1.6045463398	1.6045463297	1.6045463297
9	1.6031923497	1.6031598105	1.6031597595	1.6031597588	1.6031597588

Table 2.8b Errors in modified extrapolations $\hat{\epsilon}(p, \dots, q) = k^2 - \hat{k}^2(p, \dots, q)$
for the double-duct problem.

N=	120	144	180	228
ET=	.1670	.0980	.0910	.1000
j	$\hat{\epsilon}(1)$	$\hat{\epsilon}(1,2)$	$\hat{\epsilon}(1,2,3)$	$\hat{\epsilon}(1,2,3,4)$
1	-9.2E-08	9.6E-11	-1.6E-13	-3.6E-15
2	-4.1E-07	8.0E-10	-2.3E-12	2.9E-14
3	-5.5E-08	5.3E-11	-7.1E-14	-2.9E-15
4	-9.1E-07	2.9E-09	-1.1E-11	3.5E-14
5	-2.0E-07	4.5E-10	-9.9E-13	0.
6	-1.2E-06	7.7E-09	-2.8E-11	2.3E-13
7	-3.1E-07	1.4E-09	-1.0E-11	-5.0E-14
8	-8.8E-07	1.7E-08	-1.0E-10	-1.4E-13
9	-3.2E-07	-5.1E-10	-6.5E-12	6.1E-13

Table 2.9 Comparison of execution times using different techniques to generate initial guesses.

Number of mesh points	268	321	402	509
Bisection	3.0	3.4	4.3	5.4
1 point RE	2.8	2.2	2.7	3.4
1 point MRE	2.8	1.5	1.9	2.4
N point RE	3.0	2.3	2.2	2.4
N point MRE	2.9	1.6	1.7	1.6

Table 3.1a Numerical eigenvalues $K(p)=100xk(p)$ for the Munk profile with a shear flow.

N=	77	92	115	146	
ET=	.5990	.2950	.3320	.3740	"Exact"
j	K(1)	K(2)	K(3)	K(4)	
1	1.6683910356	1.6683900317	1.6683891873	1.6683886180	1.6683876881
2	1.6561391651	1.6561344266	1.6561304410	1.6561277537	1.6561233648
3	1.6446288764	1.6446175231	1.6446079753	1.6446015384	1.6445910275
4	1.6339082100	1.6338892127	1.6338732459	1.6338624864	1.6338449252
5	1.6245773713	1.6245529575	1.6245324471	1.6245186302	1.6244960865
6	1.6146308702	1.6145837542	1.6145440886	1.6145173250	1.6144735835
7	1.6011227064	1.6010286247	1.6009493706	1.6008958698	1.6008083855
8	1.5844601893	1.5842931934	1.5841524299	1.5840573622	1.5839018298
9	1.5650044376	1.5647281245	1.5644950558	1.5643375649	1.5640797632
10	1.5428093778	1.5423750916	1.5420084983	1.5417606387	1.5413546617
11	1.5178372599	1.5171819688	1.5166283592	1.5162538167	1.5156399269
12	1.4900109981	1.4890545443	1.4882457513	1.4876981754	1.4867999970
13	1.4592255438	1.4578672391	1.4567174252	1.4559383404	1.4546593258
14	1.4253484436	1.4234628209	1.4218647112	1.4207808749	1.4189998084
15	1.3882160453	1.3856474504	1.3834674956	1.3819874827	1.3795526272
16	1.3476266485	1.3441821866	1.3412541901	1.3392638601	1.3359851289
17	1.3033303010	1.2987703811	1.2948868579	1.2922431553	1.2878813090
18	1.2550140114	1.2490392697	1.2439393376	1.2404615173	1.2347127099
19	1.2022800638	1.1945126259	1.1878643783	1.1833210798	1.1757938037
20	1.1446133203	1.1345688075	1.1259424751	1.1200317544	1.1102106641
21	1.0813299784	1.0683735441	1.0571983426	1.0495149799	1.0367004770
22	1.0114931761	0.9947660697	0.9802559212	0.9702338116	0.9534327835
23	0.9337648270	0.9120516611	0.8930654770	0.8798657902	0.8575717465
24	0.8461226163	0.8175847393	0.7923296454	0.7745922487	0.7442700035
25	0.7452526106	0.7068053509	0.6720821039	0.6472466223	0.6037941518
26	0.6249984014	0.5704642723	0.5190682563	0.4806930362	0.4090696885

Table 3.1b Errors in numerical eigenvalues $e(p)=k-k(p)$ for the Munk profile with a shear flow.

N=	77	92	115	146
ET=	.5990	.2950	.3320	.3740
j	e(1)	e(2)	e(3)	e(4)
1	-3.3E-08	-2.3E-08	-1.5E-08	-9.3E-09
2	-1.6E-07	-1.1E-07	-7.1E-08	-4.4E-08
3	-3.8E-07	-2.6E-07	-1.7E-07	-1.1E-07
4	-6.3E-07	-4.4E-07	-2.8E-07	-1.8E-07
5	-8.1E-07	-5.7E-07	-3.6E-07	-2.3E-07
6	-1.6E-06	-1.1E-06	-7.1E-07	-4.4E-07
7	-3.1E-06	-2.2E-06	-1.4E-06	-8.7E-07
8	-5.6E-06	-3.9E-06	-2.5E-06	-1.6E-06
9	-9.2E-06	-6.5E-06	-4.2E-06	-2.6E-06
10	-1.5E-05	-1.0E-05	-6.5E-06	-4.1E-06
11	-2.2E-05	-1.5E-05	-9.9E-06	-6.1E-06
12	-3.2E-05	-2.3E-05	-1.4E-05	-9.0E-06
13	-4.6E-05	-3.2E-05	-2.1E-05	-1.3E-05
14	-6.3E-05	-4.5E-05	-2.9E-05	-1.8E-05
15	-8.7E-05	-6.1E-05	-3.9E-05	-2.4E-05
16	-1.2E-04	-8.2E-05	-5.3E-05	-3.3E-05
17	-1.5E-04	-1.1E-04	-7.0E-05	-4.4E-05
18	-2.0E-04	-1.4E-04	-9.2E-05	-5.7E-05
19	-2.6E-04	-1.9E-04	-1.2E-04	-7.5E-05
20	-3.4E-04	-2.4E-04	-1.6E-04	-9.8E-05
21	-4.5E-04	-3.2E-04	-2.0E-04	-1.3E-04
22	-5.8E-04	-4.1E-04	-2.7E-04	-1.7E-04
23	-7.6E-04	-5.4E-04	-3.5E-04	-2.2E-04
24	-1.0E-03	-7.3E-04	-4.8E-04	-3.0E-04
25	-1.4E-03	-1.0E-03	-6.8E-04	-4.3E-04
26	-2.2E-03	-1.6E-03	-1.1E-03	-7.2E-04

Table 3.2a Standard extrapolations $K(p, \dots, q) = 100x_k(p, \dots, q)$
for the Munk profile with a shear flow.

N=	77	92	115	146	
ET=	.5990	.2950	.3320	.3740	
j	K(1)	K(1,2)	K(1,2,3)	K(1,2,3,4)	"Exact"
1	1.6683910356	1.6683876838	1.6683876881	1.6683876880	1.6683876881
2	1.6561391651	1.6561233441	1.6561233648	1.6561233648	1.6561233648
3	1.6446288764	1.6445909695	1.6445910274	1.6445910275	1.6445910275
4	1.6339082100	1.6338447809	1.6338449253	1.6338449252	1.6338449252
5	1.6245773713	1.6244958572	1.6244960873	1.6244960865	1.6244960865
6	1.6146308702	1.6144735565	1.6144735845	1.6144735835	1.6144735835
7	1.6011227064	1.6008085813	1.6008083873	1.6008083855	1.6008083855
8	1.5844601893	1.5839026141	1.5839018338	1.5839018298	1.5839018298
9	1.5650044376	1.5640818679	1.5640797715	1.5640797632	1.5640797632
10	1.5428093778	1.5413593589	1.5413546784	1.5413546616	1.5413546617
11	1.5178372599	1.5156493374	1.5156399604	1.5156399268	1.5156399269
12	1.4900109981	1.4868175367	1.4868000635	1.4867999969	1.4867999970
13	1.4592255438	1.4546903600	1.4546594572	1.4546593258	1.4546593258
14	1.4253484436	1.4190526208	1.4190000663	1.4189998086	1.4189998084
15	1.3882160453	1.3796398766	1.3795531306	1.3795526280	1.3795526272
16	1.3476266485	1.3361260863	1.3359861084	1.3359851318	1.3359851289
17	1.3033303010	1.2881053849	1.2878832134	1.2878813177	1.2878813090
18	1.2550140114	1.2350652091	1.2347164262	1.2347127344	1.2347127099
19	1.2022800638	1.1763457072	1.1758011263	1.1757938710	1.1757938037
20	1.1446133203	1.1110761385	1.1102253491	1.1102108488	1.1102106641
21	1.0813299784	1.0380703099	1.0367307852	1.0367009979	1.0367004770
22	1.0114931761	0.9556437762	0.9534982038	0.9534343374	0.9534327835
23	0.9337648270	0.8612676923	0.8577232049	0.8575768475	0.8575717465
24	0.8461226163	0.7508387541	0.7446630029	0.7442896912	0.7442700035
25	0.7452526106	0.6168827464	0.6050446684	0.6038963148	0.6037941518
26	0.6249984014	0.4429167965	0.4153298464	0.4101067387	0.4090696885

Table 3.2b Errors in standard extrapolations $e(p, \dots, q) = k - k(p, \dots, q)$
for the Munk profile with a shear flow.

N=	77	92	115	146
ET=	.5990	.2950	.3320	.3740
j	e(1)	e(1,2)	e(1,2,3)	e(1,2,3,4)
1	-3.3E-08	4.2E-11	-7.2E-14	9.2E-14
2	-1.6E-07	2.1E-10	3.6E-13	4.1E-15
3	-3.8E-07	5.8E-10	4.4E-13	-1.6E-13
4	-6.3E-07	1.4E-09	-1.2E-12	7.9E-15
5	-8.1E-07	2.3E-09	-7.4E-12	1.5E-14
6	-1.6E-06	2.7E-10	-9.5E-12	2.8E-14
7	-3.1E-06	-2.0E-09	-1.8E-11	4.4E-14
8	-5.6E-06	-7.8E-09	-4.0E-11	1.0E-13
9	-9.2E-06	-2.1E-08	-8.3E-11	2.1E-13
10	-1.5E-05	-4.7E-08	-1.7E-10	3.8E-13
11	-2.2E-05	-9.4E-08	-3.3E-10	5.7E-13
12	-3.2E-05	-1.8E-07	-6.7E-10	7.5E-13
13	-4.6E-05	-3.1E-07	-1.3E-09	6.4E-13
14	-6.3E-05	-5.3E-07	-2.6E-09	-1.2E-12
15	-8.7E-05	-8.7E-07	-5.0E-09	-8.1E-12
16	-1.2E-04	-1.4E-06	-9.8E-09	-2.9E-11
17	-1.5E-04	-2.2E-06	-1.9E-08	-8.7E-11
18	-2.0E-04	-3.5E-06	-3.7E-08	-2.5E-10
19	-2.6E-04	-5.5E-06	-7.3E-08	-6.7E-10
20	-3.4E-04	-8.7E-06	-1.5E-07	-1.8E-09
21	-4.5E-04	-1.4E-05	-3.0E-07	-5.2E-09
22	-5.8E-04	-2.2E-05	-6.5E-07	-1.6E-08
23	-7.6E-04	-3.7E-05	-1.5E-06	-5.1E-08
24	-1.0E-03	-6.6E-05	-3.9E-06	-2.0E-07
25	-1.4E-03	-1.3E-04	-1.3E-05	-1.0E-06
26	-2.2E-03	-3.4E-04	-6.3E-05	-1.0E-05

Table 3.3a Modified extrapolations $\hat{K}(p, \dots, q) = 100x\hat{k}(p, \dots, q)$
for the Munk profile with a shear flow.

N=	77	92	115	146	
ET=	.5990	.2950	.3320	.3740	
j	$\hat{K}(1)$	$\hat{K}(1,2)$	$\hat{K}(1,2,3)$	$\hat{K}(1,2,3,4)$	"Exact"
1	1.6683910253	1.6683876838	1.6683876881	1.6683876880	1.6683876881
2	1.6561383254	1.6561233440	1.6561233648	1.6561233648	1.6561233648
3	1.6446223804	1.6445909679	1.6445910274	1.6445910275	1.6445910275
4	1.6338831535	1.6338447688	1.6338449253	1.6338449252	1.6338449252
5	1.6245085270	1.6244958020	1.6244960873	1.6244960865	1.6244960865
6	1.6144761774	1.6144733694	1.6144735844	1.6144735835	1.6144735835
7	1.6008183841	1.6008080613	1.6008083870	1.6008083855	1.6008083855
8	1.5839153345	1.5839013570	1.5839018327	1.5839018298	1.5839018298
9	1.5640949334	1.5640791280	1.5640797684	1.5640797632	1.5640797632
10	1.5413708831	1.5413538417	1.5413546700	1.5413546616	1.5413546617
11	1.5156569760	1.5156388948	1.5156399399	1.5156399268	1.5156399269
12	1.4868177918	1.4867987209	1.4868000164	1.4867999969	1.4867999970
13	1.4546778378	1.4546577692	1.4546593540	1.4546593256	1.4546593258
14	1.4190190244	1.4189979290	1.4189998480	1.4189998080	1.4189998084
15	1.3795725261	1.3795503753	1.3795526817	1.3795526265	1.3795526272
16	1.3360056617	1.3359824453	1.3359852024	1.3359851278	1.3359851289
17	1.2879023731	1.2878781206	1.2878814063	1.2878813073	1.2878813090
18	1.2347341097	1.2347089234	1.2347128367	1.2347127073	1.2347127099
19	1.1758151826	1.1757892933	1.1757939657	1.1757937999	1.1757938037
20	1.1102313793	1.1102052468	1.1102108660	1.1102106585	1.1102106641
21	1.0367193521	1.0366938584	1.0367007176	1.0367004686	1.0367004770
22	0.9534475727	0.9534244224	0.9534330408	0.9534327696	0.9534327835
23	0.8575778368	0.8575604638	0.8575719198	0.8575717185	0.8575717465
24	0.7442566961	0.7442525985	0.7442696390	0.7442699161	0.7442700035
25	0.6037307156	0.6037587054	0.6037905600	0.6037936151	0.6037941518
26	0.4088149578	0.4089357245	0.4090310095	0.4090601306	0.4090696885

Table 3.3b Errors in modified extrapolations $\hat{e}(p, \dots, q) = k - \hat{k}(p, \dots, q)$
for the Munk profile with a shear flow.

N=	77	92	115	146
ET=	.5990	.2950	.3320	.3740
j	$\hat{e}(1)$	$\hat{e}(1,2)$	$\hat{e}(1,2,3)$	$\hat{e}(1,2,3,4)$
1	-3.3E-08	4.2E-11	-7.1E-14	9.1E-14
2	-1.5E-07	2.1E-10	3.6E-13	4.1E-15
3	-3.1E-07	6.0E-10	4.4E-13	-1.6E-13
4	-3.8E-07	1.6E-09	-1.2E-12	9.2E-15
5	-1.2E-07	2.8E-09	-7.3E-12	1.4E-14
6	-2.6E-08	2.1E-09	-8.7E-12	2.8E-14
7	-1.0E-07	3.2E-09	-1.5E-11	4.5E-14
8	-1.4E-07	4.7E-09	-2.9E-11	1.1E-13
9	-1.5E-07	6.4E-09	-5.1E-11	2.3E-13
10	-1.6E-07	8.2E-09	-8.4E-11	4.5E-13
11	-1.7E-07	1.0E-08	-1.3E-10	7.9E-13
12	-1.8E-07	1.3E-08	-1.9E-10	1.4E-12
13	-1.9E-07	1.6E-08	-2.8E-10	2.7E-12
14	-1.9E-07	1.9E-08	-4.0E-10	4.4E-12
15	-2.0E-07	2.3E-08	-5.4E-10	7.1E-12
16	-2.1E-07	2.7E-08	-7.3E-10	1.1E-11
17	-2.1E-07	3.2E-08	-9.7E-10	1.7E-11
18	-2.1E-07	3.8E-08	-1.3E-09	2.5E-11
19	-2.1E-07	4.5E-08	-1.6E-09	3.7E-11
20	-2.1E-07	5.4E-08	-2.0E-09	5.6E-11
21	-1.9E-07	6.6E-08	-2.4E-09	8.4E-11
22	-1.5E-07	8.4E-08	-2.6E-09	1.4E-10
23	-6.1E-08	1.1E-07	-1.7E-09	2.8E-10
24	1.3E-07	1.7E-07	3.6E-09	8.7E-10
25	6.3E-07	3.5E-07	3.6E-08	5.4E-09
26	2.5E-06	1.3E-06	3.9E-07	9.6E-08

Table 3.4 Comparison of eigenvalues for Munk profile with and without a shear flow.

j	Stationary	Convected	Change
1	0.0166895	0.0166839	0.0000056
2	0.0165659	0.0165612	0.0000046
3	0.0164497	0.0164459	0.0000038
4	0.0163414	0.0163385	0.0000030
5	0.0162472	0.0162450	0.0000023
6	0.0161474	0.0161447	0.0000027
7	0.0160112	0.0160081	0.0000031
8	0.0158424	0.0158390	0.0000033
9	0.0156442	0.0156408	0.0000034
10	0.0154170	0.0154135	0.0000035
11	0.0151599	0.0151564	0.0000035
12	0.0148716	0.0148680	0.0000036
13	0.0145502	0.0145466	0.0000036
14	0.0141936	0.0141900	0.0000036
15	0.0137991	0.0137955	0.0000036
16	0.0133635	0.0133599	0.0000036
17	0.0128824	0.0128788	0.0000036
18	0.0123507	0.0123471	0.0000036
19	0.0117616	0.0117579	0.0000036
20	0.0111057	0.0111021	0.0000036
21	0.0103706	0.0103670	0.0000036
22	0.0095380	0.0095343	0.0000036
23	0.0085794	0.0085757	0.0000036
24	0.0074463	0.0074427	0.0000036
25	0.0060416	0.0060379	0.0000036
26	0.0040943	0.0040907	0.0000036

Table 3.5a Numerical eigenvalues $K(p)=0.1xk(p)$ for the aeroacoustic problem.

N=	29	34	43	55	
ET=	.1130	.0600	.0640	.0780	
j	K(1)	K(2)	K(3)	K(4)	"Exact"
1	2.9791779468	2.9786591353	2.9781475969	2.9778198593	2.9773107935
2	2.6652423256	2.6644571992	2.6636822541	2.6631851931	2.6624120617
3	2.4622206634	2.4608812904	2.4595613407	2.4587157468	2.4574020786
4	2.3007170774	2.2988227138	2.2969593731	2.2957674391	2.2939183407
5	2.1574305739	2.1546426081	2.1518887423	2.1501207769	2.1473676297
6	1.9976917863	1.9925412298	1.9874066359	1.9840851629	1.9788730950
7	1.7931851971	1.7832139036	1.7731929427	1.7666673184	1.7563582522
8	1.5320342062	1.5132312801	1.4941512707	1.4816262128	1.4616762399
9	1.1987109449	1.1635112361	1.1272494549	1.1031370029	1.0642062148
10	0.7561207089	0.6866601449	0.6125803937	0.5617222139	0.4765135425

Table 3.5b Errors in numerical eigenvalues $e(p)=k-k(p)$ for the aeroacoustic problem.

N=	29	34	43	55
ET=	.1130	.0600	.0640	.0780
j	e(1)	e(2)	e(3)	e(4)
1	-1.9E-02	-1.3E-02	-8.4E-03	-5.1E-03
2	-2.8E-02	-2.0E-02	-1.3E-02	-7.7E-03
3	-4.8E-02	-3.5E-02	-2.2E-02	-1.3E-02
4	-6.8E-02	-4.9E-02	-3.0E-02	-1.8E-02
5	-1.0E-01	-7.3E-02	-4.5E-02	-2.8E-02
6	-1.9E-01	-1.4E-01	-8.5E-02	-5.2E-02
7	-3.7E-01	-2.7E-01	-1.7E-01	-1.0E-01
8	-7.0E-01	-5.2E-01	-3.2E-01	-2.0E-01
9	-1.3E+00	-9.9E-01	-6.3E-01	-3.9E-01
10	-2.8E+00	-2.1E+00	-1.4E+00	-8.5E-01

Table 3.6a Standard extrapolations $K(p, \dots, q) = 0.1xk(p, \dots, q)$
for the aeroacoustic problem.

N=	29	34	43	55	
ET=	.1130	.0600	.0640	.0780	
6	1.9976917863	1.9787900613	1.9788845456	1.9788727947	1.9788730950
7	1.7931851971	1.7565921328	1.7563807232	1.7563577390	1.7563582522
8	1.5320342062	1.4630304519	1.4617340802	1.4616756089	1.4616762399
9	1.1987109449	1.0695336009	1.0644474316	1.0642098279	1.0642062148
10	0.7561207089	0.5012114646	0.4788249535	0.4766792927	0.4765135425

Table 3.6b Errors in standard extrapolations $e(p, \dots, q) = k - k(p, \dots, q)$
for the aeroacoustic problem.

N=	29	34	43	55
ET=	.1130	.0600	.0640	.0780
j	e(1)	e(1,2)	e(1,2,3)	e(1,2,3,4)
1	-1.9E-02	3.7E-04	-4.4E-06	3.3E-09
2	-2.8E-02	5.1E-04	-1.3E-05	2.5E-07
3	-4.8E-02	9.7E-04	-2.6E-05	6.0E-07
4	-6.8E-02	1.5E-03	-4.6E-05	1.1E-06
5	-1.0E-01	1.7E-03	-7.3E-05	1.9E-06
6	-1.9E-01	8.3E-04	-1.1E-04	3.0E-06
7	-3.7E-01	-2.3E-03	-2.2E-04	5.1E-06
8	-7.0E-01	-1.4E-02	-5.8E-04	6.3E-06
9	-1.3E+00	-5.3E-02	-2.4E-03	-3.6E-05
10	-2.8E+00	-2.5E-01	-2.3E-02	-1.7E-03

Table 3.7a Modified extrapolations $\hat{k}(p, \dots, q) = 0.1xk(p, \dots, q)$
for the aeroacoustic problem.

N=	29	34	43	55	
ET=	.1130	.0600	.0640	.0780	
j	$\hat{k}(1)$	$\hat{k}(1,2)$	$\hat{k}(1,2,3)$	$\hat{k}(1,2,3,4)$	"Exact"
1	2.9791769857	2.9772739907	2.9773112352	2.9773107932	2.9773107935
2	2.6651637893	2.6623609853	2.6624133592	2.6624120366	2.6624120617
3	2.4616036823	2.4573042366	2.4574046920	2.4574020189	2.4574020786
4	2.2982788039	2.2937558728	2.2939228992	2.2939182293	2.2939183407
5	2.1504915721	2.1471533640	2.1473748036	2.1473674436	2.1473676297
6	1.9813120748	1.9786146653	1.9788836762	1.9788727919	1.9788730950
7	1.7586553227	1.7560117723	1.7563755504	1.7563577060	1.7563582522
8	1.4637175150	1.4612162097	1.4617039503	1.4616752223	1.4616762399
9	1.0655171180	1.0635790669	1.0642442928	1.0642042047	1.0642062148
10	0.4749251844	0.4751279471	0.4764553170	0.4764974279	0.4765135425

Table 3.7b Errors in modified extrapolations $\hat{e}(p, \dots, q) = k - \hat{k}(p, \dots, q)$
for the aeroacoustic problem.

N=	29	34	43	55
ET=	.1130	.0600	.0640	.0780
j	$\hat{e}(1)$	$\hat{e}(1,2)$	$\hat{e}(1,2,3)$	$\hat{e}(1,2,3,4)$
1	-1.9E-02	3.7E-04	-4.4E-06	3.3E-09
2	-2.8E-02	5.1E-04	-1.3E-05	2.5E-07
3	-4.2E-02	9.8E-04	-2.6E-05	6.0E-07
4	-4.4E-02	1.6E-03	-4.6E-05	1.1E-06
5	-3.1E-02	2.1E-03	-7.2E-05	1.9E-06
6	-2.4E-02	2.6E-03	-1.1E-04	3.0E-06
7	-2.3E-02	3.5E-03	-1.7E-04	5.5E-06
8	-2.0E-02	4.6E-03	-2.8E-04	1.0E-05
9	-1.3E-02	6.3E-03	-3.8E-04	2.0E-05
10	1.6E-02	1.4E-02	5.8E-04	1.6E-04

Table 4.1a Numerical eigenvalues $K^2(p)=100xk^2(p)$
for the shallow water problem.

N1/N2	100/300	150/450	200/600	300/900	
ET=	7.9870	5.7940	4.7920	6.5560	
j	$K^2(1)$	$K^2(2)$	$K^2(3)$	$K^2(4)$	Exact
1	1.7805178446	1.7806674179	1.7807197867	1.7807571989	1.7807871324
2	1.6848824426	1.6854136651	1.6855997232	1.6857326642	1.6858390427
3	1.5287832832	1.5297586069	1.5301003437	1.5303445619	1.5305400092
4	1.3164975109	1.3177504076	1.3181895437	1.3185034122	1.3187546275
5	1.0562214624	1.0573243701	1.0577109025	1.0579871623	1.0582082698
6	0.7688670707	0.7692402970	0.7693704899	0.7694633464	0.7695375485
7	0.4831481449	0.4824747429	0.4822376204	0.4820677931	0.4819316589
8	0.3851153068	0.3851065403	0.3851034540	0.3851012435	0.3850994716
9	0.3582958781	0.3582725441	0.3582643672	0.3582585232	0.3582538459
10	0.3193730866	0.3193449329	0.3193351361	0.3193281560	0.3193225825
11	0.2884255951	0.2882465840	0.2881841900	0.2881397014	0.2881041566
12	0.2724371949	0.2721226385	0.2720129433	0.2719347156	0.2718722087
13	0.2465595600	0.2462779763	0.2461792850	0.2461087480	0.2460522925
14	0.1851786040	0.1847981253	0.1846653715	0.1845706765	0.1844949975
15	0.1381986509	0.1375707205	0.1373512051	0.1371944841	0.1370691507
16	0.0836556721	0.0819155609	0.0813270671	0.0809132325	0.0805860636
17	0.0486839034	0.0462087151	0.0453006868	0.0446384773	0.0441004226
18	0.0032876241	0.0024746046	0.0022004628	0.0020083102	0.0018569072

Table 4.1b Errors in numerical eigenvalues $e(p)=k^2-k^2(p)$
for the shallow water problem.

N1/N2	100/300	150/450	200/600	300/900
ET=	7.9870	5.7940	4.7920	6.5560
j	e(1)	e(2)	e(3)	e(4)
1	2.7E-06	1.2E-06	6.7E-07	3.0E-07
2	9.6E-06	4.3E-06	2.4E-06	1.1E-06
3	1.8E-05	7.8E-06	4.4E-06	2.0E-06
4	2.3E-05	1.0E-05	5.7E-06	2.5E-06
5	2.0E-05	8.8E-06	5.0E-06	2.2E-06
6	6.7E-06	3.0E-06	1.7E-06	7.4E-07
7	-1.2E-05	-5.4E-06	-3.1E-06	-1.4E-06
8	-1.6E-07	-7.1E-08	-4.0E-08	-1.8E-08
9	-4.2E-07	-1.9E-07	-1.1E-07	-4.7E-08
10	-5.1E-07	-2.2E-07	-1.3E-07	-5.6E-08
11	-3.2E-06	-1.4E-06	-8.0E-07	-3.6E-07
12	-5.6E-06	-2.5E-06	-1.4E-06	-6.3E-07
13	-5.1E-06	-2.3E-06	-1.3E-06	-5.6E-07
14	-6.8E-06	-3.0E-06	-1.7E-06	-7.6E-07
15	-1.1E-05	-5.0E-06	-2.8E-06	-1.3E-06
16	-3.1E-05	-1.3E-05	-7.4E-06	-3.3E-06
17	-4.6E-05	-2.1E-05	-1.2E-05	-5.4E-06
18	-1.4E-05	-6.2E-06	-3.4E-06	-1.5E-06

Table 4.2a Standard extrapolations $K^2(p, \dots, q) = 100xk^2(p, \dots, q)$
for the shallow water problem.

N1/N2	100/300	150/450	200/600	300/900	
ET=	7.9870	5.7940	4.7920	6.5560	
j	$K^2(1)$	$K^2(1,2)$	$K^2(1,2,3)$	$K^2(1,2,3,4)$	Exact
1	1.7805178446	1.7807870766	1.7807871316	1.7807871324	1.7807871324
2	1.6848824426	1.6858386431	1.6858390400	1.6858390427	1.6858390427
3	1.5287832832	1.5305388658	1.5305400043	1.5305400092	1.5305400092
4	1.3164975109	1.3187527249	1.3187546214	1.3187546275	1.3187546275
5	1.0562214624	1.0582066962	1.0582082648	1.0582082698	1.0582082698
6	0.7688670707	0.7695388780	0.7695375483	0.7695375485	0.7695375485
7	0.4831481449	0.4819360213	0.4819316578	0.4819316589	0.4819316589
8	0.3851153068	0.3850995272	0.3850994719	0.3850994716	0.3850994716
9	0.3582958781	0.3582538770	0.3582538465	0.3582538459	0.3582538459
10	0.3193730866	0.3193224099	0.3193225836	0.3193225825	0.3193225825
11	0.2884255951	0.2881033751	0.2881041670	0.2881041566	0.2881041566
12	0.2724371949	0.2718709934	0.2718722109	0.2718722088	0.2718722087
13	0.2465595600	0.2460527093	0.2460522917	0.2460522925	0.2460522925
14	0.1851786040	0.1844937424	0.1844950031	0.1844949974	0.1844949975
15	0.1381986509	0.1370683762	0.1370691693	0.1370691506	0.1370691507
16	0.0836556721	0.0805234721	0.0805860855	0.0805860745	0.0805860636
17	0.0486839034	0.0442285645	0.0441014410	0.0441004263	0.0441004226
18	0.0032876241	0.0018241889	0.0018559300	0.0018568930	0.0018569072

Table 4.2b Errors in standard extrapolations $e(p)=k^2-k^2(p,\dots,q)$
for the shallow water problem.

N1/N2	100/300	150/450	200/600	300/900
ET=	7.9870	5.7940	4.7920	6.5560
j	e(1)	e(1,2)	e(1,2,3)	e(1,2,3,4)
1	2.7E-06	5.6E-10	7.5E-12	2.1E-14
2	9.6E-06	4.0E-09	2.7E-11	7.0E-14
3	1.8E-05	1.1E-08	4.9E-11	1.2E-13
4	2.3E-05	1.9E-08	6.1E-11	1.2E-13
5	2.0E-05	1.6E-08	4.9E-11	8.1E-14
6	6.7E-06	-1.3E-08	2.5E-12	1.2E-14
7	-1.2E-05	-4.4E-08	1.2E-11	4.8E-14
8	-1.6E-07	-5.6E-10	-3.4E-12	-2.5E-16
9	-4.2E-07	-3.1E-10	-5.9E-12	-5.7E-15
10	-5.1E-07	1.7E-09	-1.1E-11	3.2E-14
11	-3.2E-06	7.8E-09	-1.0E-10	3.0E-13
12	-5.6E-06	1.2E-08	-2.2E-11	-2.6E-13
13	-5.1E-06	-4.2E-09	8.1E-12	-1.3E-14
14	-6.8E-06	1.3E-08	-5.7E-11	9.2E-14
15	-1.1E-05	7.7E-09	-1.9E-10	1.0E-12
16	-3.1E-05	6.3E-07	-2.2E-10	-1.1E-10
17	-4.6E-05	-1.3E-06	-1.0E-08	-3.7E-11
18	-1.4E-05	3.3E-07	9.8E-09	1.4E-10

Table 4.3a Numerical eigenvalues $K^2(p)=10^4 x k^2(p)$
for the Munk profile with an elastic bottom.

N1/N2	200/200	300/300	400/400	600/600	Exact
ET=	8.9040	7.7140	6.6490	8.3590	
j	$K^2(1)$	$K^2(2)$	$K^2(3)$	$K^2(4)$	
1	2.9038346179	2.9043777763	2.9045717303	2.9047115148	2.9048240973
2	2.7853806272	2.7853796965	2.7853793709	2.7853791383	2.7853789522
3	2.7442802497	2.7442758805	2.7442743516	2.7442732597	2.7442723862
4	2.7058505588	2.7058401277	2.7058364780	2.7058338716	2.7058317867
5	2.6688852743	2.6688658371	2.6688590395	2.6688541857	2.6688503038
6	2.6298754553	2.6298386927	2.6298258400	2.6298166640	2.6298093260
7	2.5846045345	2.5845339025	2.5845092028	2.5844915671	2.5844774627
8	2.5314592539	2.5313318617	2.5312872953	2.5312554689	2.5312300119
9	2.4703582714	2.4701445959	2.4700698176	2.4700164073	2.4699736807
10	2.4014708645	2.4011337395	2.4010157242	2.4009314209	2.4008639743
11	2.3249814954	2.3244755495	2.3242983946	2.3241718322	2.3240705683
12	2.2411039069	2.2403756422	2.2401205957	2.2399383710	2.2397925621
13	2.1501327390	2.1491218654	2.1487677992	2.1485148121	2.1483123730
14	2.0525319298	2.0511755436	2.0507004388	2.0503609612	2.0500893090
15	1.9491021271	1.9473453911	1.9467301469	1.9462905650	1.9459388267
16	1.8412749628	1.8390939512	1.8383305329	1.8377852169	1.8373489546
17	1.7313287095	1.7287528296	1.7278520436	1.7272088742	1.7266944894
18	1.6211197497	1.6181491397	1.6171101886	1.6163683147	1.6157749535
19	1.5087252241	1.5051613795	1.5039130969	1.5030211632	1.5023074328
20	1.3932928320	1.3892535163	1.3878473579	1.3868455487	1.3860457098
21	1.3017067689	1.2990759483	1.2981689802	1.2975250575	1.2970121212
22	1.2168448262	1.2119789043	1.2102506705	1.2090084277	1.2080100205
23	1.0851477799	1.0780936974	1.0756160472	1.0738436305	1.0724241279
24	0.9405899007	0.9324803764	0.9296546344	0.9276407351	0.9260324630
25	0.8153073642	0.8091597645	0.8070654825	0.8055866576	0.8044134784
26	0.7155495554	0.7073568710	0.7044198556	0.7023000120	0.7005910223
27	0.5684568836	0.5561249358	0.5517835511	0.5486751696	0.5461842154
28	0.4088321911	0.3990141967	0.3960291926	0.3940483025	0.3925541393
29	0.3557864408	0.3491632463	0.3463888083	0.3442535040	0.3424531437
30	0.2113010907	0.1980011300	0.1940565838	0.1915338313	0.1897055209
31	0.1694486681	0.1650858647	0.1628889835	0.1610428359	0.1593885055
32	0.0760223149	0.0707665231	0.0690316941	0.0678093572	0.0668369969

Table 4.3b Errors in numerical eigenvalues $e(p)=k^2-k^2(p)$
for the Munk profile with an elastic bottom.

N1/N2	200/200	300/300	400/400	600/600
ET=	8.9040	7.7140	6.6490	8.3590
j	e(1)	e(2)	e(3)	e(4)
1	9.9E-08	4.5E-08	2.5E-08	1.1E-08
2	-1.7E-10	-7.4E-11	-4.2E-11	-1.9E-11
3	-7.9E-10	-3.5E-10	-2.0E-10	-8.7E-11
4	-1.9E-09	-8.3E-10	-4.7E-10	-2.1E-10
5	-3.5E-09	-1.6E-09	-8.7E-10	-3.9E-10
6	-6.6E-09	-2.9E-09	-1.7E-09	-7.3E-10
7	-1.3E-08	-5.6E-09	-3.2E-09	-1.4E-09
8	-2.3E-08	-1.0E-08	-5.7E-09	-2.5E-09
9	-3.8E-08	-1.7E-08	-9.6E-09	-4.3E-09
10	-6.1E-08	-2.7E-08	-1.5E-08	-6.7E-09
11	-9.1E-08	-4.0E-08	-2.3E-08	-1.0E-08
12	-1.3E-07	-5.8E-08	-3.3E-08	-1.5E-08
13	-1.8E-07	-8.1E-08	-4.6E-08	-2.0E-08
14	-2.4E-07	-1.1E-07	-6.1E-08	-2.7E-08
15	-3.2E-07	-1.4E-07	-7.9E-08	-3.5E-08
16	-3.9E-07	-1.7E-07	-9.8E-08	-4.4E-08
17	-4.6E-07	-2.1E-07	-1.2E-07	-5.1E-08
18	-5.3E-07	-2.4E-07	-1.3E-07	-5.9E-08
19	-6.4E-07	-2.9E-07	-1.6E-07	-7.1E-08
20	-7.2E-07	-3.2E-07	-1.8E-07	-8.0E-08
21	-4.7E-07	-2.1E-07	-1.2E-07	-5.1E-08
22	-8.8E-07	-4.0E-07	-2.2E-07	-1.0E-07
23	-1.3E-06	-5.7E-07	-3.2E-07	-1.4E-07
24	-1.5E-06	-6.4E-07	-3.6E-07	-1.6E-07
25	-1.1E-06	-4.7E-07	-2.7E-07	-1.2E-07
26	-1.5E-06	-6.8E-07	-3.8E-07	-1.7E-07
27	-2.2E-06	-9.9E-07	-5.6E-07	-2.5E-07
28	-1.6E-06	-6.5E-07	-3.5E-07	-1.5E-07
29	-1.3E-06	-6.7E-07	-3.9E-07	-1.8E-07
30	-2.2E-06	-8.3E-07	-4.4E-07	-1.8E-07
31	-1.0E-06	-5.7E-07	-3.5E-07	-1.7E-07
32	-9.2E-07	-3.9E-07	-2.2E-07	-9.7E-08

Table 4.4a Standard extrapolations $K^2(p, \dots, q) = 10^4 x k^2(p, \dots, q)$ for the Munk profile with an elastic bottom.

N1/N2	200/200	300/300	400/400	600/600	
ET=	8.9040	7.7140	6.6490	8.3590	
j	$K^2(1)$	$K^2(1,2)$	$K^2(1,2,3)$	$K^2(1,2,3,4)$	Exact
1	2.9038346179	2.9048123031	2.9048240319	2.9048240971	2.9048240973
2	2.7853806272	2.7853789520	2.7853789522	2.7853789522	2.7853789522
3	2.7442802497	2.7442723851	2.7442723862	2.7442723862	2.7442723862
4	2.7058505588	2.7058317827	2.7058317867	2.7058317867	2.7058317867
5	2.6688852743	2.6688502873	2.6688503038	2.6688503038	2.6688503038
6	2.6298754553	2.6298092827	2.6298093259	2.6298093260	2.6298093260
7	2.5846045345	2.5844773969	2.5844774624	2.5844774627	2.5844774627
8	2.5314592539	2.5312299479	2.5312300115	2.5312300119	2.5312300119
9	2.4703582714	2.4699736555	2.4699736802	2.4699736807	2.4699736807
10	2.4014708645	2.4008640395	2.4008639738	2.4008639743	2.4008639743
11	2.3249814954	2.3240707928	2.3240705678	2.3240705683	2.3240705683
12	2.2411039069	2.2397930304	2.2397925617	2.2397925621	2.2397925621
13	2.1501327390	2.1483131665	2.1483123727	2.1483123730	2.1483123730
14	2.0525319298	2.0500904346	2.0500893082	2.0500893090	2.0500893090
15	1.9491021271	1.9459400023	1.9459388241	1.9459388267	1.9459388267
16	1.8412749628	1.8373491419	1.8373489463	1.8373489545	1.8373489546
17	1.7313287095	1.7266921256	1.7266944784	1.7266944895	1.7266944894
18	1.6211197497	1.6157726518	1.6157749752	1.6157749536	1.6157749535
19	1.5087252241	1.5023103038	1.5023074482	1.5023074327	1.5023074328
20	1.3932928320	1.3860220637	1.3860452322	1.3860457078	1.3860457098
21	1.3017067689	1.2969712918	1.2970134074	1.2970121237	1.2970121212
22	1.2168448262	1.2080861668	1.2080094850	1.2080100189	1.2080100205
23	1.0851477799	1.0724504314	1.0724238520	1.0724241280	1.0724241279
24	0.9405899007	0.9259927570	0.9260311309	0.9260324557	0.9260324630
25	0.8153073642	0.8042416848	0.8044165506	0.8044135149	0.8044134784
26	0.7155495554	0.7008027234	0.7005906830	0.7005909854	0.7005910223
27	0.5684568836	0.5462593775	0.5461825685	0.5461842115	0.5461842154
28	0.4088321911	0.3911598012	0.3925351732	0.3925567401	0.3925541393
29	0.3557864408	0.3438646907	0.3424740012	0.3424505132	0.3424531437
30	0.2113010907	0.1873611615	0.1895263121	0.1897132708	0.1897055209
31	0.1694486681	0.1615956221	0.1595540218	0.1593804660	0.1593885055
32	0.0760223149	0.0665618896	0.0668809699	0.0668366602	0.0668369969

Table 4.4b Errors in standard extrapolations $e(p, \dots, q) = k^2 - k^2(p, \dots, q)$
for the Munk profile with an elastic bottom.

N1/N2	200/200	300/300	400/400	600/600
ET=	8.9040	7.7140	6.6490	8.3590
j	e(1)	e(1,2)	e(1,2,3)	e(1,2,3,4)
1	9.9E-08	1.2E-09	6.5E-12	1.5E-14
2	-1.7E-10	2.0E-14	-6.4E-16	-7.3E-16
3	-7.9E-10	1.0E-13	2.8E-16	2.9E-16
4	-1.9E-09	3.9E-13	2.1E-16	-2.7E-16
5	-3.5E-09	1.6E-12	4.8E-15	-1.8E-16
6	-6.6E-09	4.3E-12	1.7E-14	-6.4E-16
7	-1.3E-08	6.6E-12	3.2E-14	-3.4E-16
8	-2.3E-08	6.4E-12	4.2E-14	-8.8E-16
9	-3.8E-08	2.5E-12	4.9E-14	7.4E-16
10	-6.1E-08	-6.5E-12	4.9E-14	4.2E-16
11	-9.1E-08	-2.2E-11	4.5E-14	8.0E-17
12	-1.3E-07	-4.7E-11	3.9E-14	4.5E-16
13	-1.8E-07	-7.9E-11	3.8E-14	6.8E-16
14	-2.4E-07	-1.1E-10	7.5E-14	3.2E-16
15	-3.2E-07	-1.2E-10	2.6E-13	1.8E-16
16	-3.9E-07	-1.9E-11	8.2E-13	4.4E-16
17	-4.6E-07	2.4E-10	1.1E-12	-4.7E-15
18	-5.3E-07	2.3E-10	-2.2E-12	-1.3E-14
19	-6.4E-07	-2.9E-10	-1.5E-12	1.9E-14
20	-7.2E-07	2.4E-09	4.8E-11	2.0E-13
21	-4.7E-07	4.1E-09	-1.3E-10	-2.5E-13
22	-8.8E-07	-7.6E-09	5.4E-11	1.6E-13
23	-1.3E-06	-2.6E-09	2.8E-11	-1.1E-14
24	-1.5E-06	4.0E-09	1.3E-10	7.3E-13
25	-1.1E-06	1.7E-08	-3.1E-10	-3.7E-12
26	-1.5E-06	-2.1E-08	3.4E-11	3.7E-12
27	-2.2E-06	-7.5E-09	1.6E-10	3.9E-13
28	-1.6E-06	1.4E-07	1.9E-09	-2.6E-10
29	-1.3E-06	-1.4E-07	-2.1E-09	2.6E-10
30	-2.2E-06	2.3E-07	1.8E-08	-7.7E-10
31	-1.0E-06	-2.2E-07	-1.7E-08	8.0E-10
32	-9.2E-07	2.8E-08	-4.4E-09	3.4E-11

Table 4.5 Comparison of eigenvalues for the Munk profile with an elastic bottom and a rigid bottom.

j	Elastic	Rigid
1	0.29048241E-03	
2	0.27853790E-03	0.27853790E-03
3	0.27442724E-03	0.27442742E-03
4	0.27058318E-03	0.27059198E-03
5	0.26688503E-03	0.26704188E-03
6	0.26298093E-03	0.26397293E-03
7	0.25844775E-03	0.26073984E-03
8	0.25312300E-03	0.25635956E-03
9	0.24699737E-03	0.25098018E-03
10	0.24008640E-03	0.24474192E-03
11	0.23240706E-03	0.23768501E-03
12	0.22397926E-03	0.22982337E-03
13	0.21483124E-03	0.22116310E-03
14	0.20500893E-03	0.21170732E-03
15	0.19459388E-03	0.20145785E-03
16	0.18373490E-03	0.19041582E-03
17	0.17266945E-03	0.17858200E-03
18	0.16157750E-03	0.16595691E-03
19	0.15023074E-03	0.15254093E-03
20	0.13860457E-03	0.13833434E-03
21	0.12970121E-03	0.12333734E-03
22	0.12080100E-03	0.10755009E-03
23	0.10724241E-03	0.90972717E-04
24	0.92603246E-04	0.73605315E-04
25	0.80441348E-04	0.55447959E-04
26	0.70059102E-04	0.36500712E-04
27	0.54618422E-04	0.16763621E-04
28	0.39255414E-04	
29	0.34245314E-04	
30	0.18970552E-04	
31	0.15938851E-04	
32	0.66836997E-05	

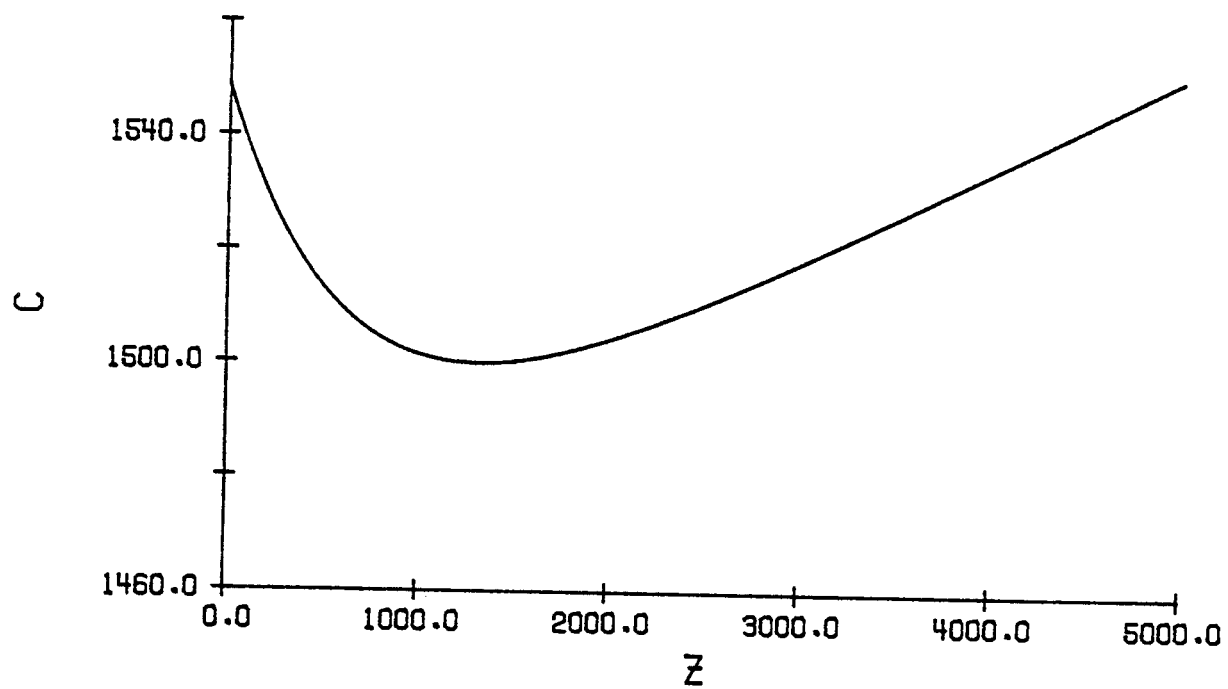


Figure 2.1 Munk sound speed profile.

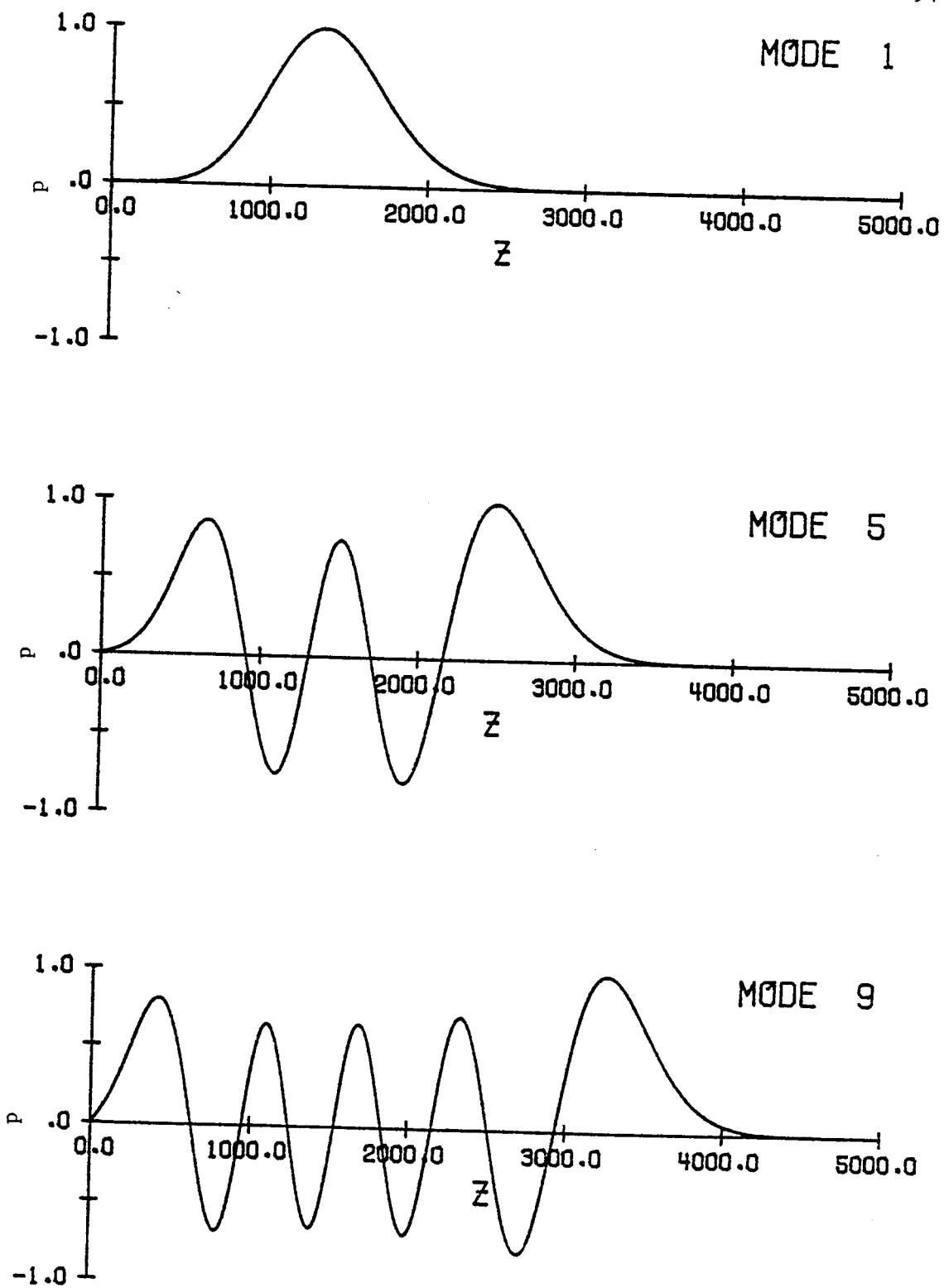


Figure 2.2a Selected modes for the Munk sound speed profile.

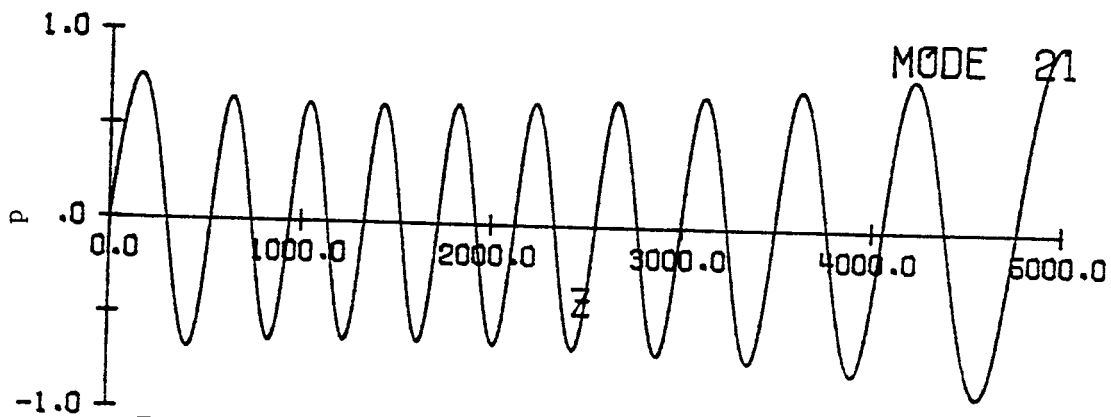
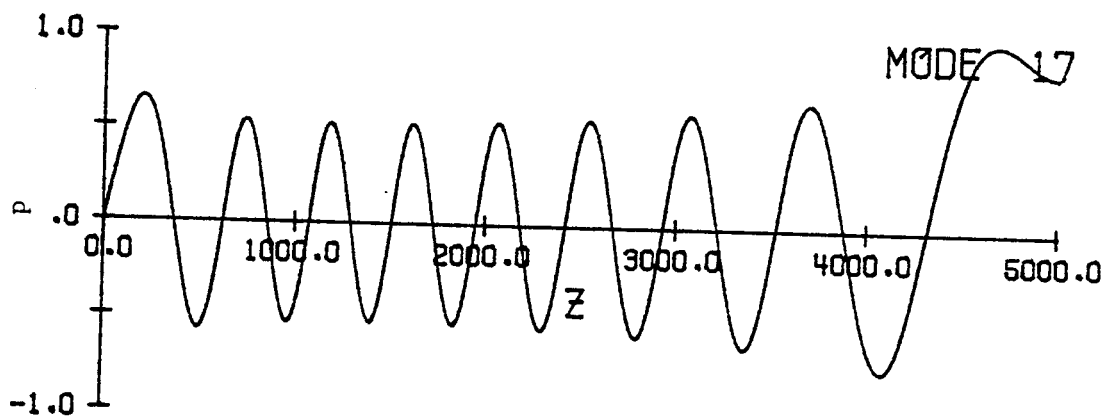
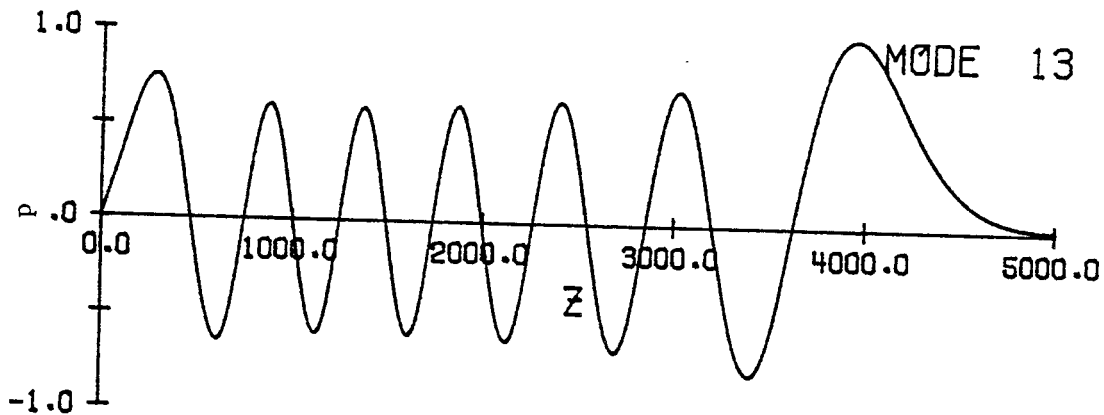


Figure 2.2b Selected modes for the Munk sound speed profile.

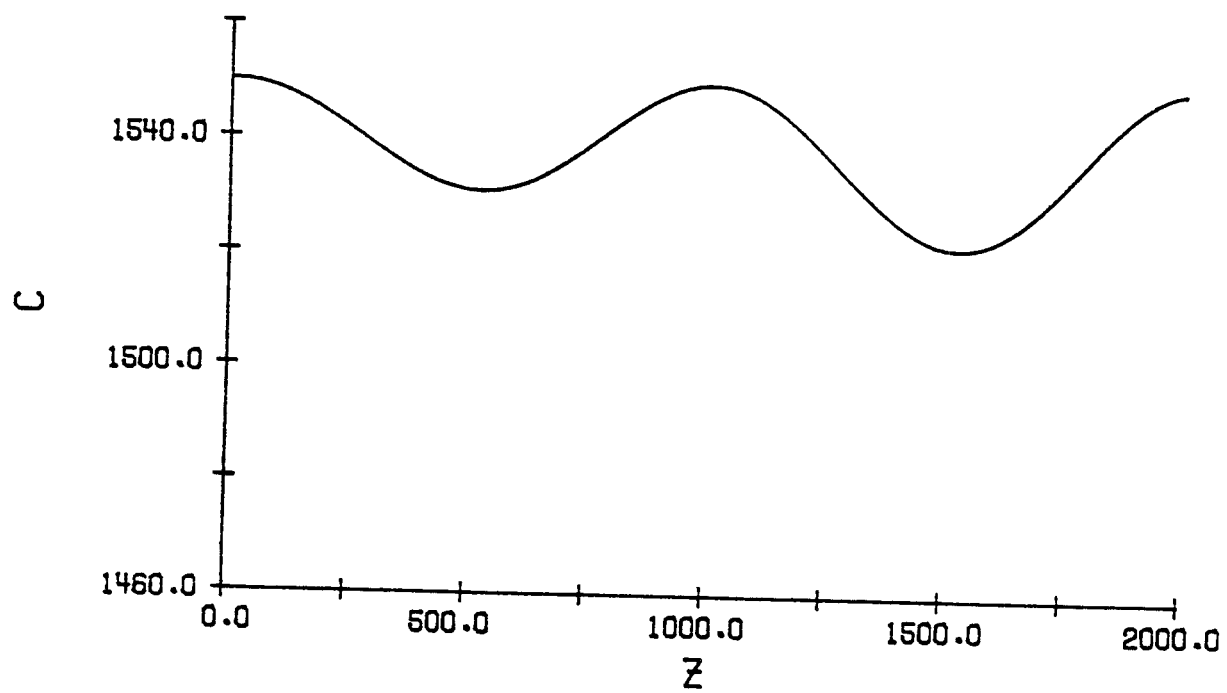


Figure 2.3 Sound speed profile for the double-duct problem.

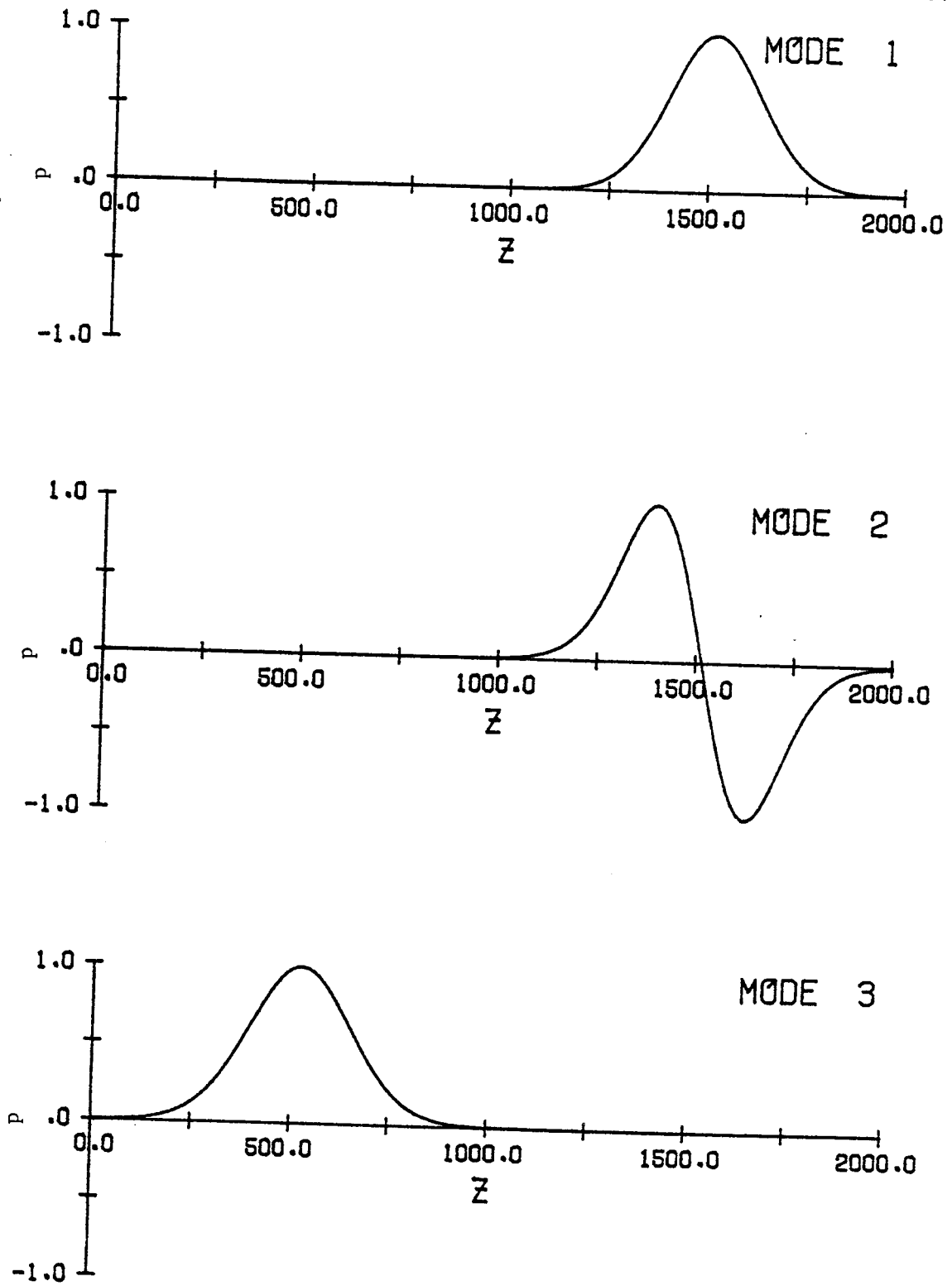


Figure 2.4a First nine modes for the double-duct problem.

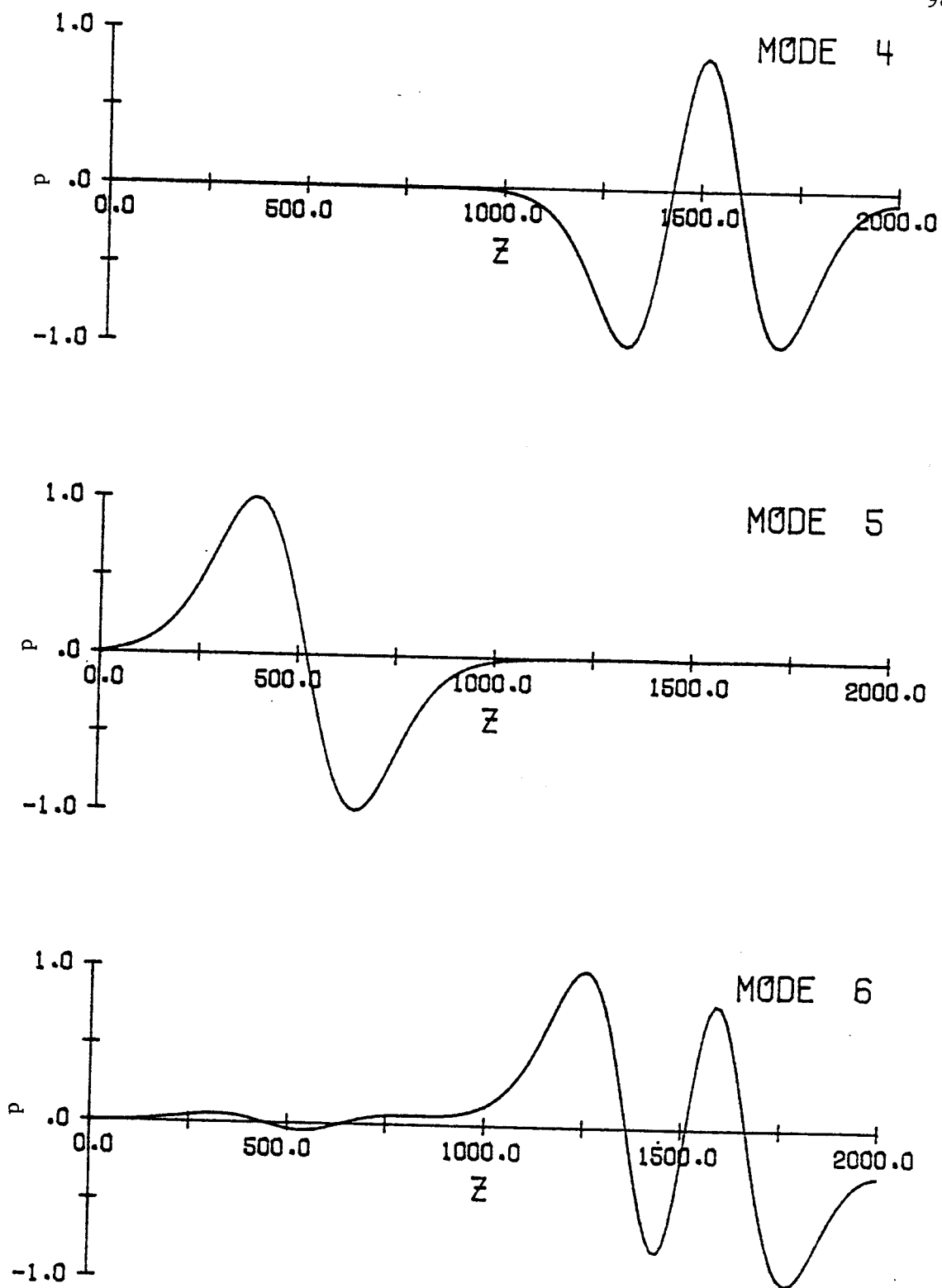


Figure 2.4b First nine modes for the double-duct problem.

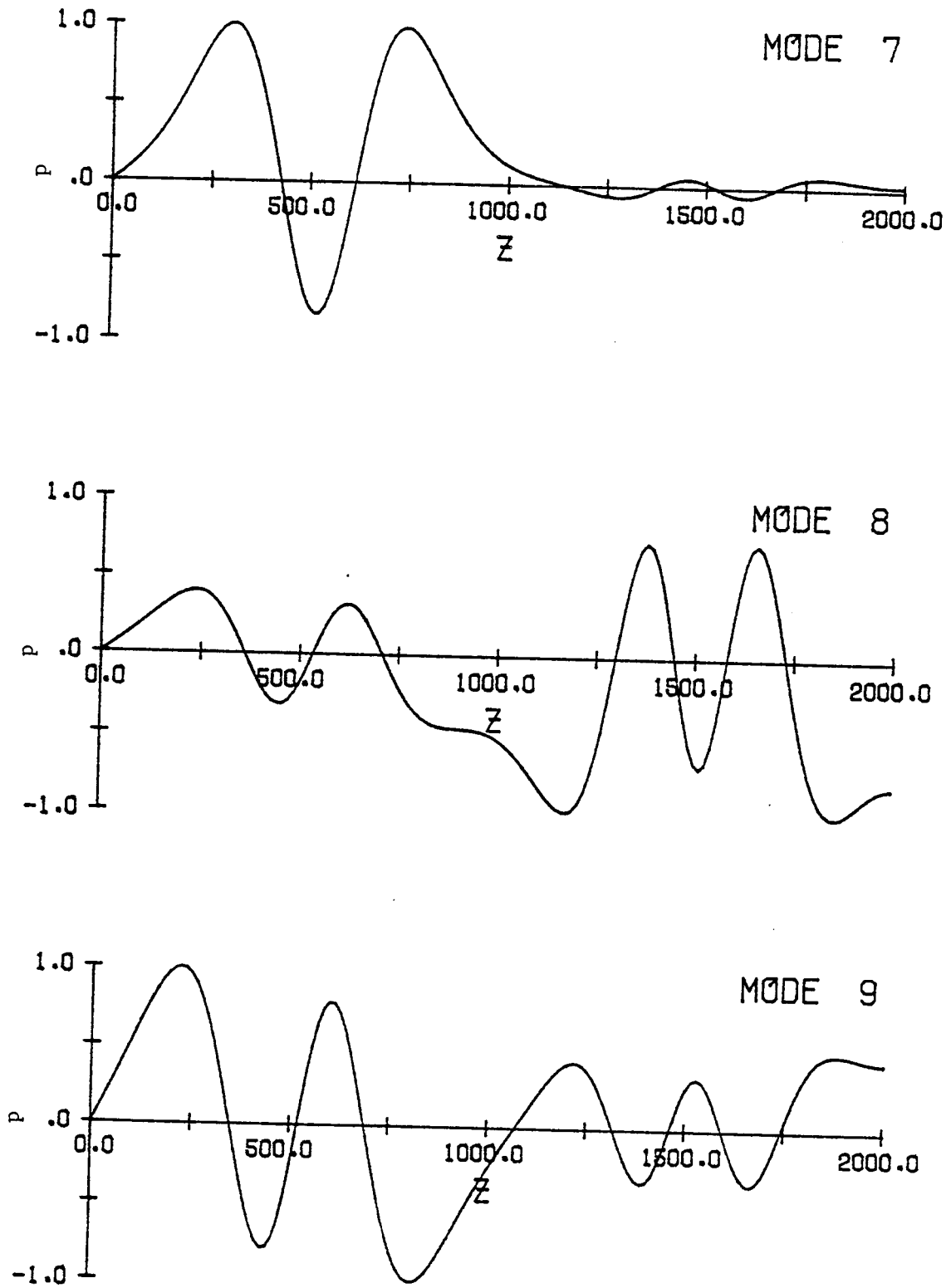


Figure 2.4c First nine modes for the double-duct problem.

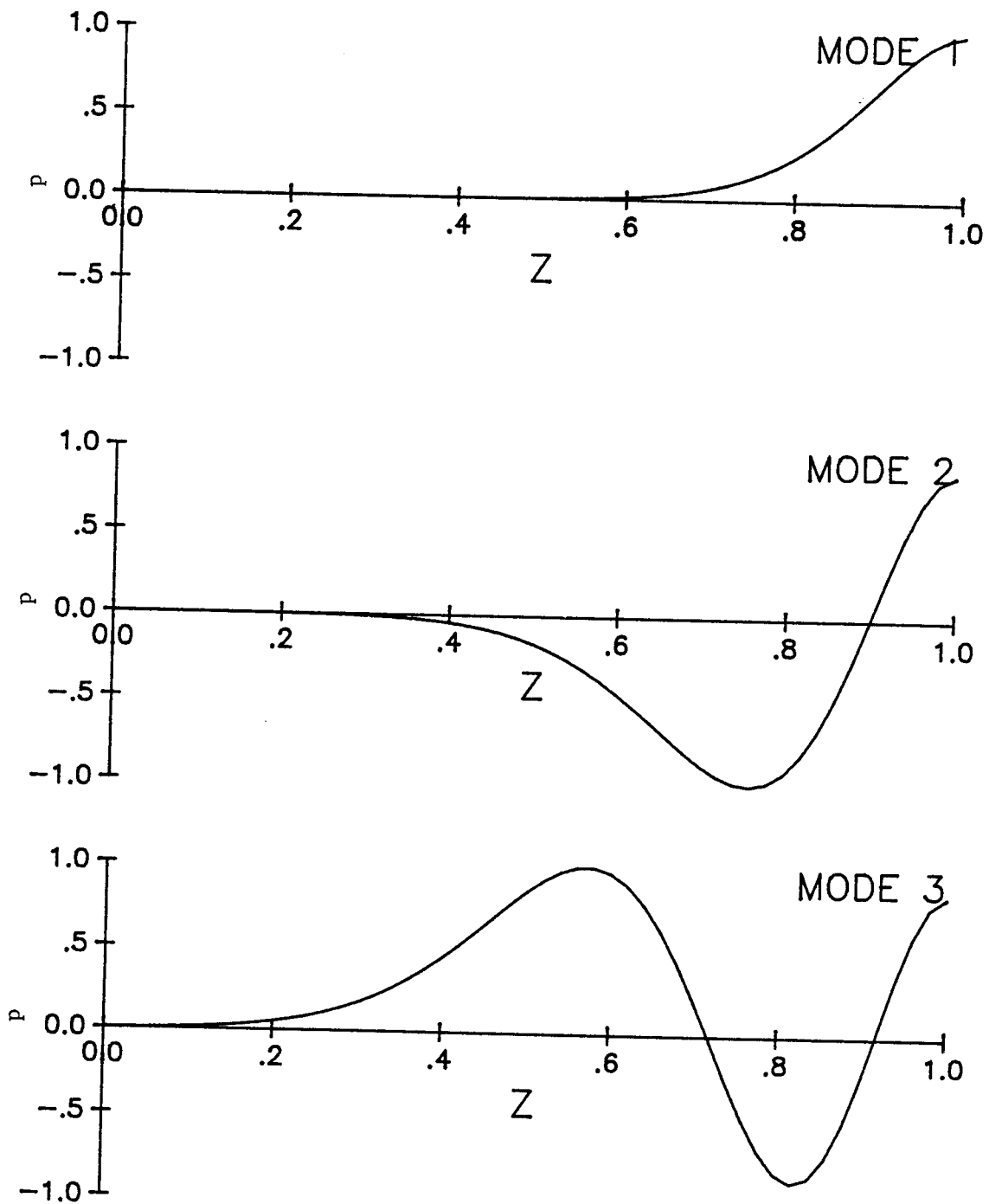


Figure 3.1a First nine modes for the aeroacoustic problem with $M=0.5$.

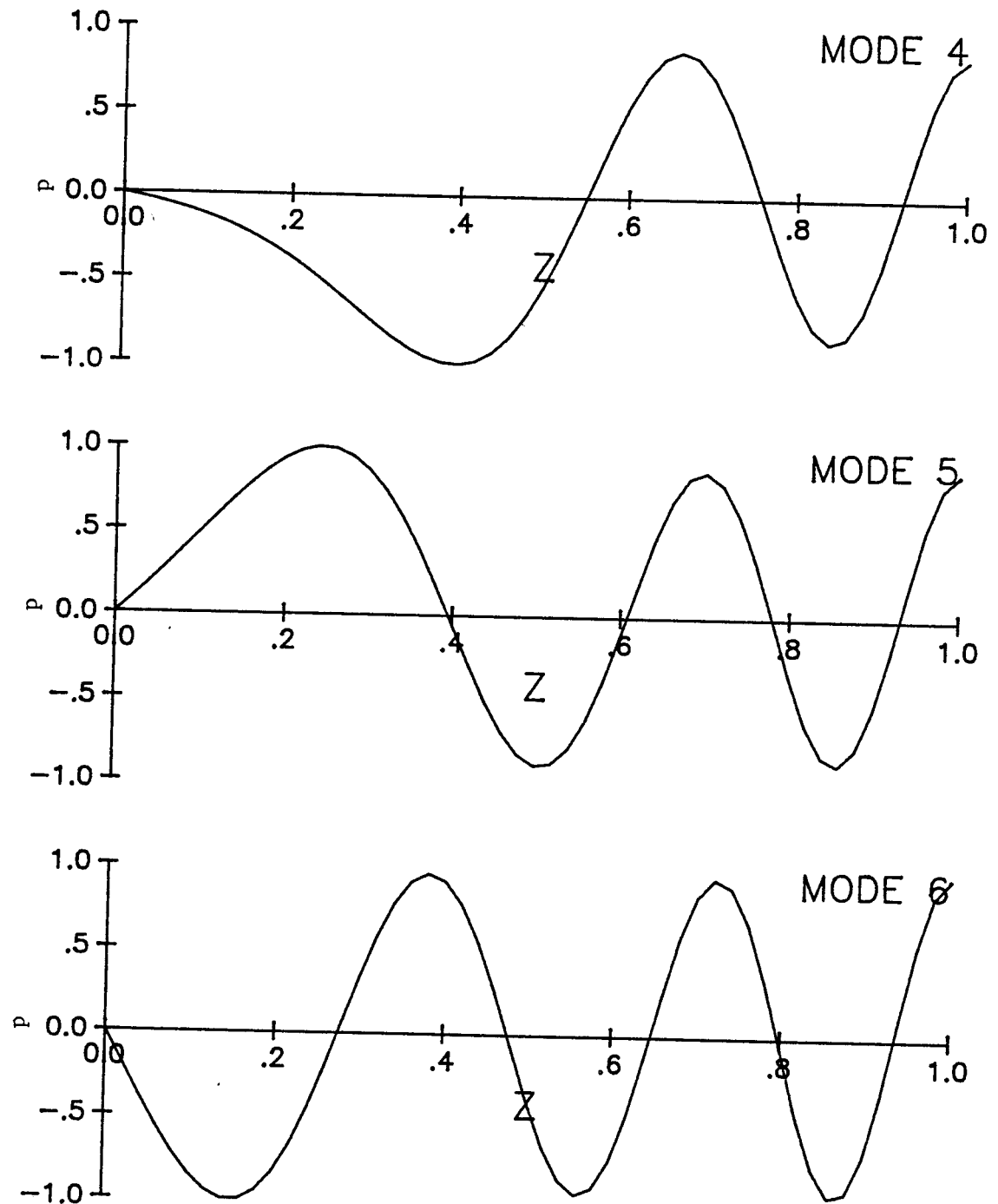


Figure 3.1b First nine modes for the aeroacoustic problem with $M=0.5$.

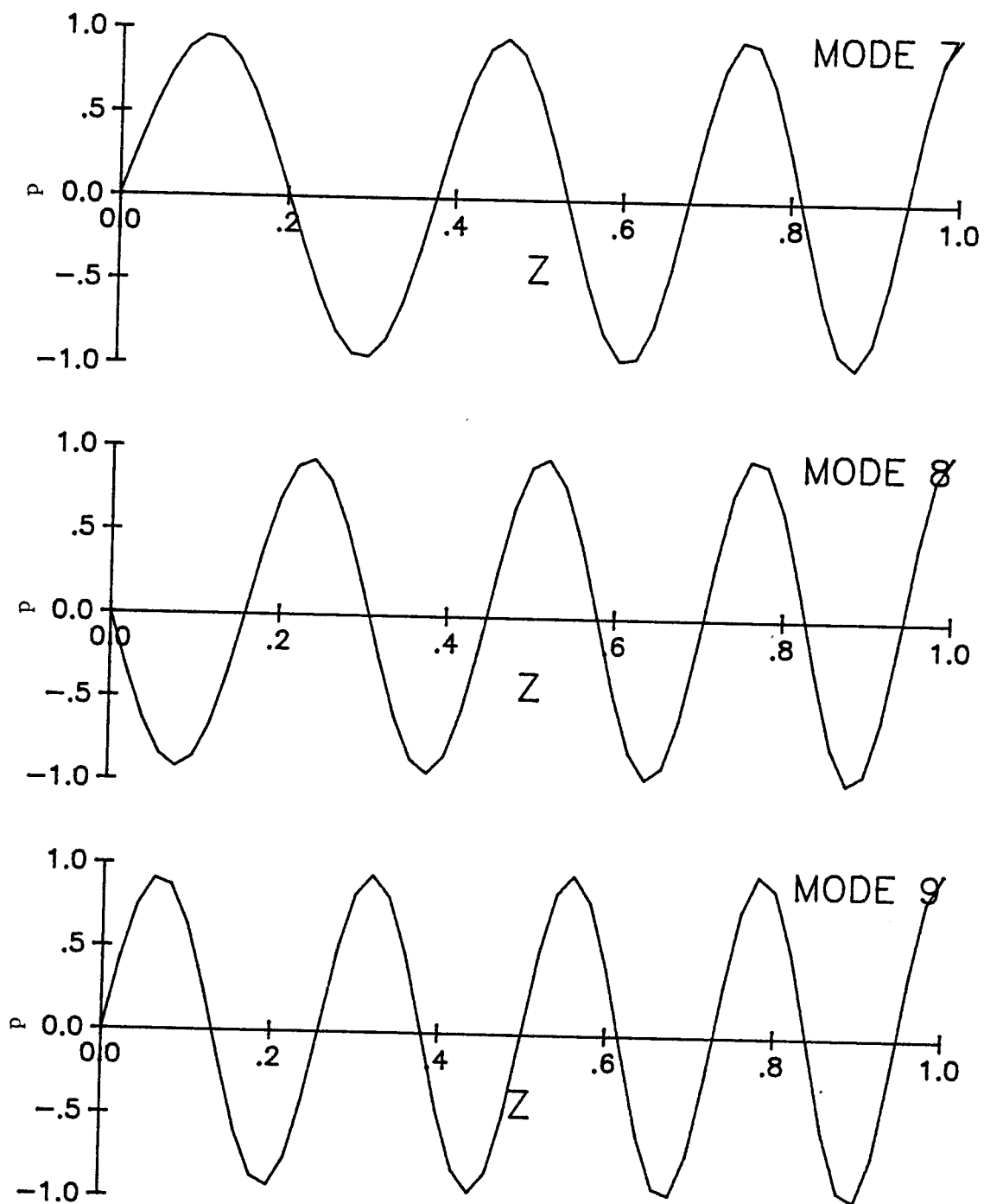


Figure 3.1c First nine modes for the aeroacoustic problem with $M=0.5$.

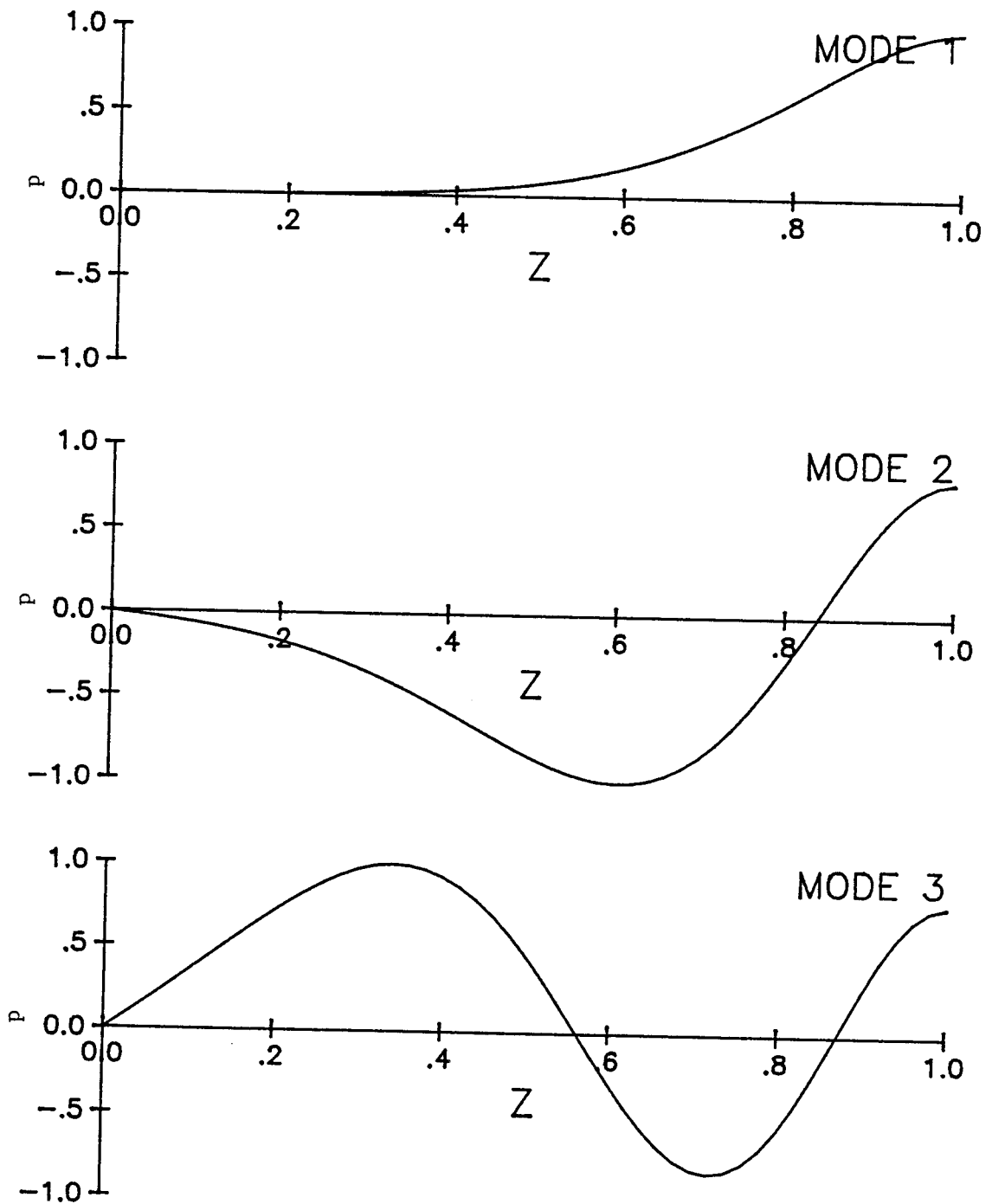


Figure 3.2a First six modes for the aeroacoustic problem with $M=1$.

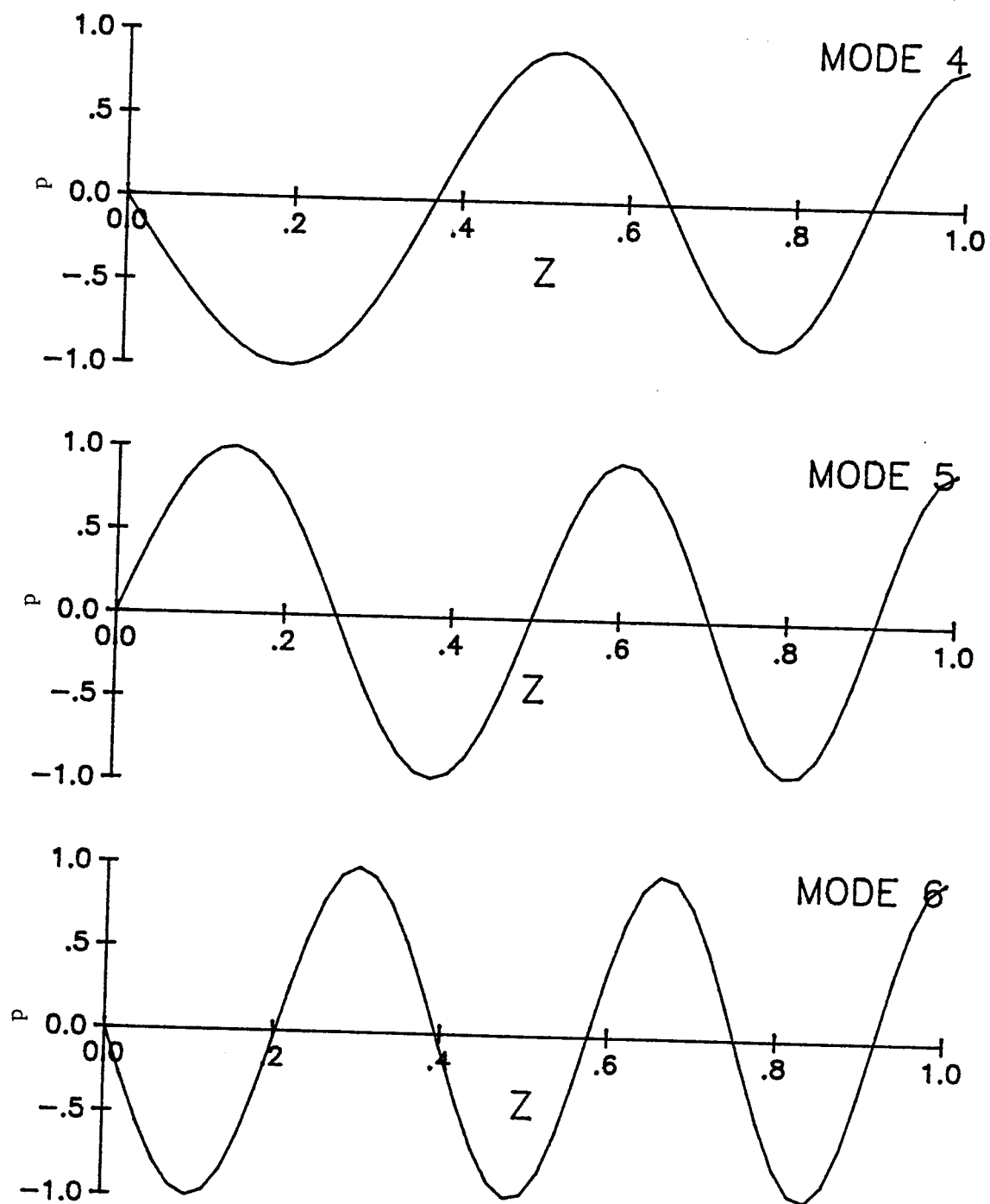


Figure 3.2b First six modes for the aeroacoustic problem with $M=.1$.

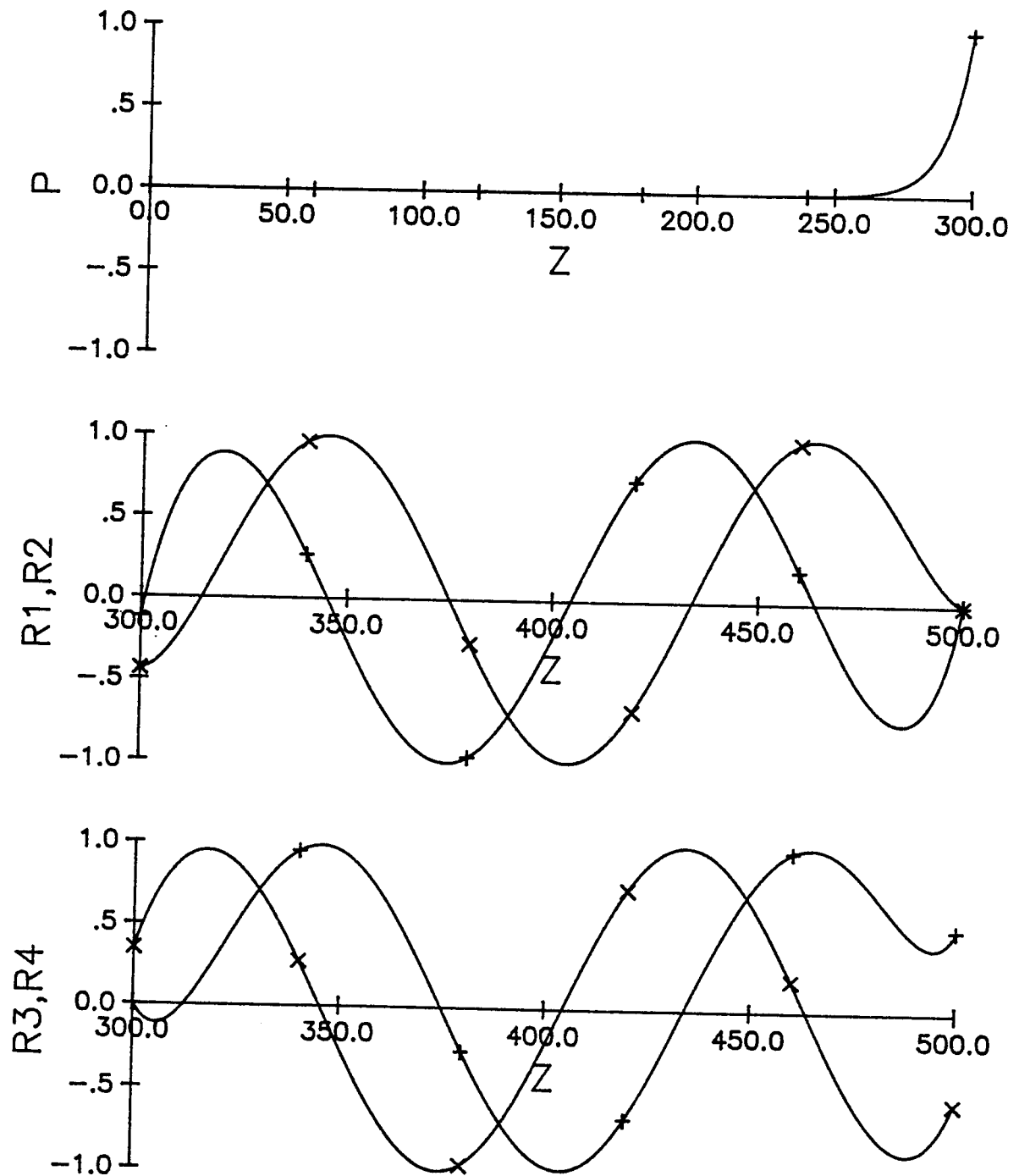


Figure 4.1 Mode 3 for the shallow water problem.

$$R_1 = -1.04E+4 \quad r_1 (+), \quad R_2 = -3.60E+4 \quad r_2 (X),$$

$$R_3 = -4.46E-2 \quad r_3 (+), \quad R_4 = -3.47E-1 \quad r_4 (X).$$

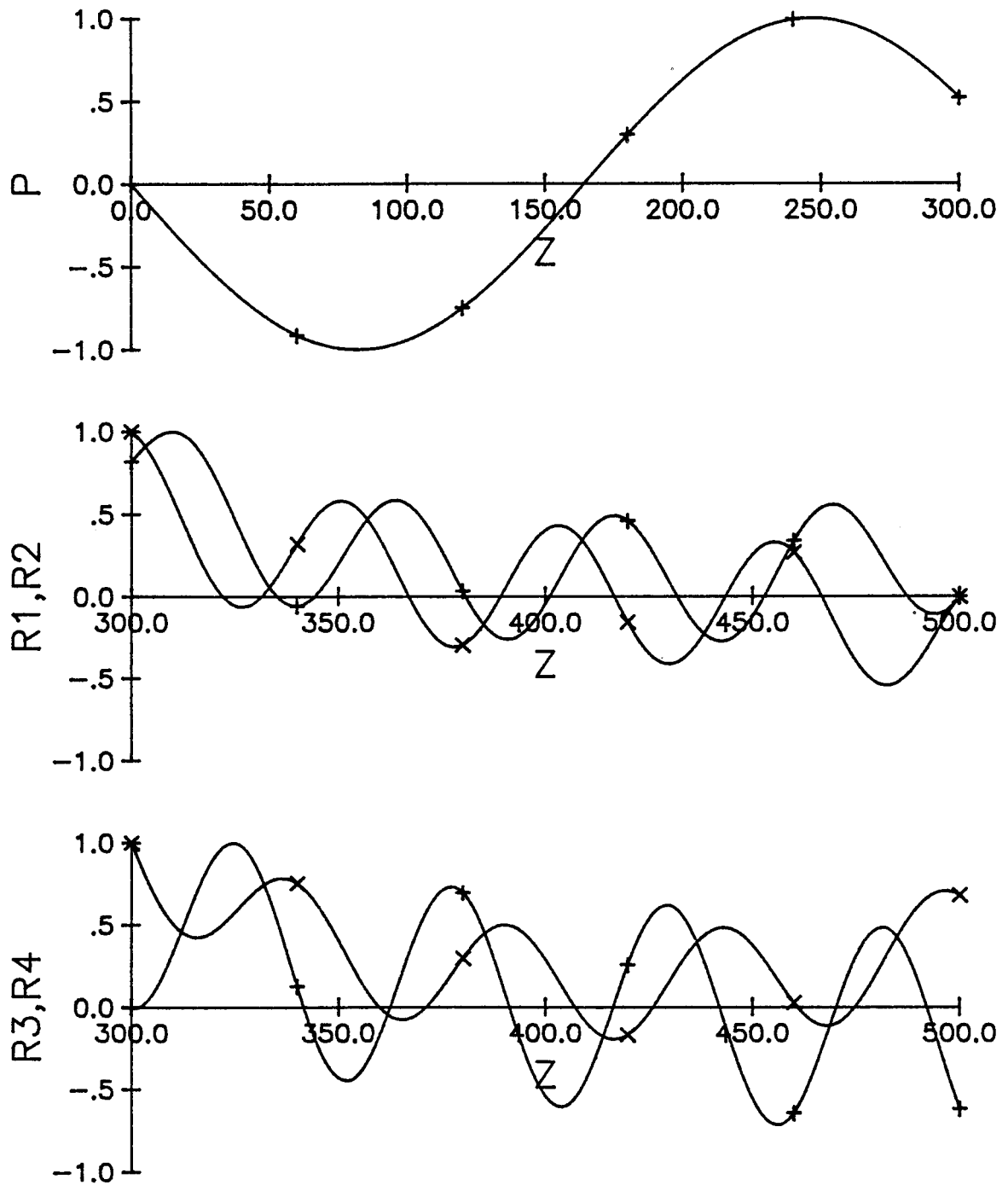


Figure 4.2 Mode 9 for the shallow water problem.

$$R_1 = +1.57E+4 \quad r_1 \quad (+), \quad R_2 = -5.44E+5 \quad r_2 \quad (X),$$

$$R_3 = -2.92E-1 \quad r_3 \quad (+), \quad R_4 = -1.93E-4 \quad r_4 \quad (X).$$

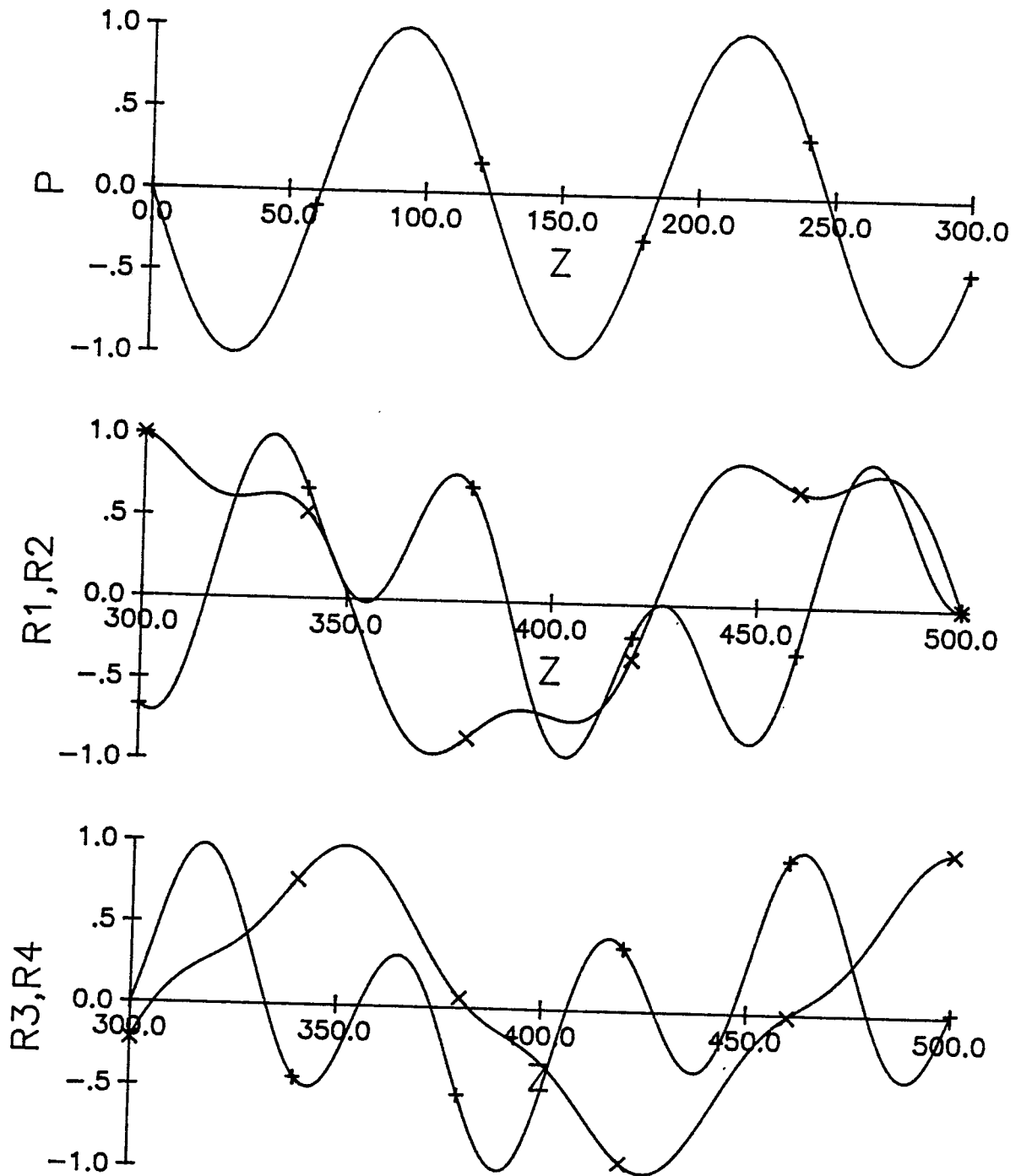


Figure 4.3 Mode 15 for the shallow water problem.
 $R_1 = +4.97E+3$ r_1 (+), $R_2 = +1.96E+5$ r_2 (x),
 $R_3 = +4.43E-2$ r_3 (+), $R_4 = -4.93E-1$ r_4 (x).

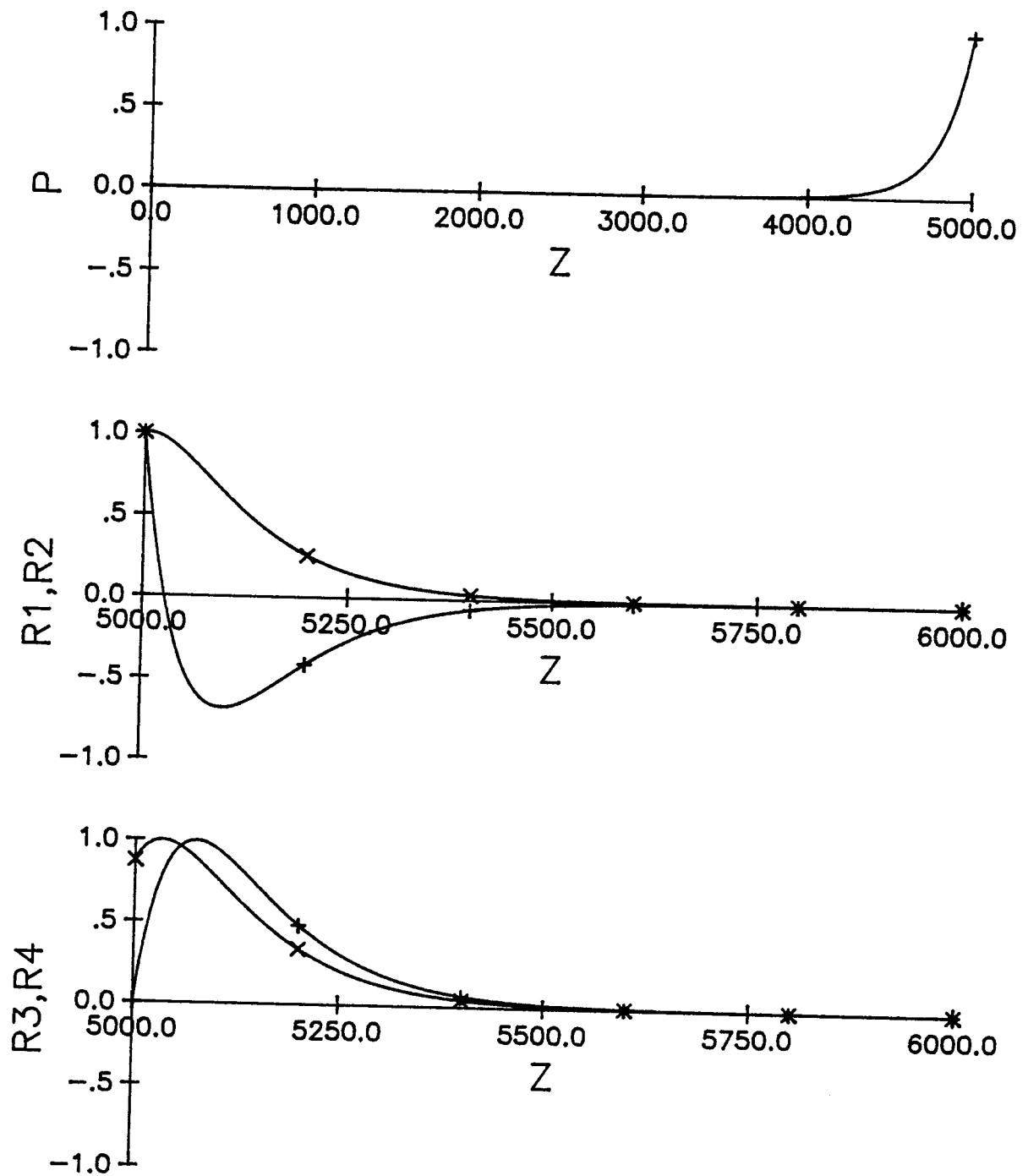


Figure 4.4 Mode 1 for the Munk profile with an elastic bottom.

$$R_1 = +6.15E+3 r_1 (+), R_2 = +1.19E+5 r_2 (x),$$

$$R_3 = +2.24E-2 r_3 (+), R_4 = -8.72E-1 r_4 (x).$$

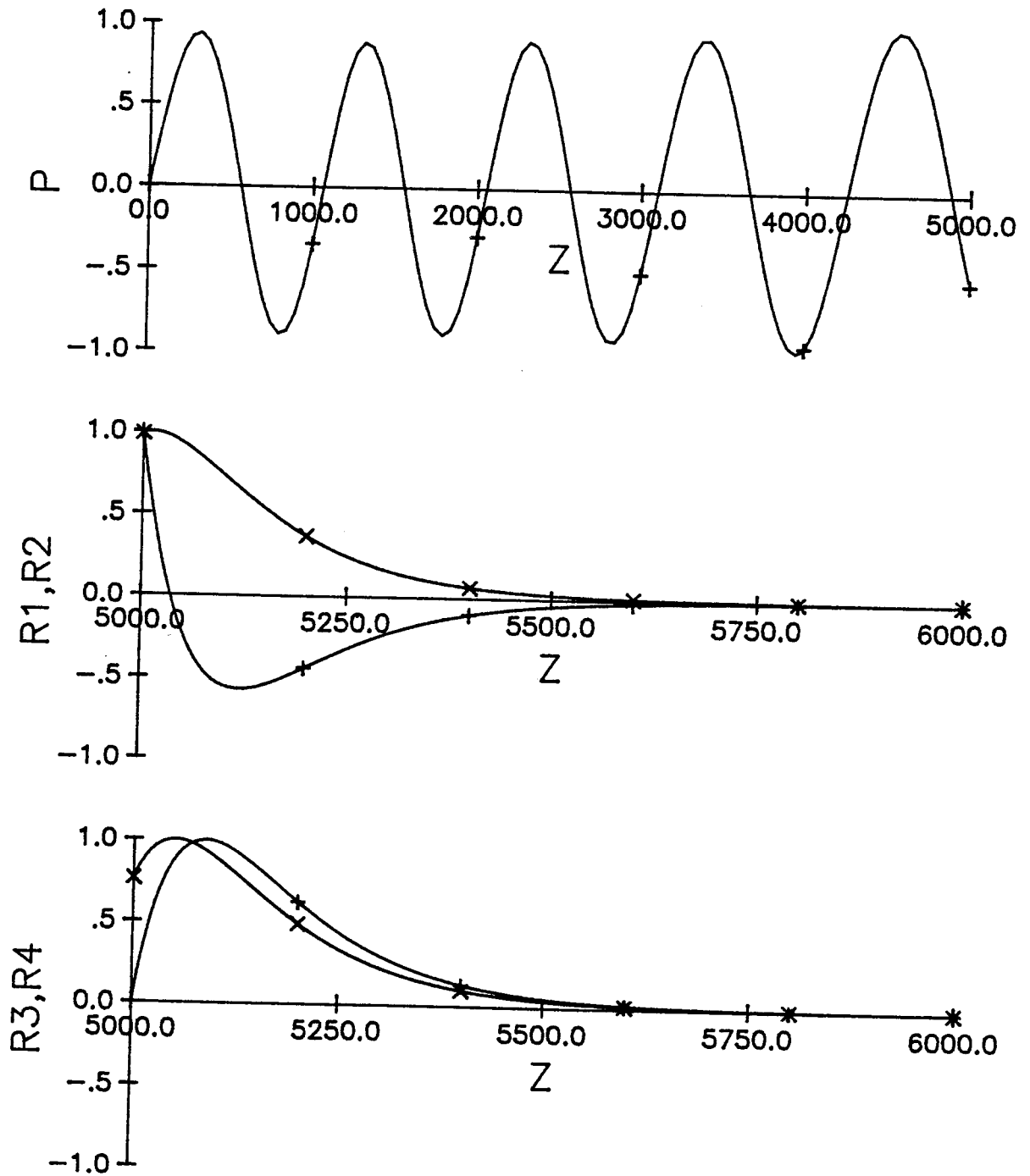


Figure 4.5 Mode 10 for the Munk profile with an elastic bottom.

$$R_1 = -6.12E+3 \quad r_1 (+), \quad R_2 = +1.52E+5 \quad r_2 (x),$$

$$R_3 = -2.73E-2 \quad r_3 (+), \quad R_4 = +1.41E+0 \quad r_4 (x).$$

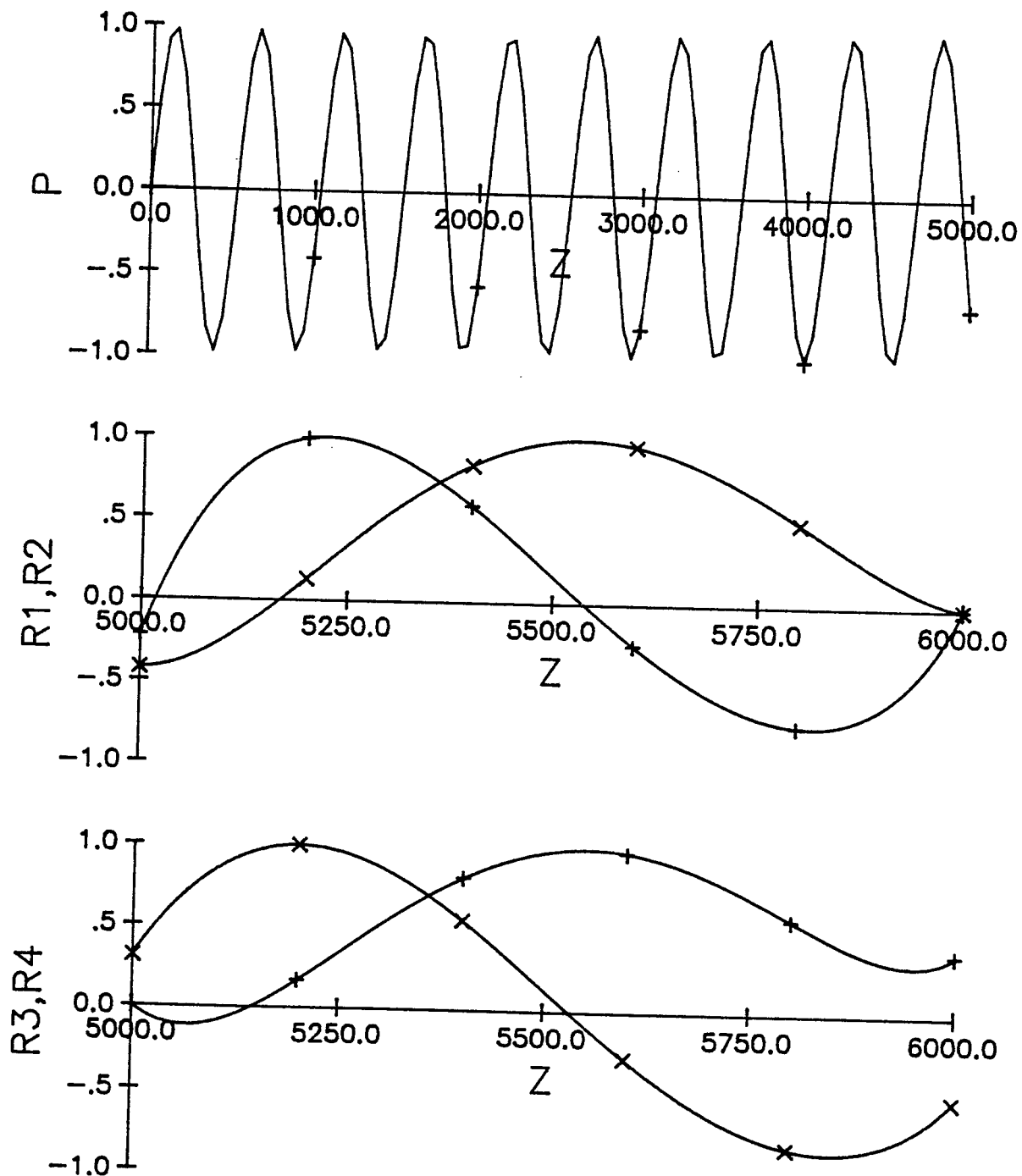


Figure 4.6 Mode 21 for the Munk profile with an elastic bottom.

$$R_1 = +1.06E+3 \quad r_1 (+), \quad R_2 = +3.27E+4 \quad r_2 (X),$$

$$R_3 = +4.45E-3 \quad r_3 (+), \quad R_4 = +4.66E-1 \quad r_4 (X).$$

REFERENCES

- Abramowitz, M. and Stegun, I. A., Handbook of Mathematical Functions, Washington, D.C., National Bureau of Standards (1964).
- Adam, Gh., "A first order perturbative numerical method for the solution of the radial Schrodinger equation", J. Comp. Physics, 22(1):1-33 (1976).
- Ageeva, N. S. and Krupin, V. D., "Structure of an infrasonic field in a shallow sea", Sov. Phys.-Acoustics, 25(3):192-195 (1979).
- Aki, Keiiti and Richards, Paul G., Quantitative Seismology: Theory and Methods, San Francisco, W. H. Freeman (1980).
- Allen, B. T., "A new method for solving second order differential equations when first derivative term is present", Comp. J., 8(4):392-394 (1966).
- Antar, Basil N., "On the solution of two point linear differential eigenvalue problems", J. Comp. Physics, 20:208-219 (1976).
- Antia, H. M., "Finite-difference method for generalized eigenvalue problem in ordinary differential equations", J. Comp. Physics, 30:283-295 (1979).
- Auld, B. A., Acoustic Fields and Waves in Solids, 2 Vols., New York, Wiley (1973).
- Avilov, K. V. and Mal'tsev, N. E., "Calculation of sound fields in the ocean by the parabolic equation method", Sov. Phys.-Acoustics, 27(3):185-188 (1981).
- Bailey, Paul B., "A slightly modified Prufer transformation useful for calculating Sturm-Liouville eigenvalues", J. Comp. Physics, 29:306-310 (1978).
- Barth, W., Martin, R. S. and Wilkinson, J. H., "Calculation of the eigenvalues of a symmetric tridiagonal matrix by the method of bisection", Num. Math., 9:386-393 (1967).
- Bathe, Klaus-Jurgen and Wilson, Edward L., "Eigensolution of large structural systems with small bandwidth", Am. Soc. Civil Eng.-Proc. Eng. Mechanics Division Journal, 99:467-479 (1973).

- Beebe, J. H. and McDaniel, S.T., "Geoacoustic models of the seabed to support range-dependent propagation studies on the Scotian shelf", p. 507-523 in Kuperman, William A. and Jensen, Finn B. (Ed.), Bottom-Interacting Ocean Acoustics, New York, Plenum Press (1980).
- Beilis, A., "Convergence zone positions via ray-mode theory", J. Acoust. Soc. Am., 74(1):171-180 (1983).
- Beisner, H. M., "Numerical calculation of normal modes for underwater sound propagation", IBM J. Res. and Dev., 18:53-58 (1974).
- Ben-Menahem, Ari and Singh, Sarva Jit, Seismic Waves and Sources, New York, McGraw-Hill (1981).
- Bolt, Bruce A., (Ed.), Methods in Computational Physics, Vol. 11, Seismology: Surface Waves and Earth Oscillations, New York, Academic Press (1972).
- Boyles, C. Allen, "Coupled mode solution for a cylindrically symmetric oceanic waveguide with a range and depth dependent refractive index and", J. Acoust. Soc. Am., 73(3):800-805 (1983).
- Bradbury, W. W. and Fletcher, R., "New iterative methods for solution of the eigenproblem", Num. Math., 9:259-267 (1966).
- Brandt, A. et al., "Multigrid methods for differential eigenproblems", SIAM J. Sci. and Stat. Comp., 4 2:245 (1983).
- Brekhovskikh, L. M., Waves in Layered Media, second ed., New York, Academic Press (1980).
- Brent, R. P., "An algorithm with guaranteed convergence for finding a zero of a function", Comp. J., 14(4):422-425 (1971).
- Brezinski, C., "A subroutine for the general interpolation and extrapolation problems", ACM Trans. on Math. Soft., 8(3):290-301 (1982).
- Burlisch, Roland and Stoer, Josef, "Numerical treatment of ordinary differential equations by extrapolation methods", Numer. Math., 8:1-13 (1966).
- Bus, J. C. P. and Decker, T. J., "Two efficient algorithms with guaranteed convergence for finding a zero of a function", Trans. on Math. Software, 1:330-345 (1975).

- Eye, John A. T., "A new method for determining eigenvalues and eigenfunctions", *Comp J.*, 10:108-111 (1967).
- Canosa, Jose, "Numerical solution of Mathieu's equation", *J. Comp. Physics*, 7:255-272 (1971).
- Canosa, Jose and de Oliveira, Roberto Gomez, "A new method for solution of the Schrodinger equation", *J. Comp. Physics*, 5:188-207 (1970).
- Carasso, Alfred, "Finite difference methods and the eigenvalue problem for nonselfadjoint Sturm-Liouville operators", *Math. Comp.*, 23:717-739 (1969).
- Caride, Anibal O. and Zanette, Susana I., "On the process of bisection to calculate the eigenvalues of quindagonal matrices", *Comp. J.*, 25(1):44 (1982).
- Chapman, D. M. F. and Ellis, Dale D., "The group velocity of normal modes", *J. Acoust. Soc. Am.*, 74(3):973-979 (1983).
- Chow, R. K. and Turner, R. G., "Attenuation of low frequency sound in the Northeast Pacific Ocean", *J. Acoust. Soc. Am.*, 72(2):888-895 (1982).
- Clay, Clarence S. and Medwin, Herman, *Acoustical Oceanography: Principles and Applications*, New York, Wiley (1977).
- Cooley, J. W., "An improved eigenvalue corrector formula for solving the Schrodinger equation for central fields", *Math. Comp.*, 15:363-374 (1961).
- Dahlquist, G. and Bjorck, A., *Numerical Methods*, Englewood Cliffs, NJ, Prentice-Hall (1974).
- Daniels, J. M. and Vidmar, P. J., "Occurrence and acoustical significance of natural gas hydrates in marine sediments", *J. Acoust. Soc. Am.*, 72(5):1564-1573 (1982).
- Davey, A., "On the removal of the singularities from the Riccati method", *J. Comp. Physics*, 30:137-144 (1979).
- Davey, A., "On the numerical solution of difficult boundary value problems", *J. Comp. Physics*, 35:36-47 (1980).
- Davey, A., "A simple numerical method for solving Orr-Sommerfeld problems", *Quart. J. Mech. App. Math.*, 26:401-411 (1973).

- DeSanto, J. A. (Ed.) Ocean Acoustics, Berlin, Springer-Verlag (1977).
- Dickinson, A. S., "Comparison of the finite difference boundary value method and the Cooley-Cashion-Zare method for solving one dimensional", J. Comp. Physics, 11:458-462 (1973).
- Dozier, Lewis B., "Calculation of normal modes in a stratified ocean", Unpublished report, : (c. 1975).
- Dozier, Lewis B. and Tappert, F. D., "Statistics of normal mode amplitudes in a random ocean (I) Theory", J. Acoust. Soc. Am., 63(2):353-365 (1978).
- Dunkin, John W., "Computation of modal solutions in layered, elastic media at high frequencies", Bull. Seism. Soc., 55(2):335-358 (1965).
- Essen, Heinz-H., "Model computations for low-velocity surface waves on marine sediments", p. 299-305 in Kuperman, William A. and Jensen, Finn B. (Ed.), Bottom-Interacting Ocean Acoustics, New York, Plenum Press (1980).
- Evans, R. B., "A coupled mode solution for acoustic propagation in a waveguide with stepwise variations of a penetrable bottom", J. Acoust. Soc. Am., 74(1):188-195 (1983).
- Eversman, W. and Beckemeyer, R. J., "The transmission of sound in ducts with thin shear layers- convergence to the uniform flow case", J. Acoust. Soc. Am., 52:216-220 (1972).
- Eversman, Walter, "Approximation of thin boundary layers in the sheared flow duct transmission problem", J. Acoust. Soc. Am., 53(5):1346-1350 (1973).
- Ewing, W. Maurice, Jardetsky, Wenceslas S., and Press, Frank, Elastic Waves in Layered Media, New York, McGraw-Hill (1957).
- Ferla, M. C. et al., "Broadband model/data comparisons for acoustic propagation in coastal waters", p. 577-592 in Kuperman, William A. and Jensen, Finn B. (Ed.), Bottom-Interacting Ocean Acoustics, New York, Plenum Press (1980).
- Ferla, M. C., Jensen, F. B. and Kuperman, W. A., "High frequency normal mode calculations in deep water", J. Acoust. Soc. Am., 72(2):505-509 (1982).

- Ferris, R. H., Ingenito, F. and Faber, A. L., "Experimental separation and identification of acoustic normal modes in shallow water", Naval Research Laboratory Report 7174, : (1970).
- Ferris, Raymond H., "Comparison of measured and calculated normal-mode amplitude functions for acoustic waves in shallow water", J. Acoust. Soc. Am., 52(3):981-988 (1972).
- Fix, Samuel P. and Marin, George J., "Variational methods for underwater acoustic problems", J. Comp. Physics, 28(2):253-270 (1978).
- Friar, J. L., "A note on the roundoff error in the Numerov algorithm", J. Comp. Physics, 28(3):426-432 (1978).
- Froberg, C., Introduction to Numerical Analysis, Reading, Mass., Addison-Wesley (1965).
- Gary, John and Helgason, Richard, "A matrix method for ordinary differential eigenvalue problems", J. Comp. Physics, 5:169-187 (1970).
- Gersting, John M., Jr., "Numerical methods for eigensystem: the Orr-Sommerfeld problem", Comp. Math., 3:47-52 (1977).
- Gersting, John M., Jr., "Numerical methods for eigensystems: the Orr-Sommerfeld problem as an initial value problem", Comp. Math., 6:167-174 (1980).
- Gersting, John M., Jr. and Jankowski, Daniel F., "Numerical methods for Orr-Sommerfeld problems", Int. J. Num. Meth. Eng., 4:195-206 (1972).
- Gilbert, Freeman and Backus, George E., "Propagator matrices in elastic wave and vibration problems", Geophysics, 31:326-332 (1966).
- Gilbert, Kenneth E., "A propagator matrix method for periodically stratified media", J. Acoust. Soc. Am., 73(1):137-142 (1983).
- Golod, O. S. and Grigor'eva, N. S., "Estimation of the influence of current on the pressure field of a monochromatic point source in a homogeneous ocean", Sov. Phys.-Acoustics, 28(6):449-451 (1982).
- Goodstein, Marvin E., Aeroacoustics, New York, McGraw-Hill (1976).
- Gordon, D. F., "Underwater sound propagation-loss program ", N.O.S.C. Rep. 393, : (1979).

- Graff, Karl F., Wave Motion in Elastic Solids, Ohio State Univ. Press (1975).
- Graham, E. W. and Graham, B. B., "Effect of a shear layer on plane waves", J. Acoust. Soc. Am., 46:169 (1968).
- Guardiola, R. and Ros, J., "On the numerical integration of the Shrodinger equation in the finite difference schemes", J. Comp. Physics, 45(3):374-389 (1982).
- Gupta, K. K., "Vibrations of frames and other structures with banded stiffness matrix", Int. J. for Num. Meth. in Eng., 2:221-228 (1970).
- Gupta, K. K., "Solution of eigenvalue problems by Sturm sequence method", Int. J. of Num. Methods, 8:379-404 (1972).
- Gupta, K. K., "Eigenproblem solution of damped structural systems", Int. J. of Num. Methods, 8:877-911 (1974).
- Gupta, K. K., "Free vibration of single-branch structural sytems", J. Inst. Math App., 5:351-362 (1965).
- Hagin, F. G., "Computation of eigenvalues for second-order differential equations using imbedding techniques", J. Comp. Physics, 3:46-57 (1968).
- Hajj, F. Y. et al, "On the numerical solution of Schroedinger's radial equation", J. Comp. Physics, 16(2):150-159 (1974).
- Hall, Marshall, Gordon, David F. and White, DeWayne, "Improved methods for determining eigenfunctions in multi-layered normal-mode programs.", J. Acoust. Soc. Am., 73(1):153-162 (1983).
- Hargrave, B. A., "Numerical approximation of eigenvalues of Sturm-Liouville systems", J. Comp. Physics, 20:381-396 (1970).
- Harkrider, David G., "Surface waves in multilayered elastic media. I. Rayleigh and Love waves from buried sources in a multilayered half-space", Bull. Seism. Soc. Am., 54(2):627-679 (1964).
- Harkrider, David G., "Surface waves in multilayered elastic media. Part II. Higher mode spectra and spectral ratios from point sources in plane", Bull. Seism. Soc. Am., 60(6):1937-1987 (1970).
- Haskell, N. A., "The dispersion of surface waves on multilayered

- media", Bull. Seism. Soc. Am., 43:17-34 (1953).
- Hawker, Kenneth E. and Foreman, Terry L., "A plane wave reflection loss model based on numerical integration", J. Acoust. Soc. Am., 64(5):1470-1477 (1978).
- Hille, Einar, Lectures on Ordinary Differential Equations, Reading, Mass., Addison-Wesley (1969).
- Hilliam, Pierre, "Numerical solution of the Helmholtz equation in optics", J. Comp. Physics, 28:232-252 (1978).
- Hindmarsh, A.C., "Optimality in a Class of Root-Finding Algorithms", SIAM Num, 9:205 (1972).
- Householder, Alston and Bauer, Friedrich L., "On certain methods for expanding the characteristic polynomial", Num. Math., 1:29-37 (1959).
- Ingenito, Frank, "Measurements of mode attenuation coefficients in shallow water", J. Acoust. Soc. Am., 53(3):858-863 (1973).
- Israeli, Moshe and Orszag, Steven A., "Approximation of radiation boundary conditions", J. Comp. Physics, 41:115-135 (1981).
- Ixary, L. Gr., "The error analysis of the algebraic method for solving the Schrodinger equation", J. Comp. Physics, 9:159-163 (1972).
- Jensen, F. B. and Kuperman, W. A., "Optimum frequency of propagation in shallow water environments", J. Acoust. Soc. Am., 73(3):813-819 (1983).
- Jensen, Finn B., "Sound propagation in shallow water: a detailed description of the acoustic field close to surface and bottom", J. Acoust. Soc. Am., 70(5):1397-1406 (1981).
- Joyce, D.C., "Survey of extrapolation processes in numerical analysis", SIAM Review, 13:435-490 (1971).
- Kausel, Eduardo and Roesset, Jose Manuel, "Stiffness matrices for layered soils", Bull. Seism. Soc. Am., 71(6):1743-1761 (1981).
- Keller, Herbert B., "Accurate difference methods for linear ordinary differential systems subject to linear constraints", SIAM Num., 6(1):8-30 (1969).
- Keller, Joseph B., "Reflection and transmission of sound by a moving medium", J. Acoust. Soc. Am., 27:1044-1047 (1955).

- Keller, Joseph B. and Papadakis, John S. (Ed.), Wave Propagation and Underwater Acoustics, Berlin, Springer-Verlag (1977).
- Kershaw, D., "QD algorithms and algebraic eigenvalue problems", Linear Alg. and Its App., 54:53-75 (1983).
- Kikina, N. G. and Sannikov, D. G., "Reflection of sound waves from a moving plane-parallel layer", Sov. Phys.-Acoustics, 15:472-474 (1970).
- Knopoff, L., "A matrix method for elastic wave problems", Bull. Seism. Soc. Am., 54:431-438 (1964).
- Ko, Sung-Hwan, "Sound attenuation in lined rectangular ducts with flow and its application to the reduction of aircraft engine noise", J. Acoust. Soc. Am., 50:1418-1432 (1971).
- Koch, Robert A. et al, "On the calculation of normal mode group velocities and attenuation", J. Acoust. Soc. Am., 73(3):820-825 (1983).
- Koch, Robert A., Vidmar, Paul J. and Lindberg, Jo B., "Normal mode identification for impedance boundary conditions", J. Acoust. Soc. Am., 73(5):1567-1570 (1983).
- Kong, J. A., "Interaction of acoustic waves with moving media", J. Acoust. Soc. Am., 48:236-241 (1970).
- Krishnamurti and Venkateswaran, "Complex zeros of a polynomial", BIT, 21:104-111 (1981).
- Krupin, V. D., "A special effect in a waveguide having a negative sound velocity gradient", Sov. Phys.-Acoustics, 18:460-465 (1973).
- Kuperman, William A. and Jensen, Finn B. (Ed.), Bottom-Interacting Ocean Acoustics, New York, Plenum Press (1980).
- Lee, Ding and Papadakis, John S., "Numerical solutions of the parabolic wave equation: An ordinary differential equation approach", J. Acoust. Soc. Am., 68(5):1482-1488 (1980).
- Lee, Ding and Peiser, S., "Generalized Adam's methods for solving underwater wave propagation problems.", Comp. Math., 7(2):195-202 (1981).
- Lee, Ding, Botseas, George and Papadakis, John S., "Finite-difference solution to the parabolic wave equation ", J.

- Acoust. Soc. Am., 70(3):795-800 (1981).
- Lee, L. H. and Reynolds, W. C., "On the approximate and numerical solution of Orr-Sommerfeld problems", Quart. J. Mech. App. Math., 20:1-22 (1967).
- Lyamshev, L. M., "Theory of sound propagation in a moving layered inhomogeneous medium", Sov. Phys.-Acoustics, 28(3):217-221 (1982).
- Lysmer, John, "Lumped mass method for Rayleigh waves", Bull. Seism. Soc. Am., 60 1:89-104 (1970).
- Malik, David J., Eccles, Joseph and Secrest, Don, "On quantal bound state solutions and potential energy surface. A comparison of the finite elt, Numerov-Cooley and f.d. methods", J. Comp. Physics, 38:157-184 (1980).
- McDaniel, Suzanne T., "Parabolic approximations for underwater sound propagation", J. Acoust. Soc. Am., 58(6):1178-1185 (1975).
- McDaniel, Suzanne T., "Mode coupling due to interaction with the seabed", J. Acoust. Soc. Am., 72(3):916-923 (1982).
- Mikhailov, Mikhail D. and Vulchanov, Nikolai L., "Computational procedure for Sturm-Liouville problems", J. Comp. Physics, 50 3:323-336 (1983).
- Mitchell, Stephen K. and Focke, Karl C., "The role of the seabottom attenuation profile in shallow water acoustic propagation", J. Acoust. Soc. Am., 73(2):465-473 (1983).
- Mungur, P. and Gladwell G. M. L., "Acoustic wave propagation in a sheared fluid contained in a duct", J. Sound and Vib., 9(1):28-48 (1969).
- Munk, W. H., "Sound channel in an exponentially stratified ocean with applications to SOFAR", J. Acoust. Soc. Am., 55:220-226 (1974).
- Murphy, C. P. and Evans, D. J., "A flexible variable order extrapolation technique for solving non-stiff ordinary differential equations", Comp. Math., 10:63-75 (1981).
- Myers, M. K., "On the acoustic boundary condition in the presence of flow", J. Sound and Vib., 71(3):429-434 (1980).
- Ng, B. S. and Reid, W. H., "An initial value method for eigenvalue problem using compound matrices", J. Comp. Physics, 30:125-136

(1979).

Ng, B. S. and Reid, W. H., "A numerical method for linear two-point boundary value problems using compound matrices", *J. Comp. Physics*, 33(1):70-85 (1979).

Ng, B. S. and Reid, W. H., "On the numerical solution of the Orr-Sommerfeld problem: asymptotic initial conditions for shooting methods", *J. Comp. Physics*, 38(3):275-293 (1980).

North, R. G. and Dziewonski, A. M., "A note on Rayleigh-wave flattening corrections", *Bull. Seism. Soc. Am.*, 66(5):1873-1879 (1976).

Officer, C. B., *Introduction to the Theory of Sound Transmission with Applications to the Ocean*, New York, McGraw-Hill (1958).

Paine, J. W. and de Hoog, F. R., "Uniform estimates of eigenvalues of Sturm-Liouville eigenvalue problems", *J. Aust. Ma. Soc.*, 21:365-383 (1980).

Paine, J. W. and de Hoog, F. R., "Correction of Sturm-Liouville eigenvalue estimates", *Math. Comp.*, 39:415 (1982).

Paine, J.W., de Hoog, F. R. and Anderssen, R. S., "On the correction of finite difference eigenvalue approximations for Sturm-Liouville problems", *Computing*, 26:123-139 (1981).

Parlett, Beresford N., *The Symmetric Eigenvalue Problem*, Englewood Cliffs, NJ, Prentice-Hall (1980).

Pederson, M. A. and Gordon, D. F., "Normal mode theory applied to short-range propagation in an underwater acoustic surface duct", *J. Acoust. Soc. Am.*, 37:105-118 (1965).

Peters, G. and Wilkinson, J. H., "Eigenvalues of $Ax=LBx$ with band symmetric A and B", *Comp J.*, 12:398-404 (1969).

Popovski, D. B., "A note on Neta's family of sixth order methods", *Comp. Math.*, 10:91-93 (1981).

Porter, L. D. et al., "Relative computer speeds for surface-wave dispersion computations", *Bull. Seism. Soc. Am.*, 70 4:1415-1420 (1980).

Pruess, S., "High order approximation to Sturm-Liouville eigenvalues", *Numer. Math.*, 24:241-247 (1975).

- Reinsch, C. and Bauer, F. L., "Rational QR transformation with Newton shift for symmetric tridaigonal matrices", Numer. Math., 11:264-272 (1968).
- Ruptis, A. D., "Two step methods for the numerical solution of the Schrodinger equation", Computing, 28:373-378 (1982).
- Rutherford, Steven R. and Hawker, Kenneth E., "Effects of density gradients on bottom reflection loss for a class of marine sediments.", J. Acoust. Soc. Am., 63(3):750-757 (1978).
- Sato, Y., "Numerical integration of the equation of motion for surface waves in a medium with arbitrary variation of material constants", Bull. Seism. Soc. Am., 49:57-77 (1959).
- Savkar, S. D., "Propagation of sound in ducts with shear flow", J. Sound and Vib., 19(3):355-372 (1971).
- Schockley, Richard C. et al, "SOFAR propagation paths from Australia to Bermuda: Comparison of signal speed algorithms and experiments", J. Acoust. Soc. Am., 71(1):51-60 (1982).
- Schwab, F. et al., "Surface wave dispersion computations: Rayleigh waves on a spherical gravitating earth.", Bull. Seism. Soc. Am., 71(3):613-654 (1981).
- Schwab, Fred and Knopoff, Leon, "Surface-wave dispersion computations", Bull. Seism. Soc. Am., 60:321-344 (1970).
- Scott, M. R. et al, "Invariant imbedding and the calculation of eigenvalues for Sturm-Liouville systems", Computing, 4:10-23 (1969).
- Scott, Melvin R., "An initial method for the eigenvalue problem for systems of ordinary differential equations", J. Comp. Physics, 12:334-347 (1973).
- Shampine, L. F. and Baca, L. S., "Smoothing the extrapolated midpoint rule", Numer. Math., 41(2):165-175 (1983).
- Shanehchi, J. and Evans, D. J., "A modified bisection algorithm for the determination of eigenvalues of a symmetric quindagonal matrix.", Comp. J., 25(4):493-494 (1982).
- Shankar, P. N., "Sound propagation in duct shear layers", J. Sound and Vib., 22(2):221-232 (1972).

- Silva, W., "Body waves in a layered anelastic solid", Bull. Seism. Soc. Am., 66(5):1539-1554 (1976).
- Stickler, D. C., "Normal Mode Program with ω^2 linear terms" and Swinbanks, M. A., "The sound field generated by a source distribution in a long duct carrying sheared flow", J. Sound and Vib., 40(1):51-76 (1975).
- Takeuchi, H. and Saito, M., "Seismic surface waves", p. 217-295 in Bolt, Bruce A., (Ed.), Methods in Computational Physics, Vol. 11, Seismology: Surface Waves and Earth Oscillations, New York, Academic Press (1972).
- Talman, James P., "Eigenvalue correction estimates for the one-dimensional Schrodinger equations", J. Comp. Physics, 37:19-40 (1980).
- Tewarson, R. P., "A seventh order num. method for solving BV nonlinear ODE's", Int. J. of Num. Methods in Eng., 18 19:1313 (1982).
- Thomson, W. T., "Transmission of elastic waves through a stratified medium", J. App. Phys., 21:89-93 (1950).
- Thrower, E. N., "The computation of the dispersion of elastic waves in layered media", J. Sound and Vib., 2:210-226 (1965).
- Tolstoy, Ivan, "Guided waves in a fluid with continuously variable velocity overlying an elastic solid", J. Acoust. Soc. Am., 32(1):81-87 (1960).
- Tolstoy, Ivan and Clay, C. S., Ocean Acoustics-Theory and Experiment in Underwater Sound, New York, McGraw-Hill (1966).
- Truhlar, D. G., "Finite difference boundary value method for solving one-dimensional eigenvalue equations", J. Comp. Physics, 10:123-132 (1972).
- Urlick, Robert J., Principles of Underwater Sound, Rev. ed. New York, McGraw-Hill (1975).
- Usmani, Riaz A., "A method of high-order accuracy for the numerical

integration of boundary value problems", BIT, 13:458-469 (1973).

Usmani, Riaz A., "An $O(h^6)$ finite difference analogue for the numerical solution of a two point boundary value problem", J. Inst. Maths Applics, 8:335-343 (1971).

Vidmar, Paul J. and Foreman, Terry L., "A plane wave reflection loss model including sediment rigidity", J. Acoust. Soc. Am., 66(6):1831-1835 (1979).

Wasserstrom, E., "A new method for solving eigenvalue problems", J. Comp. Physics, 9:53-74 (1972).

Watkins, David S., "Understanding the QR algorithm", SIAM Rev., 24(4):427-440 (1982).

Watson, D. E., "Rays, modes, interference and the effect of shear flow in underwater acoustics", J. Sound and Vib., 9(1):80-89 (1969).

Watson, T. H., "A note on the fast computation of Rayleigh wave dispersion in the multilayered elastic half-space", Bull. Seism. Soc. Am., 60:161-166 (1970).

Wicke, Brian G. and Harris, David O., "Comparison of three numerical techniques for calculation of eigenvalues of an unsymmetrical double minimum oscillator", J. Ch. P., 64:5236-5242 (1976).

Wiggins, Ralph A., "A fast, new computational algorithm for free oscillations and surface waves", Geophys. J. R. astr. Soc., 47:135-150 (1976).

Wilkinson, J. H., "Calculation of the eigenvalues of a symmetric tridiagonal matrix by the method of bisection", Numer. Math., 4:362-367 (1962).

Wilkinson, James H., The Algebraic Eigenvalue Problem, Oxford, Clarendon Press (1965).

Williams Jr., A. O., "Axial focussing of sound in the SOFAR channel", J. Acoust. Soc. Am., 41:189-198 (1967).

Wolniewicz, L. and Orlikowski, T., "On the numerical integration of the Schrodinger equation with a double-minimum potential", J. Comp. Physics, 27:169-179 (1978).

Yeh, C., "Reflection and transmission of sound waves by a moving fluid layer", J. Acoust. Soc. Am., 41:817-821 (1966).

REFERENCES

Yeh, C., "A further note on the reflection and transmission of sound waves by a moving fluid layer.", J. Acoust. Soc. Am., 43:1454-1455 (1967).

VITA

Name: Michael Blair Porter

Birth: September 19, 1958

Quebec, Canada

Education: BS Applied Mathematics

California Institute of Technology